DEVELOPMENT OF VACUUM INSULATION PANEL WITH LOW COST CORE MATERIAL

A thesis submitted for the degree of Doctor of Philosophy

By

Mahmood Alam

Department of Mechanical, Aerospace and Civil Engineering

College of Engineering, Design and Physical Science

Brunel University London

October 2015

Abstract

Buildings consume around half of the UK's total energy consumption and are responsible for almost 50% of UK's total Carbon dioxide (CO_2) emissions. Use of high thermal resistance insulation in buildings is critical to save the substantial amounts of space heating energy lost through building fabric. Conventional building insulation materials have higher thermal conductivity values ranging from 40 $mWm^{-1}K^{-1}$ (Glass fibre) - 26 $mWm^{-1}K^{-1}$ (Polyurethane foam) and require larger thicknesses to achieve stringent building regulation requirements which may not be feasible due to techno-economic constraints. Vacuum Insulation Panel (VIP) is a relatively new insulation for building applications that offers 5-8 times higher thermal resistance and can achieve significant space savings in buildings. VIPs are produced as a rigid panel comprising inner core board laminated in an outer high barrier envelope under evacuated conditions (<5mbar). However, the main challenge for large scale acceptance of VIPs in building applications is their higher cost. VIPs have been shown to have an approximately 10 times longer payback compared to conventional EPS insulation due to their high initial cost. Expensive materials currently being used for VIP manufacturing such as fumed silica contribute to high cost of VIPs and it is critical to identify alternative low cost materials for VIP components to overcome the challenge of high cost.

The aim of this thesis was to develop an alternative low cost material and investigate its suitability for use as VIP core. Expanded perlite, a low cost material was identified as a replacement of expensive fumed silica in a VIP core. Composite samples containing expanded perlite, fumed silica, silicon carbide (SiC) and polyester fibres were developed by dry mixing of the constituents in different mass ratios and their different properties were experimentally measured to identify optimum composition of composite. Gaseous thermal conductivity at different pressures was calculated from the pore size data obtained using Mercury Intrusion Porosimetry (MIP), gas adsorption and electron microscopy. Radiative conductivity of composite samples was measured using Fourier Transform Infrared (FTIR) to ascertain the opacifying effect of expanded perlite and opacifier (SiC). Centre of panel thermal conductivity of core boards of size 100mm × 100mm made of composite material at atmospheric pressure was measured by using a small guarded hot plate device. Average pore diameter values of expanded perlite decreased with the partial filling of fumed silica aggregates and was found to be in the range of 150-300 nm yielding lower gaseous conductivity values of 1.2-2.1 $mWm^{-1}K^{-1}$ at 100mbar and became negligible upon further

decreasing pressures below 10 mbar. Core boards made of optimised composite containing 30% expanded perlite and 50% fumed silica along with SiC and polyester fibres was found to achieve centre of panel thermal conductivity of 28 $mWm^{-1}K^{-1}$ at atmospheric pressure and the average radiative conductivity of 0.67 $mWm^{-1}K^{-1}$ at 300K with its gaseous thermal conductivity at 1 mbar being 0.016 $mWm^{-1}K^{-1}$. According to the results of the thesis VIP prototypes consisting of core made with optimised composite consisting (50 mass% of fumed silica, 30 mass% of expanded perlite along with 8 mass% of fibre and 12 mass% of SiC) yielded centre of panel thermal conductivity of 7.4-7.6 $mWm^{-1}K^{-1}$ at pressure of 0.53-0.64 mbar. Opacifying properties of expanded perlite were observed and quantified. Expanded perlite reduced the radiative conductivity of the composite requiring smaller quantities of high density opacifiers such as SiC. For sample containing no expanded perlite, average radiative conductivity was calculated to be 1.37 $mWm^{-1}K^{-1}$ and radiative conductivity values decreased to 1.12 $mWm^{-1}K^{-1}$, 0.67 $mWm^{-1}K^{-1}$, 0.63 $mWm^{-1}K^{-1}$ and 0.50 $mWm^{-1}K^{-1}$ with mass ratio of expanded perlite 20%, 30%, 40% and 60% respectively. It was concluded that the solid conductivity of prototypes VIPs was 1.8-2 times higher compared to those of commercially available VIPs and is the main reason for higher centre of panel thermal conductivity.

Acknowledgments

First of all, I would like to thank my supervisor, Dr. Harjit Singh for his continuous support during this research work. I would like to thank him for his supervision, guidance and encouragement which have made the completion of this research work possible. I am also indebted to him for his generous commitment of time and availability whenever I needed him.

I want to extend my appreciation to Dr. Samuel Brunner and Dr. Pär Johansson at Empa, Federal Swiss Laboratories for Material Sciences for their assistance with thermal conductivity measurement experiments.

I also gratefully acknowledge the bursary received from Brunel University for my research work.

It would be not possible for me to follow a research career without the support and encouragement from my family. I am very much thankful to all of them for their love and support.

Table of Contents

List of Figures

List of Tables

Nomenclature

Latin letters

k_c	Thermal conductivity due to the coupling effect	[$Wm^{-1}K^{-1}$]
P_{atm}	Atmospheric pressure	[Pa]
E	Young's Modulus	[Pa]
n	Mean index of refraction	-
T_r	Average temperature within the insulation material	[K]
E_c	Extinction coefficient	[m^{-1}]
e^*	Specific extinction	
K_B	Boltzmann constant	[JK^{-1}]
T	Temperature	[K]
P	Gas pressure	[Pa]
d	Diameter of gas molecule	[m]
u	Moisture content	[mass %]
Xw	Water content	[mass %]
b	Sorption isotherm constant	-
p_{gas}	Gas pressure	[Pa]
$p_{1/2,gas}$	Pressure at which the gaseous thermal conductivity equals one half of $\lambda_{free\ gas}$	[Pa]
p_g	Pore gas pressure	[Pa]
$p_{g;e}$	Atmospheric gas pressure (Pa)	[Pa]
$p_{wv;e}$	Partial water vapour pressure outside the VIP	[Pa]
t	Time	[s]
t_{get}	Time shift due to a getter	[s]
t_{des}	Time shift due to a desiccant	[s]
t_g	Time constant for gas pressure increase	[s]
t_w	Time constant for water content increase	[s]
E_a	Activation energy for permeation through the barrier envelope	[J mol^{-1}]
R	Universal gas constant	[$Jmol^{-1}K^{-1}$]
a	Regression parameter	[s $m^{-(1+c)}$]
b	Regression parameter	[mKW^{-1}]
c	Regression parameter	-
l_p	Perimeter length of VIP	[m]

s_p	Surface area of VIP	[m^2]
d_p	Thickness of panel	[$Wm^{-1}K^{-1}$]
D	Pore diameter	[m]
P	Pressure	[Pa]
L	Equivalent thickness	[m]
M	Mass of KBr pellet	[kg]
m_p	Mass fraction of sample in pellet	[%]
A	Area of pellet	[m^2]
V_{pore}	Volume of pores	[m^3g^{-1}]
V_{Bulk}	Sample bulk volume	[m^3g^{-1}]
$P_{critical}$	Critical pressure	[Pa]
C_{core}	Cost of core	[£/kg]
C_{FS}	Cost of per unit fumed silica	[£/kg]
C_{EP}	Cost of per unit expanded perlite	[£/kg]
C_{SiC}	Cost of per unit SiC	[£/kg]
C_{PF}	Cost of per unit polyester fibres	[£/kg]
m_{FS}	Mass of fumed silica	[kg]
m_{EP}	Mass of expanded perlite	[kg]
m_{SiC}	Mass of SiC	[kg]
m_{PF}	Mass of polyester fibres	[kg]
C_{ins}	Cost of insulation	[£]
$C_{A,exis}$	Annual heating cost with existing U-value	[£m^{-2} per annum]
$C_{A,imp}$	Annual heating cost with improved U-value	[£m^{-2} per annum]
C_f	Cost of fuel	[£m^{-3}]
H_V	Heating value of fuel	[Jm^{-3}]
N	Life time of insulation	[Years]
U_{avg}	Area weighted average U-value	[$Wm^{-2}K^{-1}$]
A_i	Area of a insulated building element '*i*'	[m^2]
U_i	U-value of a building element '*i*'	[$Wm^{-2}K^{-1}$]
E_A	Annual heating energy consumption	[$kWhm^{-2}$]

Greek letters

λ_{cop}	Centre of panel thermal conductivity	[$Wm^{-1}K^{-1}$]
λ_S	Solid thermal conductivity	[$Wm^{-1}K^{-1}$]
λ_R	Radiative thermal conductivity ($Wm^{-1}K^{-1}$)	[$Wm^{-1}K^{-1}$]
λ_G	Gaseous thermal conductivity	[$Wm^{-1}K^{-1}$]
ρ	Density	[kgm^{-3}]
$\lambda_{S,powder}$	Effective solid thermal conductivity of powder	[$Wm^{-1}K^{-1}$]
λ_p	Thermal conductivity of powder solid fraction	[$Wm^{-1}K^{-1}$]
ν	Poisson's ratio	-
σ	Stefan-Boltzmann constant	[$Wm^{-2}K^{-4}$]
β	Gas coefficient	-
λ_0	Thermal conductivity of air	[$Wm^{-1}K^{-1}$]
Φ	Pore size	[m]
λ_c	Core thermal conductivity	[$Wm^{-1}K^{-1}$]
φ	Relative humidity	[%]
$\lambda evac$	Thermal conductivity (in evacuated conditions)	[$Wm^{-1}K^{-1}$]
$\lambda_{free\ gas}$	Thermal conductivity of the free and still gas	[$Wm^{-1}K^{-1}$]
φ_e	Relative humidity of the air outside the VIP	[%]
λ_w	Thermal conductivity of liquid water and water vapour at equilibrium	[$Wm^{-1}K^{-1}$]
λ_{eff}	Effective thermal conductivity	[$Wm^{-1}K^{-1}$]
$\Psi_{,VIP\ edge}$	Linear thermal transmittance	[$Wm^{-1}K^{-1}$]
γ	Surface tension	[Nm^{-1}]
θ	Contact angle	[°]
τ	Transmission	[%]
$\lambda_{cop,atm}$	Centre of panel thermal conductivity at atmospheric pressure	[$Wm^{-1}K^{-1}$]
$\lambda_{cop,evacuated}$	Centre of panel thermal conductivity at evacuated pressure	[$Wm^{-1}K^{-1}$]
η	Thermal efficiency of heating system	[%]

Chapter 1

Introduction

1.1 Introduction

Rapidly increasing use of non-renewable energy resources worldwide has raised concerns over depletion of these energy resources and their environmental impact. In 2010, buildings in the European Union (EU) consumed around 40% of final energy consumption and were responsible for 36% of carbon dioxide (CO_2) emissions (Groezinger et al., 2014). Enhancing energy performance in buildings is crucial to achieve the EU goals of 20% cutback in energy use by 2020 and reduction of 88% to 91% of greenhouse gas emissions compared to 1990 in the residential and service sectors by 2050. Energy Performance of Buildings Directive 2010/31/EU require all EU countries to enhance their building regulation requirements to increase the number of nearly zero-energy buildings (European Commission, 2010). Thermal insulation of building fabric plays an important role in reducing the space heating energy consumption which accounts for 57% of primary energy demand in the EU dwellings and 52% in commercial sectors (Hall, 2010). However, meeting increasingly stringent building energy efficiency regulations require large thicknesses of conventional thermal insulation materials which reduce the internal space and may not be feasible in existing and new buildings.

Vacuum Insulation Panel (VIP) with 5-8 times higher thermal resistance is an alternative to conventional thermal insulation materials. It requires less space compared to conventional building insulation materials to achieve same resultant U-value from any building element to be insulated. Thermal conductivity of a VIP ranges from 2-8 $mWm^{-1}K^{-1}$ depending upon the materials used to manufacture therm. VIP is produced as a rigid panel made of evacuated inner core board laminated in outer high barrier envelope. Core is fabricated from porous material of suitable pore size. Its function is to maintain vacuum below a minimum critical level and physically support the VIP envelope. Heat transfer occurs through core material mainly due to conduction in the solid skeleton, gas conduction through pores and radiation (Caps and Fricke, 2000; Fricke et al., 2006; Caps et al., 2008). Lower thermal conductivity of VIP results from reduced gas conduction and convection related heat transfer through the

core material by evacuating the gas present in small size porous materials such as open porous foams, powders and fibres. Thin metal foils or multilayer metallised polymer envelopes are used to prevent the transmission of gases and water vapours into the evacuated core to enhance the service life of VIPs.

Concept of vacuum thermal insulation originated in 1892 when Sir James Dewar first used vacuum insulation in Dewar's flask to keep the gases cold enough to remain as liquid. This idea was commercially implied by Thermos GmbH in the production of vacuum flask with the name of Thermos in 1904. Since then vacuum insulation has been used in different applications where high performance thermal insulation is required. The earliest precise idea in the form of vacuum panels consisting of a load bearing material between two outer skins originated by Bovenkerk (1955) in which glass fibre kernel welded into steel foil was used as VIP. Gervais and Goumy (1979) used ultrafine silica based compact granular structure for obtaining low thermal conductivity to use it as insulating material in fields involving high and low temperatures. Young and Schreck (1984) and Nowobilski et al. (1988) used glass fibre mat as core material to develop a light weight vacuum thermal insulation panel for use in liquid nitrogen storage containers. In 1990s, the open cell polyurethane foams were also investigated as core material and for use of VIPs. These VIPs were used in different applications such as refrigeration, shipping and packaging etc. In 1998/1999 VIPs were first used for buildings applications. Buildings require different set of prerequisites from VIPs such as longer service life (more than 50 years), reasonable cost, functional and structural reliability over the useful service life under varying climatic conditions and easy handling during installation. At present VIPs lack in all of these properties to be used in buildings at large scale. Only 10% of currently produced VIPs are being used in construction industry while shipping boxes and refrigeration industry account for 30% and 60% respectively (Brunner et al., 2014). This shows that adoption of VIPs in the buildings is comparatively slow due to their high cost, uncertain service life, difficult on site handling and risk of vacuum failure. VIP handling, risk of VIP damage and size issues can be overcome by careful handling, improved quality control and design. However, high cost of VIPs is the main reason for their slow application in construction sector and can only be justified in few construction scenarios such as limited available space for insulation in buildings, economic benefit of space saving and high cost of space creation for thicker conventional insulation. Currently, high cost of VIPs is associated with the materials used in VIP production and it is of utmost importance to develop low cost materials which can be used to produce in VIPs having equal or better thermal performance.

1.2 Research objectives

The main aim of this project is to develop, characterise and experimentally evaluate the thermal performance of low cost core materials for VIPs.
The main objectives of this study are:

- Review of VIP properties and materials presently used in VIPs.
- Develop low cost core composite material for VIPs and experimentally characterise its main properties. The purpose is to identify the core material with optimal characteristics to realise high thermal performance VIPs with low cost.
- Experimentally optimise the thermal performance of core material and investigate the effect of material constituents on different modes of heat transfer occurring through VIP core material.
- Manufacture prototype VIPs using optimised low cost core material with the potential to achieve thermal performance of typical commercially available VIPs.
- Experimentally investigate the thermal performance of VIP prototypes and quantify the modes of heat transfer through core materials.
- Evaluate the cost reduction potential of optimised core material for use in VIPs and assess the energy and cost effectiveness of VIPs in building applications.

1.3 Structure of the thesis

In **Chapter 1** an introduction to the research topic of the thesis is presented along with the main aim and objectives of this research.
In **Chapter 2** a comprehensive review of existing literature on the research subject is presented.
In **Chapter 3** research materials are described along with the methods to characterise and measure different properties of VIP core materials. The results of pore size analysis carried out in this chapter led to calculate the gaseous thermal conductivity and optimisation of core material.
In **Chapter 4** experimental results of thermo-physical properties of expanded perlite-fumed silica composite material as VIP core material and the influence of presence of expanded

perlite on different properties are presented. Thermal conductivity of different core samples at atmospheric conditions is measured. Results of this chapter revealed the optimum composition of core material for use in VIPs.

In **Chapter 5** thermal conductivity of manufactured VIP prototype with optimised core material at range of pressures was measured experimentally using guarded hot plate apparatus. Results of thermal conductivity of VIP prototypes measured in this chapter and core samples in chapter 4 were used to calculate solid, gaseous and coupling conductivities of VIP core.

In **Chapter 6** material costs and thermal performance of different core samples are compared. Economic feasibility of application of VIPs in different building application scenarios are compared with conventional thermal insulation, expanded polystyrene (EPS), using simple payback period analysis. Energy efficiency potential and required thicknesses of VIPs and EPS insulation are also compared.

Finally, in **Chapter 7** the overall conclusions of the thesis and recommendations for future work are presented.

1.4 Contribution to knowledge

The main contributions of this research to knowledge are summarised as follows:

- The low cost VIP core material consisting of expanded perlite and fumed silica composite was developed and its characteristics were measured in terms of thermal and economic performance for VIP applications.

- Effect of expanded perlite on solid, gaseous, radiative and coupling conductivities in low cost VIP core material was quantified.

- The effectiveness of optimised core material in VIP application is evaluated.

Most of the work presented in this thesis has been published in two International Journal and three peer-reviewed International Conferences. These publications are listed as follows:

Journal Publications:

M. Alam, H. Singh, S. Brunner and C. Naziris. Experimental characterisation and evaluation of the thermo-physical properties of expanded perlite - fumed silica composite for effective vacuum insulation panel (VIP) core. Energy and Buildings, **2014**, 69, 442 - 450.

M. Alam, H. Singh and M.C. Limbachiya. Vacuum Insulation Panels (VIPs) for building construction industry - A review of the contemporary developments and future directions, Applied Energy, **2011**, 88, 3592 - 3602.

Conference Publications:

M. Alam and H. Singh, Methodology for thermal performance testing of Vacuum Insulation Panel (VIP). In proceedings; 11th International Vacuum Insulation Symposium (IVIS) Duebondorf, Switzerland; **2013**.

M. Alam and H. Singh, Performance analysis of expanded perlite-fumed silica composite as core material for Vacuum Insulation Panel (VIP). In proceedings; International Multiconference on Intelligent Systems, Sustainable, New and Renewable Energy Technology & Nano Technology, Haryana, India ; **2012**.

M. Alam, H. Singh and M.C. Limbachiya, Barrier performance of SiO_2 coated PET film for Vacuum Insulation Panel (VIP) envelope. In proceedings; 10th International Vacuum Insulation Symposium (IVIS) Ottawa, Canada ; **2011**.

Chapter 2

Literature Review- Vacuum Insulation Panels (VIPs)

2.1 Introduction

Buildings consume a large amount of energy which results in significant amounts of emissions worldwide. In the UK almost half of the total carbon emissions are directly related to energy consumption in buildings (DECC, 2010). In 2007, the UK government set an aim to gradually improve the energy efficiency and carbon performance of buildings to ensure all new homes to achieve zero carbon emissions from 2016 by gradually improving Part L of Building Regulations (DCLG, 2007). This carbon reduction will be realised by achieving the targets set in differ levels of Code for Sustainable Homes (CSH). CSH level 4 can be achieving by ≥19% and CSH level 5 by ≥100% improvement in Dwelling Emission Rate (DER) set in Building Regulations 2013 Part L1A ultimately improving the DER to zero net carbon emissions in 2016 achieving the CSH level 6 (DCLG, 2014). Further, the UK government also set zero carbon targets for new non domestic buildings by 2019 (DCLG, 2009). These standards are expected to assist the UK government in significantly reducing carbon dioxide (CO_2) emissions from buildings and achieving the 2050 target to reach net carbon emissions at least 80% lower than the 1990 baseline as set in the Climate Change Act 2008 (Climate Change Act, 2008). With over 60% of the energy consumed in buildings used for space heating (Palmer and Cooper, 2012), a major portion of supplied space heating energy is lost through poorly insulated building fabric leading to higher heating energy consumption. In UK average annual heating consumption levels by homes vary from 585 $kWhm^{-2}$ to 102.8 $kWhm^{-2}$ depending upon their construction year as shown in figure 2.1 (BIPE, 2011). Therefore, improving the building envelope insulation is a key to reduce the space heating energy losses of existing building stock and achieve energy efficiency targets. This reduction of heating energy consumption can be achieved by lowering the overall heat loss coefficient (U-value) of building fabric by applying insulation. U-value is the measure of the rate of heat loss through a material. Thus, building envelopes with the lowest U-values are essential to reduce space heating energy consumption.

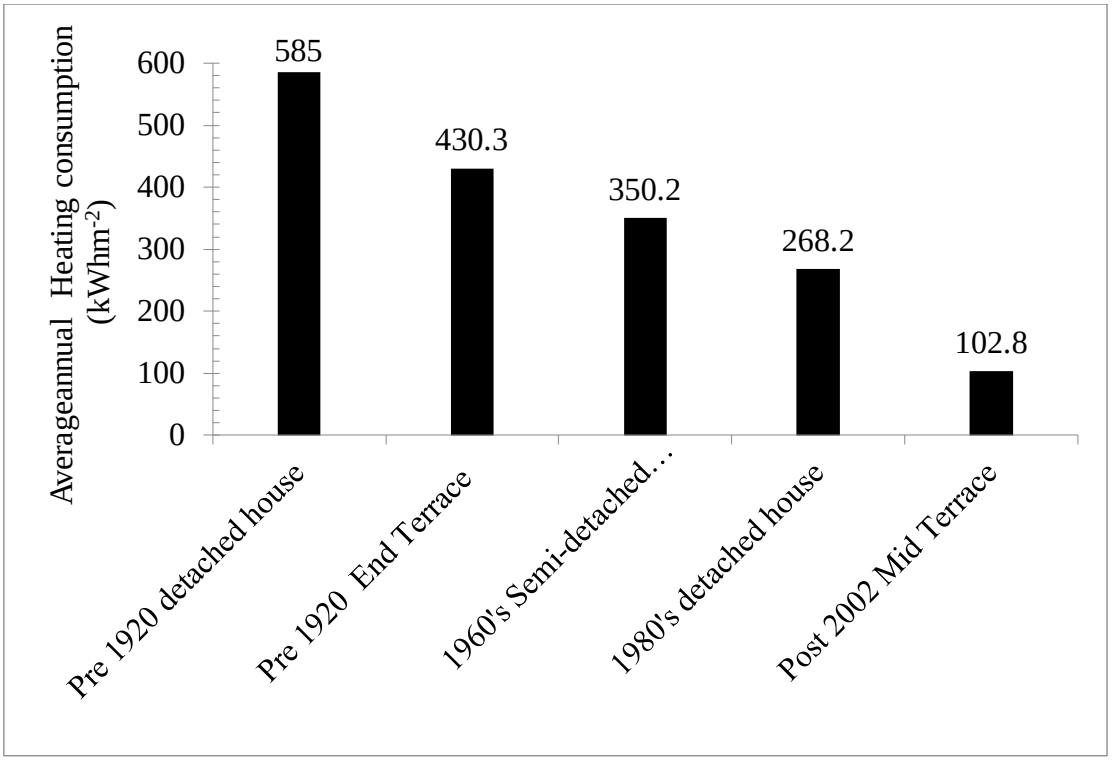

Figure 2.1 Average annual heating consumption of UK homes by their construction age (BIPE, 2011)

Conventional insulation materials such as expanded polystyrene (EPS), rock wool and glass fibre require a large thicknesses to lower the U-value of a typical masonry cavity wall of a semi-detached UK dwelling (built between 1945 and 1964) from 0.53 $Wm^{-2}K^{-1}$ to 0.20 $Wm^{-2}K^{-1}$ - 0.10 $Wm^{-2}K^{-1}$ as shown in Figure 2.2. Such large thickness of insulation may not be practicable for application in existing and new buildings due to space and technical limitations. VIPs offer thinner alternative due to their thermal resistance potentially 5-8 times higher than the conventional insulation (Brunner and Simmler, 2008; Alotaibi and Riffat, 2014). VIPs can be applied at both, external and internal surfaces, such as walls, roof, ground floor, doors, window frames, and on hot water cylinders. VIPs can also be applied on exiting historical and listed buildings (Kalnaes and Jelle, 2014; Johansson et al., 2014). However, high cost and uncertain service life are the two main challenges for VIPs in building applications. Service life of a VIP is the time period in which VIP initial thermal conductivity reaches to a critical design value. Cho et al. (2014) showed that a 40 year period life cycle cost analysis indicates that VIP could provide as much as 88.2% - 136.9% more economic benefit than conventional insulation panels and the highest cost efficiency can be achieved from 4 to 10 years in a Korean house.

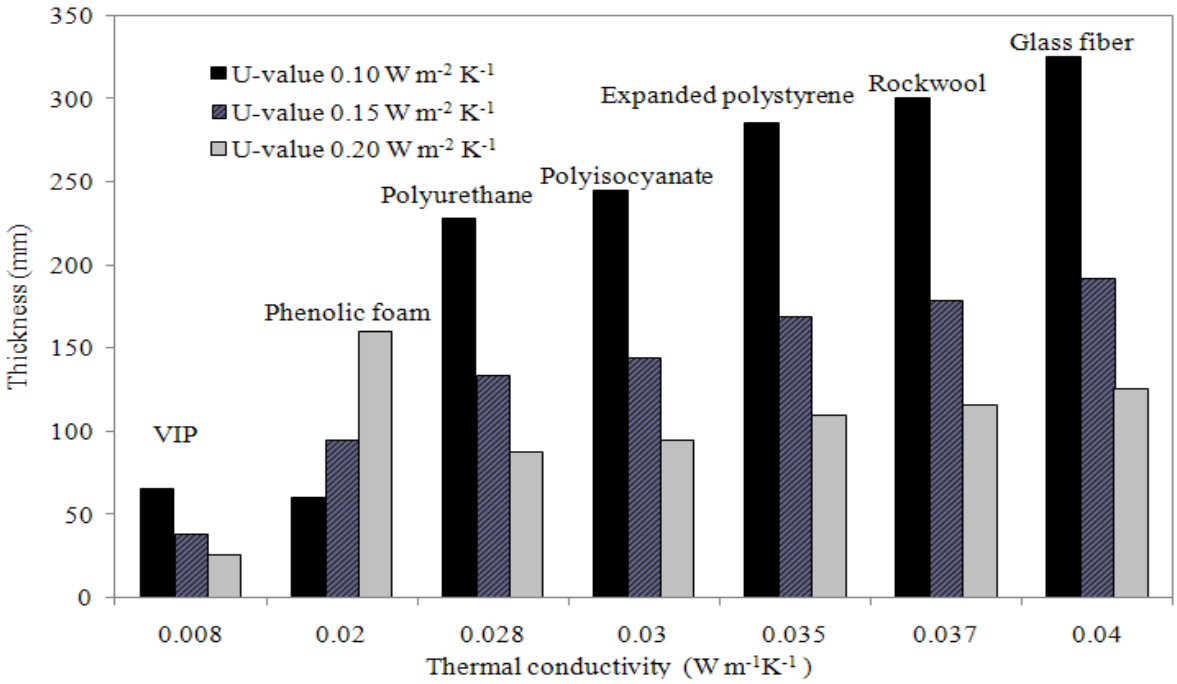

Figure 2.2 Thicknesses of different insulation materials required to achieve different U-values for a typical masonry cavity wall with a U-Value 0.53 $Wm^{-2}K^{-1}$ (Alam et al., 2011)

2.2 Vacuum Insulation Panel (VIP) - Components and materials

A VIP is a thermal insulation system consisting of an evacuated open porous material placed inside a gas barrier envelope as shown in Figure 2.3. The main components of a VIP are inner core, barrier envelope, opacifiers and getters or desiccants.

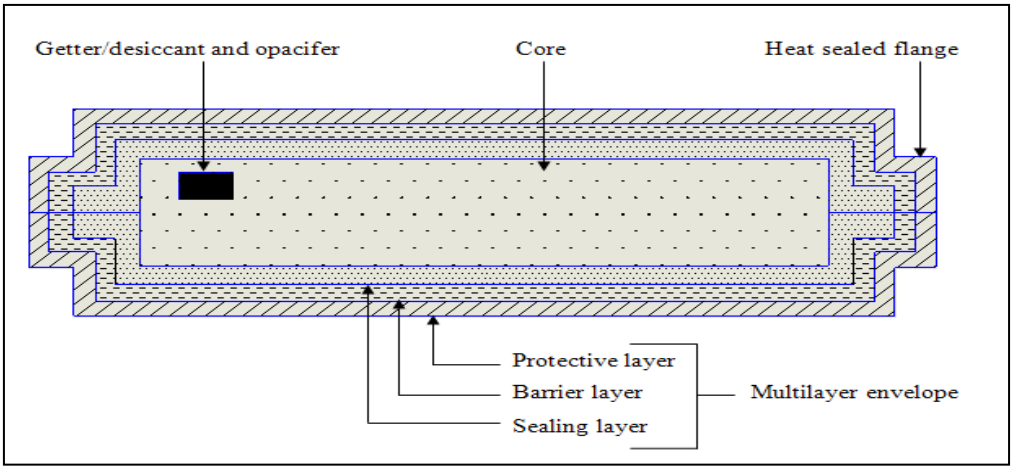

Figure 2.3 Schematic of a VIP (Alam et al., 2011)

The envelope could either consist of thick metal sheets or multilayer barrier of metalized polymeric layers to act as a barrier against the diffusion of gas and provide protection against mechanical damage to increase the durability of VIPs. Durability of VIPs can be described as its ability to withstand mechanical and environmental stresses over its design service life (>50 years for building applications) without getting physically damaged during production, transportation and installed in buildings. Any small pinhole or damage in the envelope will lead to the loss of thermal insulating ability and failure of VIP. A suitable getter or a desiccant is introduced inside the VIP core to adsorb gases and water vapours which might enter into the VIP core through envelope barrier. VIPs can be categorised as (i) sheet/foil based VIPs and (ii) polymeric film based VIPs (Tenpierik and Cauberg, 2006).

(i) **Sheet/foil based VIPs** are made with metal sheet envelope welded into one piece around the evacuated core. These VIPs demonstrate superior load bearing capacity and resistant to mechanical damage. Metal sheet envelopes offer great resistance to water vapour and gas diffusion and will be beneficial for longer service life. However, these VIP envelopes contribute a greater thermal bridging effect and will reduce the overall thermal performance of VIPs (Willems and Schild, 2005a and Willems and Schild, 2005b). Other disadvantage is their heavier weight leading to increased weight of panel. Sheet based VIPs made up of stainless steel foil were researched by Owens Corning with the name Aura® VIP shown in figure 2.4. However, these VIPs have not been used in large scale building applications due to their above mentioned draw backs.

(ii) **Polymeric film based VIPs**

Polymeric film based VIP panels are made with laminates of metallised polymeric films. These films are coated with metal oxides to improve the water vapour and gases diffusion barrier properties and have thickness in the range of 100-150µm. Contrary to sheet based VIPs, contribution of polymeric film based envelopes to thermal edge effect and weight is minimal. However, these barrier envelops provide shorter service life and are prone to damage during installation.

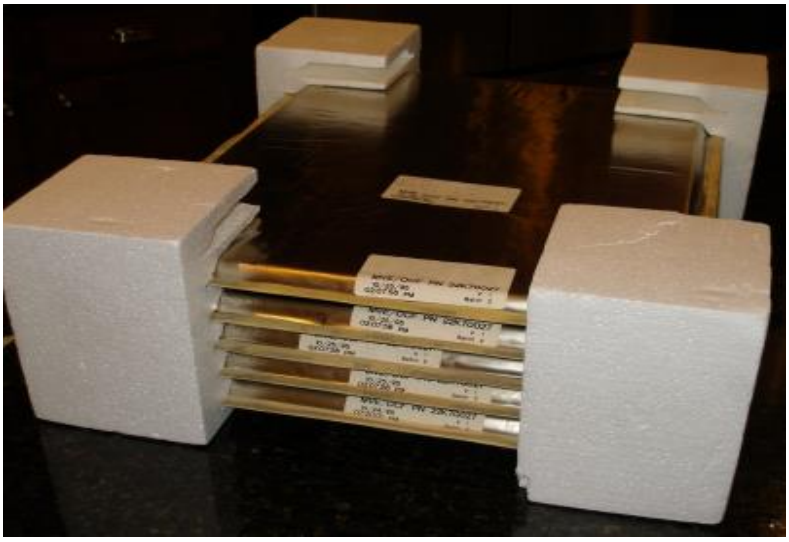

Figure 2.4 Aura® VIPs produced by Owens Corning (Rusek, 2009)

2.2.1 VIP core

Core, the internal part of a VIP as shown in Figure 2.3, is made of porous material of appropriate pore size such as open porous foams, powders and fibres. Its purpose is to physically support the VIP envelope against the atmospheric pressure after evacuation, decrease radiation heat transmission and establish small size pore spaces that are smaller or same order of size as the mean free path length of gas molecule present in pores. Gaseous heat transfer is further suppressed within the core material by evacuating the porous materials. Main research studies investigating different materials as core materials of VIP has been detailed in Table 2.1.

2.2.1.1 Foams

Foams with open cell structure and small pore sizes in the range of 30-300 μm can be used as a core in VIPs. These foams such as phenolic foam and polyurethane (PUR) have high thermal resistance at low pressure conditions owing to their low density (25-100 kgm^{-3}), high porosity and smaller pore sizes. However, it is difficult to achieve a normally accepted centre of panel thermal conductivity value of 4 $mWm^{-1}K^{-1}$ by using foams in VIP core. For foams with a mass density of 70 kgm^{-3} the radiative and solid conductivities at 300 K were reported as 2.7 $mWm^{-1}K^{-1}$ and 3-7 $mWm^{-1}K^{-1}$ respectively (Kwon et al., 2009). By adding the solid and radiative conductivity a centre of panel thermal conductivity in the range of 5.7-9.7 $mWm^{-1}K^{-1}$ can be obtained which is higher than the normally adopted centre of panel VIP thermal conductivity value of 4 $mWm^{-1}K^{-1}$. Clearly, it would be difficult to achieve such a

low thermal conductivity value using foams in VIPs even with zero gaseous conductivity. Kwon et al. (2009) calculated the overall thermal conductivity value of polyurethane foam (pore size 100 μm) as 7.8 $mWm^{-1}K^{-1}$ at 0.1 mbar. Phenolic foams required an even lower pressure of 0.01 mbar to achieve an effective thermal conductivity of 5 $mWm^{-1}K^{-1}$ due to large pore size of 260 μm (Kim et al., 2012). However, such a low pressure of <0.1 mbar is not easily preserved over the service life of the VIP, which is expected to be 50-100 years for building applications. This suggests that VIPs with foams can only be realistic for applications with shorter service life such as refrigerators, insulated boxes etc. Out gassing from foam materials is also a concern and increases core pressure which reduces their thermal performance. Pre-treatment of PUR foam by baking at 120°C temperature for 15 minutes prior to sealing in the VIP envelope reduces the out gassing rate of foam (Yang et al., 2007).

Table 2.1 Main studies investigating different core materials and their findings

Authors	**Core material**	**Main findings**
Nemanič and Žumer, (2015)	Organic Melamine-formaldehyde fibre fleece core materials for VIP	λ = 2.3 $mWm^{-1}K^{-1}$, density 250 kgm^{-3}
Nemanič et al., (2014)	Open pore melamine - formaldehyde rigid foam	λ = 6 $mWm^{-1}K^{-1}$
Li et al, (2013)	Glass fibre	λ = 2-3 $mWm^{-1}K^{-1}$
Karami et al., (2014)	Granular silica	λ = 14 $mWm^{-1}K^{-1}$at 0.1 mbar at density of 130 kgm^{-3} when granules were compressed with 1 bar pressure
Di et al., (2014)	Glass fibre chopped strand Glass wool	λ=1.5 $mWm^{-1}K^{-1}$ at inner pressure below 0.1 mbar λ = 2.8 $mWm^{-1}K^{-1}$ at inner pressure below 0.1 mbar
Kim et al., (2012)	Phenolic foam	λ = 5 $mWm^{-1}K^{-1}$ below 0.01 mbar
Tseng and Chu, (2009)	Polystyrene-Poylethylene core material with carbon black, and calcium stearate	λ = 4.4 - 9.0 $mWm^{-1}K^{-1}$ at 10^{-4} torr
Mukhopadhyaya et al., (2009)	Glass mineral oxide fibre and wood fibre with pumice and zeolite powder	Thermal conductivity comparable to precipitated silica and nanogels for a pressure below 0.1 mbar and density was in the range of 320-340 kgm^{-3}
Fricke et al., (2008)	Fumed silica kernel	λ = 4 $mWm^{-1}K^{-1}$ below 1 mbar pressure

Thermal resistance of foams can be increased by reducing the size of pores. Wong and Hung (2008) prepared open porous polystyrene foam with calcium carbonate and high density polyethylene fillers produced by the mixture of CO_2 and fluorocarbon or the mixture of CO_2 and nitrogen (N_2) as foaming agents and found their thermal conductivity comparable to that of polyurethane foams when used as a core of VIP. Nemoto et al. (2008) developed rubber blended polypropylene and polyethylene nano/microcellular foam with average cell diameter of 0.5-2 µm by CO_2 pressure quench method. Such foams with small pores are potential candidates for VIP core materials. However, foams have a potential of causing fire toxicity because of the release of dangerous emissions mainly carbon monoxide (CO) and hydrogen cyanide (HCN) (Hull and Stec, 2011).

2.2.1.2 Powders

2.2.1.2.1 Fumed silica

Powders such as fumed silica or pyrogenic silica, silica aerogels and expanded perlite are commonly used for VIP cores. Fumed silica is the most used core material for VIPs due to its low density, high specific surface area and low thermal conductivity. Fumed silica was first developed by Degussa AG (currently Evonik Industries) in Germany in 1942 by the combustion of silicon tetrachloride in an oxygen-hydrogen flame (Evonik Industries, 2006). This process yields molten particle of silicon dioxide. These particles fuse with each other to form chain-like aggregates with mean aggregate size of 0.2-0.3µm. Fumed silica has low thermal conductivity 3-6 $mWm^{-1}K^{-1}$ at a pressure in the range of 20-100 mbar (Wang et al., 2007) due to low density, high porosity, small pore size of 300 nm and a specific surface area in the range of 5 - 60 × 10^{-2} m^2kg^{-1}. However, the main drawbacks of fumed silica are its low resistance to radiative heat transfer (Caps et al., 1983) and high cost. It is comparatively expensive material and a contributing factor to the present high cost of VIPs. The cost of VIPs must be comparable with conventional insulation to increase their extensive application in the construction industry. Cost reduction potential can be achieved by substituting or reducing the quantity of fumed silica with low cost alternative materials.

2.2.1.2.2 Silica aerogels

Silica aerogels, first developed by Kistler in 1931 using sodium silicate (Kistler and Caldwell, 1934), are nano porous materials with pore size of approximately 20 nm and a density in the range of 3 to 350 kg m^{-3}. In general, aerogels are made by two steps (i) wet gel

formation by acidic condensation or sol-gel process (ii) drying of wet gel by using supercritical or ambient drying to produce silica aerogel (Potter, 2001). A low density and a smaller pore size (1-100 nm) render silica aerogel has a thermal conductivity of approximately 1-3 $mWm^{-1}K^{-1}$ in evacuated and opacified conditions depending on temperature and can even achieve a value of 4 $mWm^{-1}K^{-1}$ at 50 mbar or less making it suitable for VIP applications (Baetens et al., 2011). The advantage of silica aerogel is that it is considered as non-reactive and non-flammable. However, due to its high cost it has not been widely used in VIPs for building applications. Silica aerogels are also considered as optically transparent and leads to higher radiative conductivity. Other drawback of Silica aerogel is that it is extremely brittle and difficult to handle. This can be improved by preparing composites of silica aerogels with other mechanically stable materials. Wang et al. (2011) prepared the silica aerogel in the pores of expanded perlite to make a low cost mechanically stable composite for thermal insulation. Thermal conductivity of expanded perlite-silica aerogel composite was observed to be reduced slightly compared to pure expanded perlite.

2.2.1.2.3 Expanded Perlite

Expanded Perlite is another potential candidate as a more economically viable material for incorporation in core of a VIP in the form of composite with fumed silica. Perlite is a low cost glassy amorphous mineral rock and can be expanded on heating at temperature of 760-1100 °C (Tekin et al., 2006). It has been used for different construction applications such as lightweight cement aggregate, insulation and ceiling tiles (Sari and Karaipekli, 2008) due to its low density (35-120 kgm^{-3}), porous nature, low thermal conductivity, ease of handling and non-flammability (Perlite Institute, 1983). However, the thermal resistance of expanded perlite is rather limited; its thermal conductivity is between 45-70 $mWm^{-1}K^{-1}$ at 300K (Pfundstein et al., 2008). Due to its porous nature it is well suited for use under vacuum conditions (Perlite Institute, 1983) and has been used in cryogenic insulation systems at a temperature range of 20K-90K (Augustynowicz et al., 1999) and liquid hydrogen storage tanks (Sass et al., 2008) and can also be applied to ambient temperature applications, for example, building applications. Fricke et al. (2006) showed that at 0.1 mbar pressure, thermal conductivity values of expanded perlite are comparable to that of micro silica powders. Beikircher and Demharter (2013) measured the effective thermal conductivity of evacuated perlite powder to be 9.2 $mWm^{-1}K^{-1}$ at 0.08 mbar pressure. This measurement was carried out

with a low density of 92.4 kgm^{-3} due to self-compression only, however, for making of VIP cores, material needs to be compressed under pressure and the density of core is usually higher compared to lose powder which increases its solid conductivity and results in effective thermal conductivity higher than that of self-compressed expanded perlite. The pore size of expanded perlite is relativity large in micrometric range (approximately 3 μm) (Zhang et al., 2007) and requires a high level of vacuum (<0.01 mbar) to limit its gaseous thermal conductivity. Such a low pressure is difficult to maintain for long service life of VIP for building applications. Initial required pressure can be raised to reasonable level for expanded perlite modifying the pores of expanded perlite by filling or partially filling them with nano materials. Wang et al. (2011) made an attempt to produce low cost composite by synthesizing silica aerogel in expanded perlite pores and measured slight reduction in thermal conductivity of composite material at atmospheric pressure. Nevertheless, synthesis of silica aerogel is an expensive process and may lead to an overall high production cost.

2.2.1.3 Glass fibre

Glass fibre can also be used as the core of a VIP for buildings (Boafo et al., 2014) and high temperature applications due to its low density and high thermal stability (>1000°C) . Kwon et al. (2009) reported a radiative conductivity of 7 $mWm^{-1}K^{-1}$ and a solid conductivity of approximately 2.1 $mWm^{-1}K^{-1}$ for glass fibre with a density of 250 kgm^{-3} and a fibre diameter of 0.5-0.7 μm at 300 K. Collectively this results in an overall VIP thermal conductivity of 2.8 $mWm^{-1}K^{-1}$. However, a very low pressure of 0.01 mbar is required to suppress the gaseous thermal conductivity to a negligible level (Swimm et al., 2009). Kwon et al. (2009) also reported a theoretical total thermal conductivity value of 3.6 $mWm^{-1}K^{-1}$ for a glass fibre core at 0.1 mbar. Araki et al. (2009) investigated the performance of glass fibre based VIPs for insulating hot water cylinders. Although the glass fibre VIPs can achieve a lower initial thermal conductivity compared to fumed silica VIPs, but these are very sensitive to pressure increase due to their large pore size and moisture. Li et al. (2013) has observed that 1 mbar is the critical pressure for glass fibre core material and any rise in core pressure above this critical pressure led to an exponential rise in thermal conductivity. Glass fibre VIPs also require getters/desiccants to continuously adsorb gases which penetrate through envelope over time to reduce the increase in thermal conductivity due to increased moisture content inside the core. Di et al. (2013) found the thermal conductivity of glass fibre core VIP to be

1.5 $mWm^{-1}K^{-1}$ at 0.1 mbar pressure and estimated a maximum service life of 15 years. However, such shorter service life is not suitable for building applications.

2.2.1.4 Fibre/powder composites

Fibre-powder composites are other alternative materials which can potentially be used as core material in VIPs. Mukhopadhyaya et al. (2009) considered the use of layered composites of glass mineral oxide fibre and wood fibre with pumice and zeolite powder as an alternative low cost VIP core material. In these composites alternate layers of fibre and powder boards were placed on top of each other in order to reduce the pore size and thermal conductivity. Main drawback of such composites was their high density ranging between 320-340 kgm^{-3} compared to other core materials. Thermal conductivity of these materials was found to be comparable to precipitated silica and nanogels for a low pressure range of 0.1-1 mbar. However, upon increasing the pressure the exponential rise in thermal conductivity suggests that pore sizes were not effectively reduced by alternate layering method. This pore size reduction can be realised with developing new low cost composite materials in which large fibre pores are filled with smaller powder particles. However such composites need to be optimised in order to achieve a cost reduction potential and high thermal performance so that these can be used as an alternative low cost material in VIP cores.

2.2.2 VIP envelope

Envelope is external cover that contains the VIP core. It retains the vacuum inside the VIP core by acting as a barrier against the transmission of gases from outside and also offers mechanical strength to endure handling stresses during transportation and installation. The key requirements for the development of barrier envelope are:

i) Low permeation of water vapour transmission rate (WVTR) of 0.003-0.005 $gm^{-2}d^{-1}$ and oxygen transmission rate (OTR) of 0.001-0.002 $cm^3m^{-2}d^{-1}$
ii) Low thermal conductivity (0.15-0.30 $Wm^{-1}K^{-1}$)
iii) Flexible and mechanically stable against handling stresses
iv) Ability to be heat sealed

Thermal performance of VIP over its service life depends upon the thermo-physical properties of the core material and barrier properties of envelope. Envelopes with lower transmission rates and offering minimum thermal bridging effect are suitable for use in VIPs. Envelope materials with water vapour transmission rate (WVTR) of approximately 0.001 g

$m^{-2}d^{-1}$ and oxygen transmission rate (OTR) of $0.001cm^3m^{-2}d^{-1}$ are expected to provide a service life of approximately 30-50 years for building applications (Simmler et al., 2005). However, the range of service life of 30 to 50 years is a broad range which needs to be specified more precisely and for building applications life time of more than 50 years also needs to be considered to encourage the large scale application of VIPs in construction sector. Currently steel, aluminium foil and metallised polymeric films are used as barrier envelope to avoid the rise of internal pressure and the accumulation of moisture in the core material (Simmler et al., 2005 and Fricke et al., 2006). These are able to ensure a service life of longer than 50 years due to virtually non-permeable nature of metallic foils. A typical VIP envelope with three metalized films was reported to have a WVTR and an OTR of 0.003-0.005 $gm^{-2}d^{-1}$ and 0.001-0.002 $cm^3m^{-2}d^{-1}$ respectively at 23°C and 50% RH (Simmler et al., 2005). For a two-layered metallised envelope panel predicted useful life time is 16 to 38 years depending upon panel size and climatic conditions (Schwab et al., 2005). Clearly, envelopes which offer higher barrier properties and a minimum thermal bridging effect are required to attain low effective thermal conductivity and a long service life of VIP (>50 years) for building applications. Aluminium foil envelope provides higher barrier properties compared to a metallised polymeric envelope. However, the main drawback of aluminium foil envelope is its higher thermal bridging effect (linear thermal transmittance 70 $mWm^{-1}K^{-1}$) compared to metalized film envelope (linear thermal transmittance 10 $Wm^{-1}K^{-1}$) due to its higher thermal conductivity (Simmler and Brunner, 2005). Therefore, for VIP applications envelopes made from materials which are thermally less conducting and offering superior barrier against gases are preferred.

Unfortunately, the metallic layers contain a high density of defects (mainly pinholes) (Jung, 2013). Because of this defect distribution, barrier performance to atmospheric gases is not as good as laminated aluminium foils. This effect is reduced by the superposition of several metalized layers, so that the path length and tortuosity are increased for the permeant molecules. However, multilayer laminate requires a layer of polyurethane as an adhesive in between the metalized layers which is the softest layer and subject to a hydrolytic degradation with time and loosens the polymer network and forms oligomers in the envelope and hence prone to degradation (Brunner and Simmler, 2008). Other disadvantage of multilayer laminate is the presence of multilayer of polyethylene terephthalate (PET) which leads to accumulative large thickness and has complex influence on heat sealing of envelope (Marouani, 2012).

2.2.1 Structure of envelope

A typical VIP envelope comprises of three thin layers; (i) outer protective layer (ii) barrier layer and (iii) inner sealing layer, each serving a different purpose, as shown in figure 2.5. A detailed cross section of multilayer envelope is shown in Figure 3 where three aluminised PET films and a high density polyethylene (HDPE) or low density polyethylene (LDPE) are joined together to produce an envelope by using a suitable adhesive such as polyurethane.

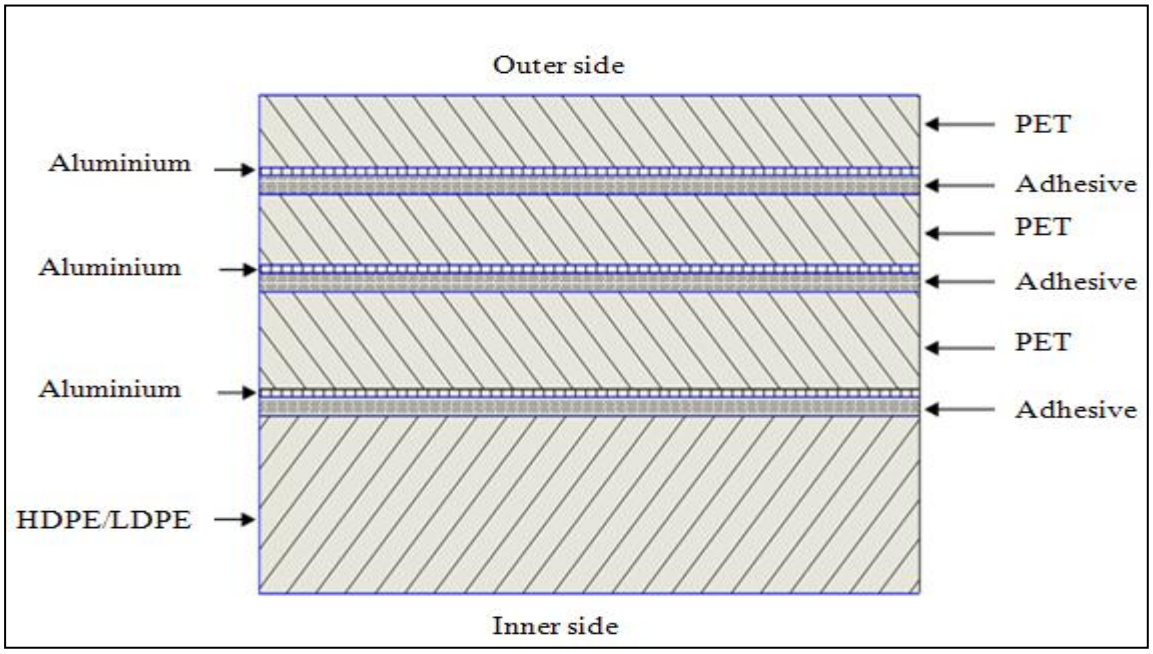

Figure 2.5 A cross section of typical multilayer barrier envelope containing metalized barrier layers (Alam et al., 2011)

Kwon et al. (2010) and Jung et al. (2014) suggested a double envelope with an additional porous core material sandwiched between the inner envelope and outer envelope to reduce the gas permeation through the envelope as shown in Figure 2.6. This method may provide an additional protection against the transmission of gases and leads to longer service lifetime compared to single Al-metallized film envelop and may be suitable for core materials which are susceptible to increase in pressure such as glass fibres. However, such additional envelope and core material may increase the thickness and cost of VIP and any increase in pressure in outer core will also contribute towards degradation of VIP performance. Thus, efforts should be focused on to developing and using high barrier materials in single envelope

to keep the thickness and cost at minimum. Jung et al. (2014) proposed the aluminium foil envelope with another layer of aluminium foil bonded to the VIP metallised envelope except at the edges and found that this method of double enveloping decreased the permeation of gases virtually to zero through the aluminium foil bonded region without increasing the heat conduction at edges. However, in this method edges still have higher permeation rates compared to aluminium foil boded region and could act as weak spot for gas permeation leading to overall higher pressure inside the VIP.

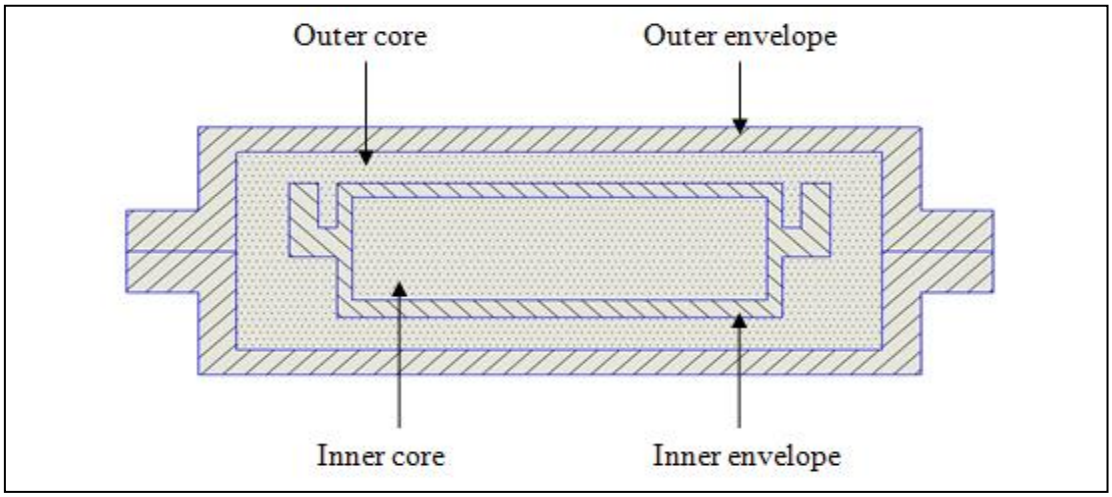

Figure 2.6 Schematic of a double envelope VIP (Alam et al., 2011)

2.2.1.1 Protective Layer

It is the outer most layer of the envelope as shown in Figure 2.3, which protects the VIP from environmental and handling stresses and also acts as a substrate for barrier layer. Different polymers such as PET, polypropylene (PP), polyethylene (PE) can be used for this purpose. Barrier properties of these three polymer films of 13 µm thickness at 20 °C and 50% R.H have been compared in table 2.2. It has been found that PP and PE have poor barrier properties against oxygen and have better barrier properties water vapour transmission compared to that of PET. Currently, PET is used as protective layer due to its low cost and better barrier properties. Use of other materials for envelope is being investigated, for example Araki et al. (2009) investigated Polyamide (Nylon 6) as a protective layer in VIP envelope for high temperature application such as heat pumps and water storage tanks due to its high melting point (225°C). A drawback of Nylon 6 is its high cost. However, barrier

properties of protective layer alone are not sufficient to fulfil the key prerequisite of low permeation of water vapours and gases for VIP envelope.

Table 2.2 Comparison of oxygen and water vapour transmission rates of PET, PP and LDPE [NORNER Industrial Polymer Institute]

Substrate	Thickness (µm)	OTR ($cm^3m^{-2}d^{-1}$)	WVTR ($gm^{-2}d^{-1}$)
PET	13	47.6	7.16
PP	13	725.9	1.62
LDPE	13	3215.0	3.29

2.2.1.2 Barrier Layer

The middle layer (Figure 2.3) which acts as a barrier against air and water vapour transmission consists of coating layer of inorganic material on the polymer substrate such as metal or silica oxide. This coating improves the barrier properties by one or two orders of magnitude. The mass transmission occurs through a defect free polymer and coated polymer film by Fick's diffusion and through pinholes, grain boundaries and micro-cracks (Alam et al., 2011 and Bouquerel et al., 2012). The permeation rate through the defects free areas is negligible. However, pin hole and micro-defects are much more effective paths through the coating layer for gas permeation. Thin metal oxides such as Silicon oxide (SiO_2) and Aluminium oxide (Al_2O_3) coatings on PET are predominately studied coatings owing to their excellent barrier properties and transparency. Other transparent thin oxide barrier coatings include Titanium oxide (TiO_2), Zinc oxide (ZnO), Zinc tin oxide ($ZnSn_xO_y$) and Indium tin oxide (ITO) have also been used as barrier in various application such as food packaging, flat panel displays, organic light emitting diodes and organic solar cells. However, the use of these coatings for VIP envelope application has not been proposed. Oxygen and water vapour transmission rates of these coatings along with substrate thickness and coating thicknesses are shown in table 2.3.

Table 2.3 Oxygen and water vapour transmission rates along with coating thickness of various oxides

Substrate	Thickness (µm)	Coating	Thickness (nm)	OTR ($cm^3m^{-2}d^{-1}$)	WVTR ($gm^{-2}d^{-1}$)
PET[(1)]	75	Al_2O_3	280	0.08	0.03
PET[(2)]	12	AlO_x	14	2.54	0.99
PET[(3)]	13	SiO_2	170	0.03	7.86
PET[(1)]	75	SiO_2	240	0.14	0.15
PET[(1)]	75	TiO_2	340	0.55	0.3
PET[(1)]	75	ZnO	100	0.13	0.05
PET[(1)]	75	$ZnSn_xO_y$	310	0.05	0.01
PET[(2)]	12	ITO	37	0.78	0.10

[(1)] Fahlteich et al., (2011) [(2)] Henry et al., (2001) [(3)] Alam et al., (2011)

From all of these coatings Al_2O_3 and ZnO oxide have advantage of good barrier properties and low cost. In order to increase the barrier properties, the number and size of the micro-defects should be minimized. The number of barrier layers in a VIP envelope can vary from one to three; though a three layer structure is widely used due to its better barrier properties against air and water vapour transmission. Currently PP and PET are being used as substrates. Araki et al. (2009) investigated the use of multilayer laminate of ethylene vinyl alcohol copolymer (EVOH) and metallised layer of PET with Nylon 6 and HDPE in VIP envelope and found that WVTR and OTR index for this type of envelope were high as compared to the envelope with aluminium foil. Teniers (2009) reported the better barrier properties of metalized layer of EVOH. However, due to the presence of high thermal conductivity metal in such barrier layers the thermal bridging effect on edges of VIP becomes dominant. Thermal bridging effect can be reduced by replacing the metalized barrier layer with silicon oxides (SiO_x) and silicon nitride (SiN_x) coatings. Barrier properties and mechanical properties of these materials are comparable to the metalized barrier layer (Lange and Wyser, 2003; Amrerg-Schwab et al., 1998; Howells et al., 2008; Wolf et al., 2007; Yun-Jin et al., 2008 and Lim et al., 2010). Miesbauer et al. (2014) developed a novel barrier envelope films for VIPs by depositing a hybrid polymer material ORMOCER®, aluminium and aluminium oxide layers on PET substrate for achieving lower gas permeation rates. OTR of this multilayer film

has found to be lower than the limit of measurement (5×10^{-14} $m^3m^{-2}day^{-1}Pa^{-1}$) of Mocon OX-TRAN equipment.

2.2.1.3 Sealing Layer

In an envelope formation process two laminates are joined together by sealing layer which is the inner most layers in a multi-layered VIP envelope (Figure 2.3). Seam area represents the weakest point of the envelope through which gases can penetrate to the core and degrade the vacuum inside the core. Therefore, seals with maximum strength are required for VIP envelope to perform its function over longer time period. Heat sealing is a commonly used process to join the laminates. In sealing process the laminates surfaces are sandwiched between two hot bars and pressure is applied to create a fusion bonding (inter-diffusion of macromolecular chains of two polymer surfaces) between two polymer layers of laminate. The heat sealing parameters such as the temperature and time play an important role for achieving strong seal (Malsen et al., 2008 and Marouani, 2012). Conventionally LDPE and HDPE thicknesses between 50-70 µm have been used in VIPs as a sealing layer (Brunner et al., 2006)]. Marouani (2012) identified temperature of 140°C and time of 5 seconds for three layer metalized PET with LDPE as a sealing layer to achieve the maximum peel strength. Araki et al. (2009) reported the use of other materials such as polybutylene (PBT) and high retort-cast polypropylene (HR-CPP) as sealing layers for high temperature applications. Malsene et al. (2008) experimentally found no significant difference between the seal strength of LDPE and HDPE. Hence it is better to use a material which has lower air and water vapour permeability and at the same time provide better seal strength.

2.2.3 Getters and desiccants

Getters and desiccants are integrated inside the core material to extend the useful life time of a VIP by continuously adsorbing water vapours (desiccants) and gases (getters) which may penetrate into it over its useful life time through either permeation from the outside environment or via out gassing of core and envelope materials or both. In the case of silica core VIPs, core itself acts as a desiccant but for other core materials a small amount of silica gel desiccant is required. For adsorbing residual gases in VIP core chemical getters are effective to maintain the pressure below the minimum required for long time and improve the life span of VIPs. Permeated or out gassed gases are combined chemically or by adsorption on the surface of getters leading to removal of gases from the evacuated systems.

Performance of getters depends upon their sorption capacity. Fumed silica core VIPs does not usually contain getters due to their already longer service life. However for glass fibre VIPs, getters are usually adopted to increase their short life span. Araki et al. (2009) used synthetic zeolite getters to adsorb gases for a glass fibre core. Di et al. (2014) investigated the use of a novel low cost adsorbent made up of modified calcium oxide (CaO) and copper oxide (CuO) for use in glass fibre core of VIPs and predicted the slower increase in pressure leading to service life of 10-15 years.

2.2.4 Opacifiers

Opacifiers are used to reduce the radiative conductivity of the core material by making it opaque to infrared radiation. Silicon carbide (SiC) is the most commonly used opacifier in fumed silica core. Other opacifiers such as carbon black, titanium dioxide (TiO_2) and iron oxide (Fe_3O_4) are also being used. Caps and Fricke (2000) reported that at room temperature thermal conductivity of pure silica is higher by 2-3 $mWm^{-1}K^{-1}$ than that of SiC opacified precipitated silica. Nonetheless, caution has to be exercised when using opacifiers as these typically have high solid thermal conductivity which means higher content of opacifier will lead to a higher solid thermal conductivity offsetting any benefit it provides by reducing the radiative conductivity; On the other hand, an insufficient amount of opacifier in a VIP core will lead to a higher radiative conductivity. Hence, an optimum mass proportion of a given opacifier needs to be identified to achieve a minimum radiative conductivity in VIP cores.

2.3 Manufacturing of VIPs

VIPs are manufactured by placing the core material inside the VIP envelop and heat sealing in evacuated conditions. This is a semi-automated process which involves steps described in sections 2.3.1-2.3.3.

2.3.1 Preparation of core material

Core materials powder or fibres are prepared and dried at suitable temperature to remove the moisture. This dried core material is then pressed into core boards. The pressure requires for making core board is varied for different materials. Abe et al. (2005) reported the use of pressure between 0.6-1.5 MPa to obtain the fumed silica and fibre composite boards with

sufficient handling strength. For fumed silica based core a polymeric fleece is used to cover the core to avoid the contamination of sealing portion of envelope.

2.3.2 Preparation of envelope

Envelope is made of two or three layers of metallised polymeric films joined together with suitable adhesive in the form of laminates. Two laminates are heat sealed together from two or three sides to make an envelope which is open from one side.

2.3.3 Insertion of the core and vacuum sealing

Core is inserted into the envelope through the open end and placed in the vacuum sealing chamber. Chamber is evacuated to the required pressure and then open end of the envelope is sealed. Heat sealing of the envelope could either be a three sided seal or a four sided seal. Three sided seal has the advantage of reduced gas permeation through the seal flanges compared to four-sided seal (Kwon et al., 2010).

2.4 Heat transfer theory in a VIP core

Main modes of heat transfer through a VIP core are solid conduction, radiation and gaseous conduction. All these modes of heat transfer can be added together by assuming a simplistic approach of thermal resistance in parallel connection supposing that all the modes of heat transfer take place independently and centre of panel thermal conductivity of a VIP (λ_{cop}) core can be quantified as equation (2.1) (Fricke 1993)

$$\lambda_{cop} = \lambda_S + \lambda_R + \lambda_G + k_c \quad (2.1)$$

where

λ_S is the solid thermal conductivity ($Wm^{-1}K^{-1}$)

λ_R is the radiative thermal conductivity ($Wm^{-1}K^{-1}$)

λ_G is the gaseous thermal conductivity ($Wm^{-1}K^{-1}$)

k_c is the thermal conductivity due to the coupling effect ($Wm^{-1}K^{-1}$)

Centre of panel thermal conductivity (λ_{cop}) of VIP core can be lowered by decreasing the thermal conductivity terms shown in the right hand side of equation (1) to minimum and is expected to be in the range of 4-5 $mWm^{-1}K^{-1}$ (Fricke, 1993). In equation (1) k_c represents coupling effect which is a result of complex interaction of other modes of heat exchange.

This becomes evident at higher pressures for powders and fibre materials with large size pores.

2.4.1 Solid conduction

Solid conduction takes place through the structure of core material and heat is transferred via the physical contact of the particles of the core material. Solid conduction is the dominant mode of heat transfer under evacuated conditions in the core material. Solid conductivity of a porous solid is usually much smaller than the thermal conductivity of pure solid fraction. Its magnitude depends upon material, density and pressure exerted on the core material. In case of powders, heat transfer occurs through small contact area between adjacent particles which reduces the heat transfer rate. Furthermore, the additional resistances due to tortuous nature of heat path also reduce the effective heat conduction through its solid structure. The following correlation (2.2) was proposed for the variation of solid conductivity with density of the core material (Fricke, 1993).

$$\lambda_S \approx \rho^{\alpha} \tag{2.2}$$

where ρ is density (kgm^{-3}) and the index α has an approximate value of 1 for foams and ranges from 1 to 2 for powders materials depending upon the material structure. It is clear from equation (2.2) that the materials with lower bulk densities will have a smaller solid conductivity values due to the decrease in volume ratio between solid fraction and pores. Typical approximate values of λ_S for fibres range from 1-3 $mWm^{-1}K^{-1}$, for powders 3-10 $mWm^{-1}K^{-1}$ and for foams 5 $mWm^{-1}K^{-1}$ (Fricke et al., 2006). In case of powder materials, it is very difficult to theoretically calculate exact solid conduction in porous powder due to the uneven particle size and arrangement in random manner. Kwon et al. (2009) presented two models for theoretically calculating the solid conductivity of using Hertz contact theory. The first model equation (2.3) assumed that the powder particles are loosely arranged in simple cubic arrangement with the second assuming them to be in a hexagonal packed arrangement (equation (2.4)).

$$\lambda_{S,powder} = \lambda_p(3(1-\nu^2)P_{atm}/E)^{1/3} \tag{2.3}$$

$$\lambda_{S,powder} = \lambda_p(96(1-\nu^2)P_{atm}/E)^{1/3} \tag{2.4}$$

where

$\lambda_{S,powder}$ is the powder effective solid thermal conductivity ($Wm^{-1}K^{-1}$)

λ_p is the thermal conductivity of powder solid fraction ($Wm^{-1}K^{-1}$)

ν is the Poisson's ratio i.e. the ratio of the relative contraction strain (or transverse strain) normal to the applied load - to the relative extension strain (or axial strain) in the direction of the applied load

P_{atm} is the atmospheric pressure exerting on the powder particle (Pa)

E is the Young's Modulus (Pa)

Results for fumed silica powder were found to be 4 to 12 times higher compared to reported value of 3 $mWm^{-1}K^{-1}$ (Kwon et al., 2009). This anomaly was thought to be caused by higher effective porosity due to uneven and random arrangement of particles. This discrepancy can be higher in the case of composite mixture of powders with particles of different sizes. This suggests that reliable experimental data for different powder materials is required to measure their accurate solid conductivity.

2.4.2 Radiation

Heat transfer in the form of long wave radiation is a significant mode of transferring heat in vacuum conditions. Radiative heat transfer in porous insulation is reduced by scattering and absorption by adding opacifier to the core material and values below 1 $mWm^{-1}K^{-1}$ can be achieved with adding suitable opacifier (Bouquerel et al., 2012). Diffusion approximation approach is commonly used to the case of optically thick medium and hence applicable for calculating the temperature dependent radiative conductivity of a porous insulation material. It can be calculated by using equation (2.5) (Fricke, 1993) which is analogous to Fourier law of heat conduction.

$$\lambda_R = 16n^2\sigma T_r^3/3E_c(T_r) \quad (2.5)$$

where

n is the mean index of refraction

σ is the Stefan-Boltzmann constant (5.67×10^{-8} $Wm^{-2}K^{-4}$)

E_c is the extinction coefficient of the insulating material (m^{-1})

T_r is the average temperature within the insulation material (K) and can be calculated as

$$T_r = \sqrt[3]{\frac{1}{4}(T_1^2 + T_2^2)(T_1 + T_2)}$$

where T_1 and T_2 are the temperature of VIP surfaces.

Extinction coefficient can be calculated by multiplying the specific extinction (e^*) and density (ρ) of specimen. e^* can be calculated using the measured transmission values which can be obtained by Fourier Transform Infrared spectroscopy (FTIR). FTIR analysis for loose powder can be employed by two methods:

i) Kuhn et al. (1993) described a method in which layer of loose powders were spread onto supporting layer of polyethylene (PE) or Potassium bromide (KBr) and placed in horizontal plane instead of mixing sample powder with KBr to avoid the change in scattering behaviour. A complex arrangement of mirrors for redirecting the IR beam on horizontal plane was employed. However, this method involves the supporting layer (PE) or (KBr). The PE supporting layer has a transmission between 85-90% and hence there is a chance of error of 10-15% in the transmission and it is difficult to prepare stable layer of 0.3 mm thick KBr. Other error could arise from exteranl optical device which was used to redirect the IR beam on a horizonal sample because of the imprefections of mirrors, attenuation of IR due to passing through the atmosphere and energy losses due to IR divergence. The uniform distribution of powder layer on the support layer is also a challenge and depends upon the powder dispersion methods.

ii) Wei et al. (2013) used the KBr method by mixing the small amount of silica aerogel powder sample with KBr powder and then pressed into discs. The effect of KBr on infrared light scattering losses was accounted by subtracting a background measurement of pure KBr disc.

2.4.3 Gaseous thermal conduction

In porous solids heat transfer also occurs through the gas molecules present in pores. Gaseous thermal conductivity of a porous medium depends upon the number of gas molecules (the internal pressure) as well as the size of the pores. If a gas is present in a pore which is in the same order of size as a mean free path (an average distance a gas molecule travels before it collide with another molecule) of the gas molecule then all collisions occur between the gas

molecules and pore walls are highly elastic and no transfer of energy occurs. This leads to reduction in gaseous thermal conductivity. Ratio of molecular mean free path length (l) to the pore size diameter (Φ) is described as the Knudsen number as shown in equation (2.6) (Simmler et al., 2005).

$$K_n = l/\Phi = k_B T/\sqrt{2}\ \pi\ d^2 P\Phi \quad (2.6)$$

where

k_B is the Boltzmann constant (1.3807×10^{-23} JK^{-1})

T is the temperature (K)

d is the diameter of gas molecule (m)

P is the gas pressure (Pa)

At low pressures the Knudsen number becomes much higher than 1 that means the mean free path is larger than the pore size and all the molecules collide elastically with pores walls and no energy is transferred leading to lower gaseous thermal conductivity. However, as the gas pressure increases the mean free path reduces due to larger number of molecules are available for collision and mean free path starts to reduce which leads to more collision between gas molecules and increase in gaseous thermal conductivity. At higher pressure when Knudsen number becomes much smaller than 1 the mean free path becomes very small and gas molecules are freely colliding with each other and leading to higher gaseous thermal conductivity. Kaganer (1969) proposed the following correlation equation (2.7) to estimate the gas conductivity, λ_G, as a function of Knudsen Number.

$$\lambda_G = \lambda_0 /(1 + 2\beta K_n) \quad (2.7)$$

where

λ_0 is the thermal conductivity of free gas ($Wm^{-1}K^{-1}$)

β is the gas coefficient

Kwon et al. (2009) employed the following correlation, equation (2.8), to estimate the gaseous thermal conductivity of air at 25 °C using ß = 0.016/P.

$$\lambda_G = \lambda_0/(1 + 0.032/P\Phi) \quad (2.8)$$

By using equation (2.8) the calculated values of gaseous thermal conductivity of air for different pore sizes are shown as a function of pressure in figure 2.7. It can be seen that materials with smaller pore size range 100-300 nm have negligible gaseous thermal conductivity at low pressures of 10 mbar. On the other hand, materials with larger pore size require a further low pressure of 0.1 to 0.01 mbar to yield low gaseous thermal conductivity.

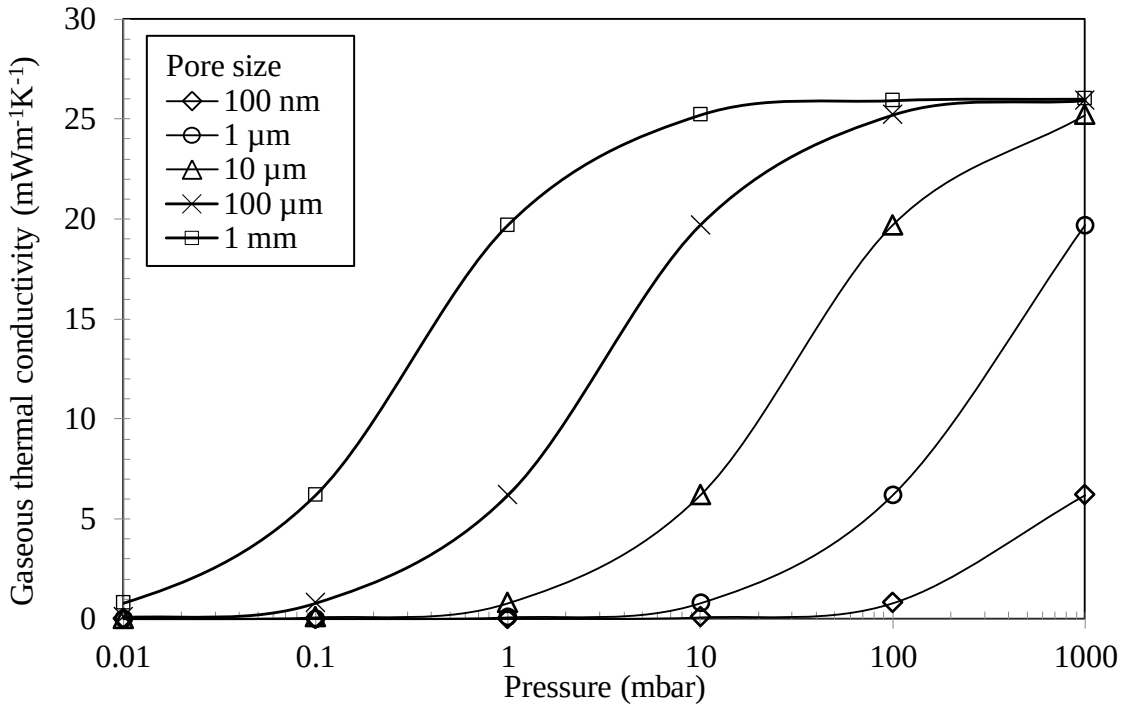

Figure 2.7 Dependence of gaseous thermal conductivity on pore diameter as a function of gas pressure

It is clear from figure 2.7 that with increasing pore size comparatively much lower pressure is required to suppress gaseous thermal conductivity. Therefore, materials with smaller pores, especially the nano pore materials, are ideal for use in VIP core to yield minimum thermal conductivity.

2.4.4 Coupling effect

The coupling effect (k_c) arises due to a short circuit for the heat flow from one particle to the other through the gas present in the pores. k_c is negligible for foams with non-broken structure and can be significant at high gas pressures due to the presence of large number of molecules in voids. However, at low pressure this term can be negligible. For powder materials such as perlite and diatomite the values of coupling effect can range between 20 - 30 $mWm^{-1}K^{-1}$ at atmospheric pressure (Fricke et al., 2006). This effect cannot be distinctly

separated from the other mode of heat transfer and cannot be measured directly. The semi-empirical approximate models presented by Swimm et al. (2009) and Beikiricher and Demharter (2013) for aerogels and expanded perlite respectively are limited to the interaction of gas and solid conduction. Beikiricher and Demharter (2013) measured the sum of coupling and gaseous conductivity to be 43.9 $mWm^{-1}K^{-1}$ at atmospheric pressure and coupling effect at a pressure of 0.08 mbar was estimated to be 0.03 $mWm^{-1}K^{-1}$ for expanded perlite powder. The coupling effect at specific pressure can also be calculated by measuring the thermal conductivity of panel both at atmospheric condition and under evacuated conditions provided the gaseous conductivity at atmospheric and vacuum states is known.

2.5 Measurement of basic properties of VIPs

2.5.1 Pressure measurement

Gas pressure rise inside a VIP core is an important factor to predict its service life. Pressure increase can be due to addition of gases from one or more of these sources (i) residual gases present inside VIP after manufacturing (ii) out gassing of materials present in envelope and core and (iii) permeation through barrier envelope and seal flange (Simmler et al., 2005 and Baetens et al., 2010). Pressure measurement in a VIP is a challenging process as the core is sealed inside an outer envelope. The following techniques (sections 2.5.1.1-2.5.1.2) are employed to measure pressure inside a VIP.

2.5.1.1 Spin router gauge method

In spin router gauge method a stainless steel tube is attached to the VIP with a steel ball suspended in magnetic field and made to spin at a specific speed. Due to pressure of gas inside the tube it reduces the spinning speed of ball and this deceleration is used to measure the relative pressure inside the panel (Caps et al., 2008). However, attaching the tube to the panel has the propensity of facilitating leakage in the panel

2.5.1.2 Foil lift off method

Foil lift off method is based on the pressure equilibrium between inside and outside the panel. Pressure around the vacuum panel is gradually decreased and when it reaches the value of slightly lesser then inside the panel, the envelope of VIP start detaching from the core. This detachment distance is measured and used to calculate the critical pressure inside the panel at which the envelope of a VIP begins detaching (Simmler et al., 2005 and Caps et al., 2008).

This method can only be used on individual panels in uninstalled conditions and is limited to the VIPs with flexible envelope. VIP envelope does not lift off uniformly and forms a curvature and hence distance at edges will be not the same as in centre and to overcome this problem an average of few points is required.

2.5.1.3 Radio frequency identification technique (RFID)

RFID method is suitable for installed VIPs. A chip based RFID tag is placed inside each panel and data is retrieved by a remotely located data acquisition system by identifying radio waves emitted by RFID tag. Some of the tags require internal power source and are called as active tags and some take power from the reader and called as passive tags. By using this method pressure can be measured without any physical contact with the panel. If the pressure inside the panel exceeds a certain value (e.g. 600 mbar for fumed silica core) the switch disconnects the signal from the tag and the reader cannot detect any signal (Caps et al., 2008 and Caps and Beyrichen, 2005). This is a fast method for measuring pressure inside the VIP and can be applied to large number of VIPs. However, this device can only work if the panel is made of thin metallised foils as thick metal foils obstruct the signals from the tag.

2.5.1.4 Thermal measurement of gas pressure

This method is based on the measurement of thermal conductivity of thin fibre sensor fleece disk located under VIP envelope on a metal plate. Thermal conductivity of fleece disk is obtained by measuring the heat flux and temperature difference between the metal plate under the disk and measurement sensor over the envelope. A relationship of this thermal conductivity with a known pressure samples is developed to predict the gas pressure of VIP samples (Caps et al., 2008 and Caps and Beyrichen, 2005).

2.5.2 WVTR measurement

WVTR through the barrier envelope of a VIP can be measured by using gravimetric method in which specimen is sealed to the open side of a test dish containing a desiccant or an aqueous saturated salt solution. This assembly is placed in a controlled atmosphere and weighed periodically to establish a water vapour transmission rate (BS EN 12086:1997). Another method, electrolytic method uses a carrier gas flowing underneath the sample foil and carries away the permeated moisture in a measurement cell where the electrolysis of phosphorous penta oxide (P_2O_5) coated on electrodes occurs. The amount of electrolyte

current generated is used to measure WVTR. Mocon test can also be used to measure the water vapour transmission rate of films but its detection limit for water vapours is limited to 0.005 $gm^{-2}d^{-1}$ (Howells et al., 2008). Calcium test is another method available to measure the WVTR of films in the range of 10^{-1} - 10^{-5} $gm^{-2}d^{-1}$ and can be used for measuring WVTR of VIP envelope (Simmler et al., 2005).

2.5.3 Thermal conductivity measurement

Heat flow meter and guarded hot plate apparatus methods are used to determine the thermal resistance of building elements and insulation materials. Centre of panel thermal conductivity of VIP can be determined by using either of these methods described in BS EN 12667:2001. The heat flow meter is an assembly that measures the heat flux through the sample while between both sides of sample are at different temperatures. Heat flow meter apparatus generally consist of a heating and cooling unit, heat flux sensors and temperature sensors. Heat flow meter is a quick method of measuring thermal resistance or thermal conductivity; however it is limited in its requirement of a calibration factor to be included for measuring the thermal resistance of specimen, which is not needed in the case of the guarded hot plate apparatus. In a guarded hot plate apparatus the heat flow rate is obtained from the measurement of the power input to the heating unit in the metering area. Guarded hot plate apparatus is generally considered as main absolute method for measuring the thermal transmission properties of insulation materials. Guarded hot plate method is slow, expensive and requires auxiliary guard section and edge insulation around the specimen to avoid any heat transfer from the edges.

2.6 VIP aging

2.6.1 Service life estimation of VIP

Service life of a VIP is the period in which VIP thermal conductivity (i.e. centre of panel thermal conductivity) increases over a threshold value (ASTM C1484, 2001 and Tenpierik et al., 2007). The rise in thermal conductivity with time depends upon initial pressure and moisture content of the core material, the barrier properties of envelope for gas and water vapour and environmental conditions such as temperature and relative humidity. Slow permeation of gases and water vapours over time through the VIP envelope leads to increase in pressure and moisture content inside VIPs. This increase in pressure and moisture content

in core material causes the change in thermal conductivity. This change in thermal conductivity over time is used to estimate the service life of a VIP.

Simmler and Brunner (2005) calculated the change in thermal conductivity for a VIP with silica core and metalized envelope for environmental conditions of 23ºC and 50% relative humidity using equation (2.9) to be approximately 0.1 $mWm^{-1}K^{-1}a^{-1}$ and recommended the preliminary thermal design values of centre of panel thermal conductivity for silica VIPs to be 6 $mWm^{-1}K^{-1}$ for aluminium foil envelope and 8 $mWm^{-1}K^{-1}$ for metalized polymeric envelope for 20 mm thick and 250 mm wide VIP.

$$\frac{\partial \lambda_c}{\partial t} = \frac{\partial \lambda_c}{\partial P}\frac{\partial P}{\partial t}(T, \varphi) + \frac{\partial \lambda_c}{\partial u}\frac{\partial u}{\partial t}(T, \varphi) \tag{2.9}$$

where

λ_c is the core thermal conductivity ($Wm^{-1}K^{-1}$)

u is the moisture content (mass%)

T is the temperature (K)

φ is the relative humidity (%)

P is the pressue (Pa)

Centre of panel thermal conductivity design values are higher for metalized polymeric envelope due to the fact that it has small thermal bridging effect compared to aluminium foil envelope.

Schwab et al. (2005) used a correlation (2.10) for predicting thermal conductivity as a function of time for a fumed silica kernel VIP. In correlation (2.10) initial thermal conductivity is limited to only solid and radiative conductivity and thermal conductivity due to increase in gas pressure and water content over time was added to calculate the time dependent thermal conductivity, $\lambda(t)$.

$$\lambda(t) = \lambda evac + \frac{\lambda_{free\ gas}}{1 + (p_{1/2,gas}/\ p_{gas}(t))} + b.Xw(t) \tag{2.10}$$

where

$\lambda evac$ is the thermal conductivity (in evacuated conditions) ($W\ m^{-1}\ K^{-1}$)

$\lambda_{free\ gas}$ is the thermal conductivity of the free and still gas ($W\ m^{-1}\ K^{-1}$)

$p_{1/2,gas}$ is the pressure at which gaseous thermal conductivity equals to one half of $\lambda_{free\ gas}$ (Pa)

p_{gas} is the gas pressure (Pa)

b is the sorption isotherm constant

Xw is the water content (mass %)

In VIPs, moisture influences the thermal conductivity by increasing the pore gas pressure and the solid conduction by changing the contact between particles of core material. Simmler et al. (2005) calculated that unit increase in moisture content (mass%) led to 0.05 $mWm^{-1}K^{-1}$ increase in thermal conductivity and 30 mbar increase in gas pressure led to a 1 $mWm^{-1}K^{-1}$ increase in thermal conductivity. Tenpierik et al. (2007) and Tenpierik (2009) proposed an analytical model equation for estimating changes in thermal conductivity over time and useful life time for a VIP. This equation (2.11) includes the effect of getters and desiccants on rate of change of thermal conductivity and more suitable for VIPs containing getters and desiccants e.g. VIPs with glass fibre and PU foam core.

$$\Delta\lambda_c(t) \approx \frac{\partial\lambda_c}{\partial p_g}\Delta p_{g;e}\left(1-e^{-(t-t_{get})/t_g}\right)+\frac{\partial\lambda_c}{\partial p_{wv}}p_{wv;e}\left(1-e^{-\frac{t-t_{des}}{t_w}}\right)+\frac{\partial\lambda_c}{\partial u}\frac{du}{d\varphi}\varphi_e\left(1-e^{-\frac{t-t_{des}}{t_w}}\right) \quad (2.11)$$

where

p_g is the pore gas pressure (Pa)

$p_{g;e}$ is the atmospheric gas pressure (Pa)

$p_{wv;e}$ is the partial water vapour pressure outside the VIP (Pa)

t is the time (s)

t_{get} is the time shift due to a getter (s)

t_{des} is the time shift due to a desiccant (s)

t_g is the time constant for gas pressure increase (s)

t_w is the time constant for water content increase (s)

φ_e is the relative humidity of the air outside the VIP (%)

For compressed fumed silica a simplified model, (2.12), was used to approximate rapid estimation of useful life time by assuming no effect of VIP life using getter and desiccant (Tenpierik et al., 2007) and (Tenpierik, 2009).

$$Tsl \approx a.e^{b(\lambda_{lim} - \lambda_0 - \lambda_w)}.d_p.\left(\frac{l_p}{s_p}\right)^c.\frac{T_0}{T}\ e^{(E_a/R)\left(\frac{1}{T}-\frac{1}{T_0}\right)} \quad (2.12)$$

where

a ($s\ m^{-(1+c)}$), b (mKW^{-1}) and c are regression parameters

E_a is the activation energy for permeation through the barrier envelope ($Jmol^{-1}$)

R is the universal gas constant ($Jmol^{-1}K^{-1}$)

l_p is the perimeter length of VIP (m)

s_p is the surface area of VIP (m^2)

λ_w is the thermal conductivity of liquid water and water vapour at equilibrium ($Wm^{-1}K^{-1}$)

λ_0 is the thermal conductivity of air at atmospheric pressure ($Wm^{-1}K^{-1}$)

T_0 is the reference laboratory temperature (K)

T is the absolute temperature (K)

This simplified model is restricted to specific panel parameters and environmental conditions such VIP in the range of 10-50 mm thickness, temperature in the range of 268-318 K, perimeter length to surface area ratio in the range of 2-12 m^{-1} and a 50% constant relative humidity. However, for building applications constantly changing environmental conditions require a model that is able to predict VIP useful life time under real life changing conditions. Beck et al. (2009) presented a dynamic model for a silica VIP core under varying temperature and relative humidity conditions and was able to estimate the moisture transmission and temperature profile at the same time.

2.6.2 Thermal bridging effect

Thermal conductivity of VIPs is expressed either as centre of panel or effective thermal conductivity with later including thermal bridging effect around the edges. Thermal bridges also known as linear thermal transmittance occur and at edges and corners due to the relatively high thermal conductivity of envelope materials surrounding the evacuated core (Quenard and Sallee, 2005, Tenpierik and Cauberg, 2007 and Sprengard and Holm, 2014). The linear thermal transmittance or thermal bridging effect depends upon the type of

envelope, panel thickness, length of edges and surface area. Effective thermal conductivity of a VIP can be calculated by adding up linear thermal transmittance to the centre of panel thermal conductivity as expressed in equation (2.13) (Wakili et al., 2004).

$$\lambda_{\text{eff}} = \lambda_{\text{cop}} + \Psi_{,\text{VIP edge}} \cdot d_p \cdot l_p / s_p \quad (2.13)$$

where

λ_{cop} is the centre of panel thermal conductivity ($Wm^{-1}K^{-1}$)

$\Psi_{,\text{VIP edge}}$ the is linear thermal transmittance ($Wm^{-1}K^{-1}$)

λ_{eff} is the effective thermal conductivity ($Wm^{-1}K^{-1}$)

d_p is the thickness of panel (m)

l_p is the length of perimeter (m)

s_p is the surface area of panel (m^2)

Wakili et al. (2004) performed numerical simulation to predict the effective thermal conductivity and also carried out measurements using a guarded hot box. Linear thermal transmittance calculated by Wakili et al. (2004) for a square VIP of area 1 m^2 are given in figure 2.8. It can be seen that linear thermal transmittance values are higher for a VIP with an aluminium foil (8µm) envelope as compared to that of aluminium coated polymeric foil envelopes. Binz et al. (2005) estimated that linear thermal transmittance values in the range of 8-10 $mWm^{-1}K^{-1}$ for a 10-40 mm thick VIP with envelopes composed of three 12 µm metalized PET layers, whereas for a 6 µm aluminium foil it ranged between 22 $mWm^{-1}K^{-1}$ and 40 $mWm^{-1}K^{-1}$. Simmler and Brunner (2005) calculated the design values of VIP including linear thermal transmittance to be 7 $mWm^{-1}K^{-1}$ and 10 $mWm^{-1}K^{-1}$ respectively for an aluminium foil and a metallised envelope. Clearly, an aluminium foil envelope is not suitable for use in VIP envelope due to their higher thermal bridging effect.

Thorsell and Kallebrink (2005) considered the use of serpentine edge design to reduce the thermal bridging effect at VIP edges. For a stainless steel straight edge linear thermal transmittance value of 28 $mWm^{-1}K^{-1}$ was estimated and reduced to 9.6 $mWm^{-1}K^{-1}$ for the envelope with 17 serpentines of 20 mm depth. However, these linear thermal transmittance values were comparatively larger as compared to those of metallised and aluminium foil envelopes measured by the Wakili et al. (2004) and Schwab et al. (2005).

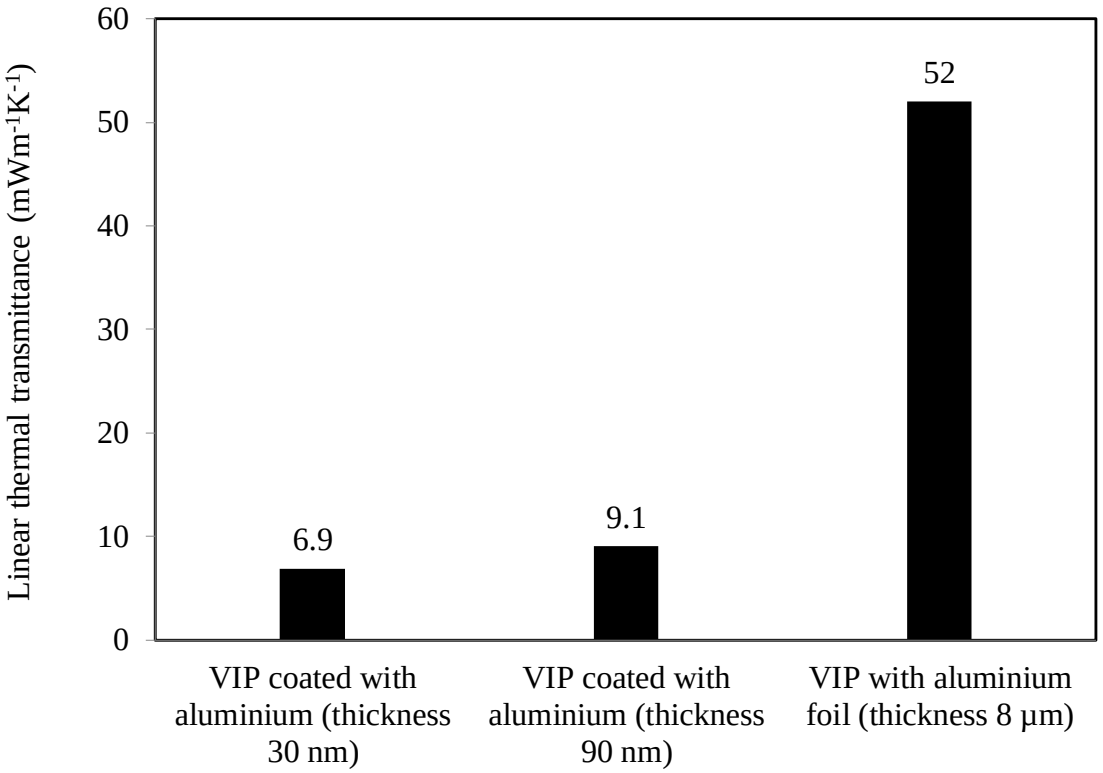

Figure 2.8 Linear thermal transmittance for different envelope configurations (Alam et al., 2011)

Tenpierik et al. (2008) and Tenpierik and Cauberg (2007) presented an analytical model assuming steady state boundary conditions, no lateral heat transfer between adjacent VIPs and zero thermal conductivity of core presented an analytical model to calculate thermal bridges due to VIP envelope. A separate modal for non-zero core thermal conductivity was also presented. The results of model for non-zero core thermal conductivity were validated against the predictions obtained from commercially available software, TRISCO. Linear thermal transmittance was found to be a complex function of laminate thickness, laminate thermal conductivity, panel thickness and core thermal conductivity. Results of their research (figure 2.9) showed that materials such as aluminium and steel foil with higher thermal conductivity in the VIP envelope produced higher values of linear thermal transmittance and metalized film caused smaller thermal bridge effect compared to that of aluminium foil and stainless steel envelope.

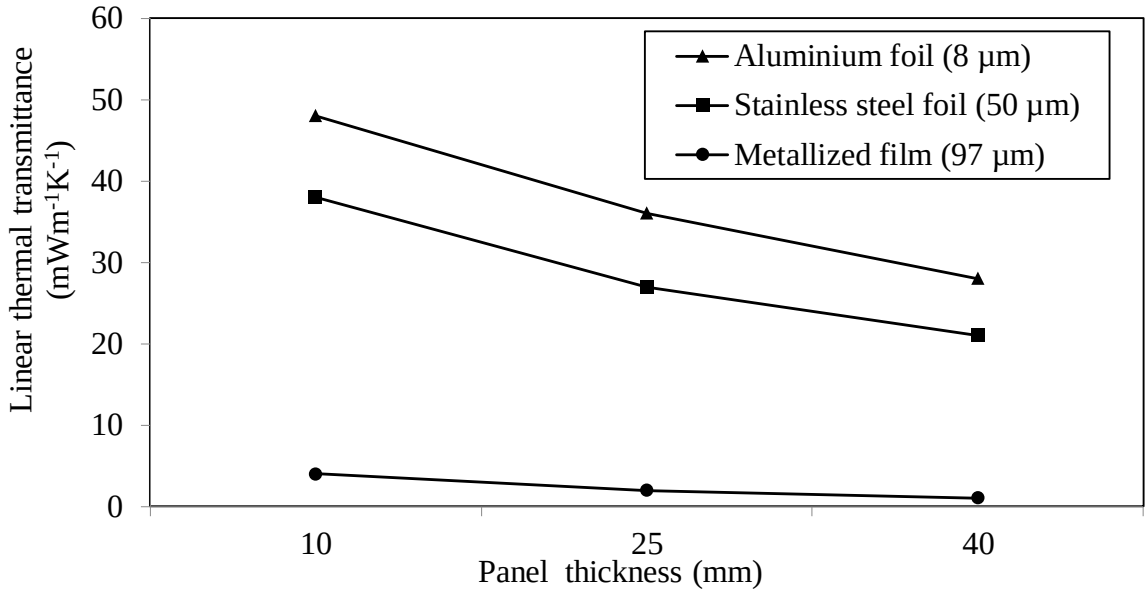

Figure.2.9 Comparison of linear thermal transmittance of different envelope materials with specified thicknesses (Tenpierik and Cauberg, 2008)

For building applications, VIPs usually covered with external protecting facings or skins on sides of the panels to protect from mechanical damage. Linear thermal transmittance values of aluminium and stainless steel facing caused larger values of linear thermal transmittance as compared to that of polyester facing such as expanded polystyrene facings (Tenpierik and Cauberg, 2010; Nussbaumer et al., 2006; Schwab et al., 2005; Quenard and Sallee, 2005 and Mukhopadhyaya et al., 2014). To reduce these thermal bridges designers should be careful with design by minimising the thickness of perimeter insulator or use a better insulator for perimeter.

2.7 Conclusion

VIPs have thermal performance 5-8 time higher than that of conventional insulation materials. As a result, VIPs offer higher thermal insulation while taking less space in buildings. VIP is made of an evacuated core material covered by a multilayer metallised barrier film to preserve the vacuum for a specified time. Core is porous material which provides resistance and against compression and does not allow heat transfer. Envelop is a multilayer barrier often metalized polymeric layers which provides protection against environmental and handling stresses. Heat transfer across insulation occurs through solid conduction, radiation and gaseous heat transfer. In conventional insulation materials the dominant heat transfer is through the gas present in hollow pores of the core material and in

VIP this gaseous heat transfer is suppressed by means of creating vacuum inside the core material.

Application of VIPs in buildings is limited due to their limitations such as

- Vulnerability to mechanical damage during installation and transportation
- Uncertain service life
- Thermal birding effect
- High material cost

Risks of VIP damage, uncertain service life and thermal birding effect can be managed by careful handling, improved quality control and improved designing of VIPs. However, high cost is associated with materials being used in VIPs. Fumed silica an expensive material is mostly used core material in VIPs and contributes to the overall high cost of VIPs. There is a scope of VIP cost reduction by replacing currently used core material (fumed silica) completely or partially with low cost materials.

Currently, VIP research is focused on developing alternative low cost material, improving design, better understanding of performance and developing tools to accurately predict life time. Reviewed research studies have also investigated the use of glass fibre, open cell foams and porous mineral as VIP core materials. However, none of the reviewed research studies considered the use of low cost expanded perlite as replacement of proportion of expensive fumed silica. In this research thesis, expanded perlite and fumed silica composite material as low cost VIP core material has been investigated. The main research work carried out during this research work is given as follows:

- Development of expanded perlite and fumed silica composite material for low cost core of VIPs.

- Experimentally optimise the main thermo-physical properties of developed core material composites.

- Manufacture prototype VIPs using optimised low cost core material with the potential to attain thermal conductivity of commercial VIPs.

- Cost reduction potential assessment of optimised core material for use in VIPs for building applications.

Chapter 3

VIP Core Material and Characterisation Methods

3.1 Introduction

Thermal conductivity of VIPs depends on the core material. The most important properties required for a suitable core material are (i) low density (ii) low thermal conductivity (iii) high resistance to infrared radiative heat transfer (iv) small pore diameter and (v) high porosity to reduce the gaseous conductivity. Pore size of VIP core material has to be less or at least in the same order as the mean free path of air molecules in order to achieve the lowest gaseous thermal conductivity. Generally, fumed silica is used as core material of VIP due to its low thermal conductivity, low density and smaller pore size. However, it is an expensive material and a contributing factor to high cost of VIPs. For reducing the cost of VIPs alternative cheap materials are required to be developed to completely or partially replace the fumed silica. The objective of this study was to develop an alternative low cost material and evaluate its effectiveness as a core material for VIPs. Expanded perlite is an economical material which has low thermal conductivity, low density and porous structure. However, its pores are relatively larger in size and required to be small enough to limit the gaseous thermal conductivity. Fumed silica aggregates containing smaller pores can fill the larger pores of expanded perlite and reduce the gaseous thermal conductivity leading to overall reduction in thermal conductivity of such composite. In this research, expanded perlite and fumed silica composites along with fibre and suitable opacifier as a low cost VIP core material are developed, characterised and experimentally tested. This chapter provides the details of materials, composite sample preparation, characterisation methods and experimental techniques to measure different properties. Pores size and porosity analysis was carried out using Transmission Electron Microscopy, Scanning Electron Microscopy, Mercury Intrusion Porosimetry and Gas adsorption. Fourier Transform Infrared spectroscopy was used to measure the radiative conductivity of composite samples. VIP core material samples were prepared and guarded hotplate method was used to measure the thermal conductivity of core boards.

3.2 Research materials

3.2.1 Expanded perlite

For this research, Ultrafine P05 expanded perlite (EP) was sourced from William Sinclair Ltd., UK. Its properties are given in table 3.1. Perlite is a low cost glassy amorphous mineral rock and average price of processed crude perlite was $53 per metric ton (Bolen, 2012). Raw perlite is expanded by heating at temperature of 760-1100 °C and water present in the perlite vaporises and gives porous structure to perlite particles rendering the light weight and excellent insulating properties (Tekin et al., 2006). In 2012 an average price of expanded perlite was $310 per ton (Bolen, 2012).

Table 3.1 Properties of Ultrafine P05 Expanded perlite (William Sinclair Ltd., UK)

Property	Value
Thermal Conductivity ($Wm^{-1}K^{-1}$)	0.05
Free Moisture (%)	0.5
Softening Point (^{o}C)	890-1100

Expanded perlite is a white inorganic lightweight aluminium silicate powder with a typical composition as shown in table 3.2. It has low bulk (35-120 kgm^{-3}) density which makes it an ideal material for insulation. It has been used for different construction applications such as lightweight cement aggregate, insulation and ceiling tiles (Sari and Karaipekli, 2008) due to its low thermal conductivity (45-70 $mWm^{-1}K^{-1}$), low density, ease of handling, non-combustibility, non-flammability and porous nature (Perlite Institute USA, 1983). Due to its porous nature it is also well suited for use under vacuum conditions (Perlite Institute, USA) and has been used in cryogenic insulation systems at a temperature range of 20K-90K (Dubé et al., 1991 and Augustynowicz et al., 1999), liquid hydrogen storage tanks (Sass et al., 2008) and can also be used as light weight building material at ambient temperature (Sengul et al., 2001) and (Demirboğa and Gül, 2003). However, the pore size of expanded perlite relativity large in micrometric range approximately 3 µm (Zhang et al., 2007) which will yield higher gaseous conductivity and requires to be reduced in size to decrease its gaseous conductivity.

Table 3.2 Typical composition of expanded perlite (William Sinclair Ltd., UK)

Chemical constituent	Mass ratio (%)
Silica (SiO_2)	73
Aluminium oxide (Al_2O_3)	15
Potassium oxide (K_2O)	5
Sodium oxide (Na_2O)	3
Calcium & Magnesium oxides (CaO + MgO)	1
Iron oxide (Fe_2O_3)	2
Others	1

3.2.2 Fumed silica

For filling the pores of expanded perlite a high purity, hydrophilic fumed silica (FS), SUPASIL™ BIL-FS200 was obtained from Baltimore Innovations Ltd. Different physical properties of SUPASIL™ BIL-FS200 fumed silica are given in table 3.3. Fumed silica (amorphous) is a non-flammable white fluffy powder composed of small primary particles (5-50 nm) fused into branched aggregates (secondary particles) of short chains of length 0.2-0.3 µm. These aggregates tend to further agglomerate into tertiary particles. Fumed silica aggregates are arranged in pseudo circular form and the hollow spaces between the chains form the pores structure. Pore size of fumed silica ranges from 100-300 nm. Fumed silica powder has high porosity (>90%), low density and high surface area ranging from 100 - 400 m^2g^{-1}. It is produced by a continuous flame hydrolysis of silicon tetrachloride ($SiCl_4$). During this process $SiCl_4$ is converted to the gas phase and is burned in a flame of hydrogen and oxygen (at approximately 1800 ºC) to yield the fumed silica and gaseous hydrochloric acid as a by-product. This process yields molten particle of silicon dioxide. The chemical reaction involved in this process is shown in equation (3.1):

$$2H_2 + O_2 + SiCl_4 \longrightarrow SiO_2 + 4HCI \qquad (3.1)$$

Properties such as particle size and surface area of fumed silica can be varied for different applications depending on process parameters such as temperature, concentration of reactants and dwell time of silica in combustion chamber (Evonik Technical bulletin Fine Particles, Number 11, 2006). Fumed silica has overall thermal conductivity less than 5 $mWm^{-1}K^{-1}$ at 10 - 20 mbar pressure (Caps and Fricke, 2000) due to is low density and small pore size.

Table 3.3 Physical properties of SUPASIL^{TM} BIL-FS200 (Baltimore Innovations Limited UK)

Appearance	White powder
Specific surface area (BET)	200 ± 25 m^2g^{-1}
Silica content	≥ 99.8 wt %
Tapped Density (dried for 2 h@105 ºC)	25-60 Kgm^{-3}
Carbon Content	< 0.2 wt %
Melting Point	1700 ºC

3.2.3 Polyester fibre

Polyester fibres (PF) with diameter of 12 µm, length of 1.6 mm and melting point 230-260 ºC were obtained from Goonvean Fibres Ltd. for adding into fumed silica and expanded perlite powders to increase mechanical strength of the core board. Polyester fibres are extremely strong, durable resistant to most chemicals, stretching and shrinking. Polyester fibres burns slowly and melts at high temperatures. Polyester is hydrophobic in nature and dries quickly which is an advantage for rapid drying of the VIP cores.

3.2.4 Opacifiers

Opacifiers are radiation absorbing and scattering materials which are integrated into core material in order to make it opaque to infrared radiation to reduce the radiative conductivity. A major drawback of addition of opacifiers in the core material is that it might lead to higher solid thermal conductivity because some opacifiers, such as silicon carbide (SiC) and titanium oxide (TiO_2), have a higher solid conductivity than pure core materials such as fumed silica and glass fibre. Therefore, it is essential to determine the critical doping mass of opacifier for addition into VIP core. Performance of an opacifier depends upon number of factors such as wavelength, temperature, particle size and refractive index. Opacifiers can be selected depending upon the intended application of VIP. In this research SiC has been investigated in mixture with expanded perlite and fumed silica composite to evaluate its opacifying effect and optimise the critical doping mass in the composite.

3.3 Preparation of composite samples

Composite samples consisting of different constituent materials in varying mass proportions were prepared by dry mixing using mixer device SpeedMixer™ DAC 150 FVZ-K shown in figure 3.1 (a). It works by spinning a high speed mixing arm in opposite directions. The material components were weighed individually and powder samples (0.5g) were mechanically mixed at approximately 1500 rpm for 1 minute to ensure the uniform mixing of all sample constituents. This device is limited to prepare only small samples and suitable for preparing samples for FTIR study and pore size analysis which require small amounts of samples. However, for manufacturing of core board samples and VIP prototypes, powder samples were required in large quantities (>30 g). For this purpose samples were prepared by dry mechanical mixing of different constituent materials in varying mass proportions using an electrical hand mixer containing metal whisk attachment as mixing device as shown in figure 3.1 (b) .

(a) (b)

Figure 3.1 (a) SpeedMixer^{TM} DAC 150 FVZ-K used for composite sample preparation (b) electrical hand mixer with metal whisks attachment

Materials were weighed individually and placed into a container and mixed with electrical hand mixer using one metal whisk attachment at approximately 1200-1500 rpm for 5 minutes at room temperature. Container was kept fully covered with lid to avoid any powder materials to become airborne and a small hole was made in the container lid for allowing the whisk to go into the container. Both methods of mixing exhibited no airborne fumed silica particles in mixed samples and this demonstrate the uniform mixing of sample contents. Mixing speed used in both these method of mixing is approximately in the same range to realise a similarity

in the mixing processes adopted. However, more time was required for conventional electrical hand mixer due to the greater amounts of samples employed.

3.4 Pore size analysis

Thermal conductivity of VIP core at different pressures mainly depends upon gaseous conductivity, radiative and solid conductivity of core material. Determining of gaseous conductivity requires the data related to porosity and pore size of the material. Materials with pore size in the range of free mean path of air are required to limit the gaseous conductivity under evacuated conditions. This section discusses the methods used for characterisation of pore size and porosity of developed fumed silica and expanded perlite composite samples.

3.4.1 Pore size measurement of composite samples

Pores of porous materials are generally classified in terms of their pore diameter or width. Sing et al. (1985) classified pores in three categories (i) micropores with pore diameter <2 nm (ii) mesopores with pore diameter range from 2-50 nm (iii) macropores with pore diameter >50 nm. The most common methods for quantitative pore size analysis are Mercury Intrusion Porosimetry (MIP) for the macropore range and gas adsorption for the micropore and mesopore ranges. Qualitative pore size analysis is performed using Electron Microscopy techniques such as Scanning Electron Microscopy (SEM) or Transmission Electron Microscopy (TEM). For pore size analysis, choice of technique depends upon the expected pores size and nature of material being investigated. A single porosimetry technique alone is not able to determine pore size distribution throughout the entire range of pore sizes due to their limitations. Composite materials developed in this research was expected to have wide range of pore size distribution, therefore, a range of techniques including Electron Microscopy, MIP and Gas adsorption were employed to obtain porosity and pore size distribution information throughout the entire range of pore sizes.

3.4.2 Transmission Electron Microscopy (TEM)

TEM is a microscopy technique used to visually characterise nano material to acquire quantitative information of pore size, particle size and morphology. This technique has already been used for characterising nano-silica powders by Temmerman et al. (2012) and Feng et al. (2011). In the TEM technique a focused beam of electrons is transmitted through the sample. As the electrons interact with sample material an image is formed, magnified and

displayed onto an imaging device. This technique enables to characterise nano-scale materials at significantly higher resolution. However, this technique is limited to only providing 2D representation and provides only the size of neck of the pores and is not able to offer the information of depth of the pores. Fumed silica powder sample was analysed to assess the pore size and morphology of fumed silica. The sample was suspended in ethanol and supported on a copper grid that was coated with a thin layer of carbon and imaged using JEOL 2100 field emission gun transmission electron microscope (FEG TEM) at a magnification of 30000 times. Figure 3.2 shows the TEM image of fumed silica powder sample displaying amorphous fumed silica aggregate in which primary particles are linked together in a chain arrangement. Furthermore, a number of nano-size pores are formed between primary particles. These pores varied in size and the largest pores analysed by TEM imaging analysis software were approximately 135.15 nm, 100.83, 93.15 and 67.28. Clearly, the pore sizes of fumed silica measured were in the same range as the mean free path of air, which could limit the gaseous thermal conductivity to be lower than that of still air under ambient conditions and could be further lowered in evacuated conditions.

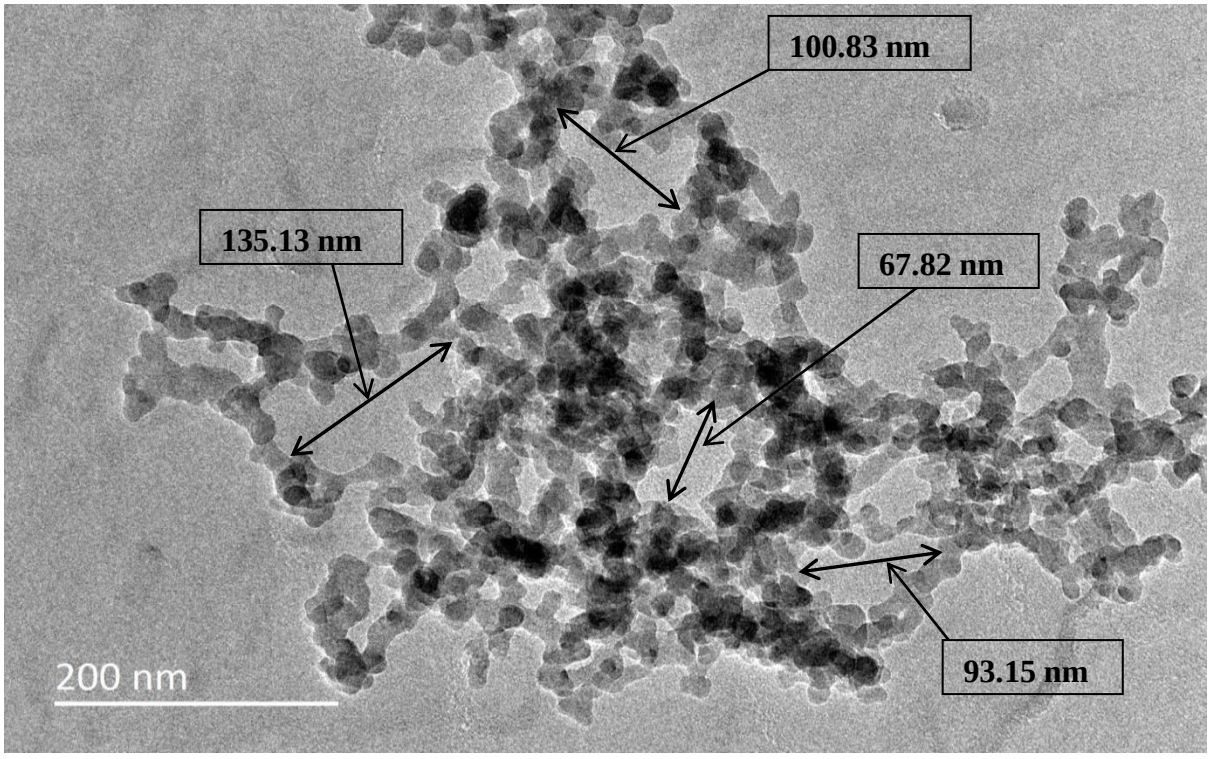

Figure 3.2 TEM image of fumed silica powder sample displaying chain aggregate and pore sizes (Alam et al., 2014)

3.4.3 Scanning Electron Microscopy (SEM)

In order to characterise the morphology of the fumed silica and expanded perlite composite SEM technique was also used. As the expanded perlite has coarser particles, SEM is suitable method to visualise the integration of fumed silica aggregates in large pores of expanded perlite. Powder sample of pure expanded perlite was analysed to observe the structure of expanded perlite particles and pores. Powder sample containing expanded perlite (30 mass%) fumed silica (62 mass%), and polyester fibre (8 mass%) was also analysed to visualise the integration of fumed silica aggregates into the pores of expanded perlite. Both powder samples were mounted on a stub with carbon tape and coated with gold. Micrographs were taken using a Zeiss Supra 35 VP SEM. Surface images were taken and stored in TIF format. Figure 3.3 shows the SEM image of porous particles of expanded perlite showing the pores of size between 3-10 µm. Figure 3.4 shows the SEM image of powder sample containing expanded perlite (30 mass%) fumed silica (62 mass%), and polyester fibre (8 mass%) and it can be seen that fumed silica aggregates got into pores of expanded perlite randomly filling them completely or partially which made the much large pores of expanded perlite loaded with fumed silica containing mesopores and micropores. This effect of fumed silica in reducing the pore size of expanded perlite helps in reducing the gaseous thermal conductivity of composite sample due to the reduction in its pore size.

Figure 3.3 SEM image of expanded perlite powder containing porous particles

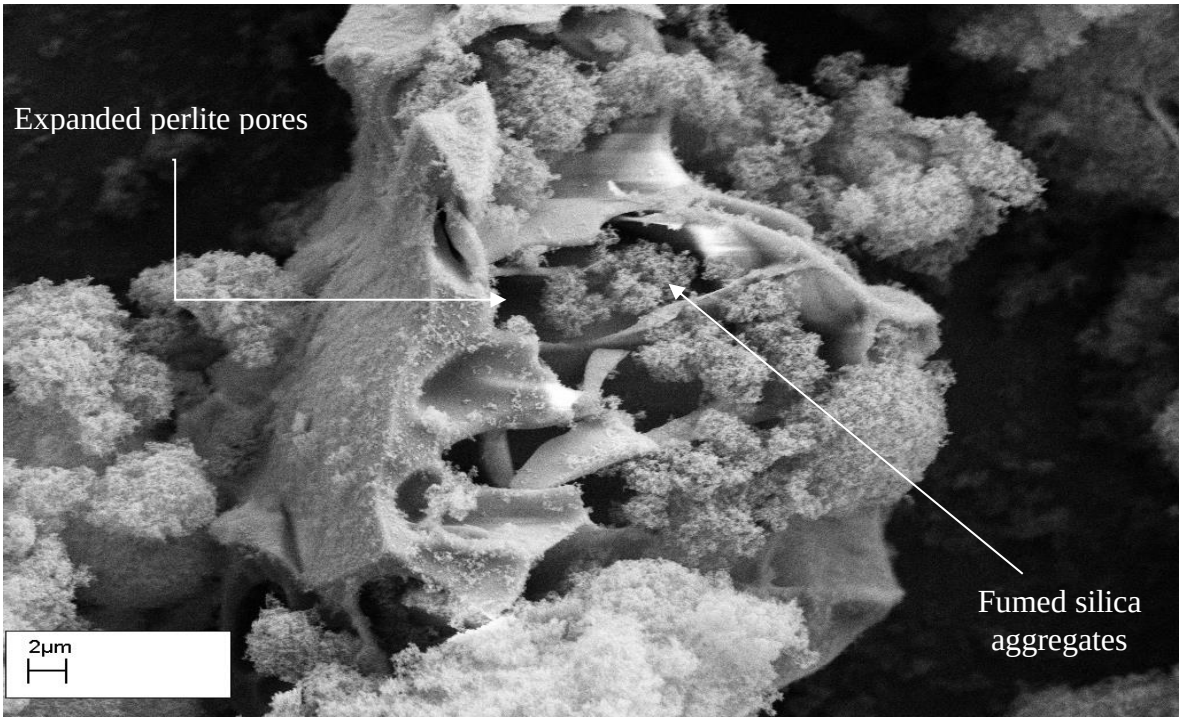

Figure 3.4 SEM image of powder sample containing expanded perlite (30 mass%) fumed silica (62 mass%), and polyester fibre (8 mass%) showing expanded perlite pores fully or partially filled with fumed silica aggregates

However, TEM and SEM images were not able to provide pore size distribution due to the limitation of equipment. Hence, other techniques such as gas adsorption and MIP were employed to ascertain the effect of fumed silica integration on pore size distribution of composite samples.

3.4.4 Gas adsorption

Nitrogen (N_2) adsorption analysis technique is used to determine the surface area and pore size distribution of microporous to mesoporous materials with pore sizes ranging from 2 nm to 100 nm (BS ISO 15901-2:2006). However, it is not able to determine pores with larger diameter. Other limitation is that it is a slow method which may take up to 24 hours for a sample. In case of composite samples containing both macropores and mesopores other techniques such as Mercury Intrusion Porosimetry (MIP) or Electron microscopy are also essential to be employed to evaluate the pore size distribution over a whole range (Alam et al., 2014). Pore size analysis of composite sample A (fumed silica 80 mass%, expanded perlite 0%, SiC 12 mass% and fibres 8 mass%) and composite sample B (fumed silica 50 mass%, expanded perlite 30%, SiC 12 mass% and fibres 8 mass%) was carried out using

nitrogen adsorption analysis at 77.3 K using Quantachrome Nova 2200. Samples were out gassed by evacuating at 250 ºC for 24 hours. After the degassing procedure, samples were weighed to determine the analysis weight of the sample. The sample tube is then placed on the analysis port of the instrument and adsorption and desorption isotherms were collected. Prior to adsorption isotherm measurement, free space of the sample tube was measured volumetrically using helium. Helium was evacuated and sample tube was kept in cryogenic liquid nitrogen with a known amount of N_2 at successions of controlled pressures. The pressure programme comprised 21 adsorption and 17 desorption points measured at equilibrium with a maximum relative pressure of 0.999. Figure 3.5 shows the nitrogen adsorption-desorption isotherms of samples A and B.

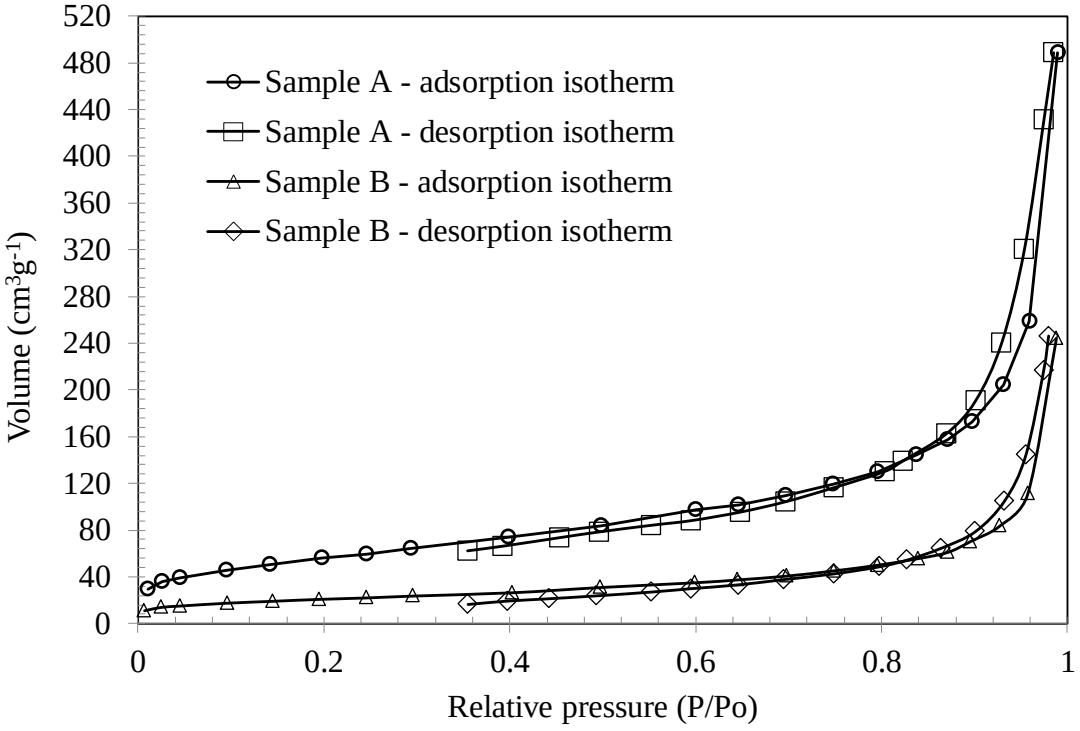

Figure 3.5 Nitrogen adsorption and desorption isotherms for samples A and B

Adsorption isotherms of both samples A and B exhibit shape characteristic of type II adsorption isotherm classified by the International Union of Pure and Applied Chemists (IUPAC) and is associated with macroporous materials containing pores >50 nm. This indicates that for these samples pore size distribution continues in macropores region (>50 nm) and is also confirmed by the pore size distribution obtained by TEM. However, gas

adsorption was not able to resolve the entire macropore range and required the MIP analysis of fumed silica and expanded perlite composite.

3.4.5 Mercury Intrusion Porosimetry (MIP)

MIP is based on the capillary law governing liquid penetration into small pores. This law in case of a non-wetting, non-reacting liquid like mercury and cylindrical pores, is expressed by equation (3.2) (Webb, 2001)

$$D = -(4\gamma\cos\theta)/P \quad (3.2)$$

where

D is the pore diameter

P the applied pressure (Pa)

γ the surface tension (Nm^{-1})

θ the contact angle (°)

In MIP, a sample is inserted into an evacuated container and mercury is allowed to fill the container. Pressure is increased causing the mercury to fill the pores while the volume of mercury entering pores in the sample is observed. The volume of mercury that enters into the sample due to rise in pressure is equivalent to the volume of the pores. MIP technique is limited by the associated compression of material due to pressure applied for intrusion of mercury into small pores of highly porous silica and may compress or damage the sample and be considered as pore volume instead of compression (Brown and Lard, 1974). However, an advantage of this method is that it is a quick method of measuring the open pores (pores that reach the surface of sample). In case of composite samples of fumed silica and expanded perlite both these limitations may affect the results. However, this technique can be useful to obtain first approximation of the porosity information for these composites due to the presence of a large range of pore sizes, which is not coverable by gas sorption. Porosity, pore volume, pore size distribution and surface area was measured using MIP technique employing a Micromeritics Autopore IV mercury porosimeter over a pressure range of 0 - 413.6 MPa and the total intrusion volume was measured. The surface tension of 0.48 Nm^{-1} and a contact angle of 140º were used for mercury. Other parameters used for the MIP are listed in table 3.4. Total pore volume was calculated by software package Autopore IV 9500 V 1.09 by subtracting intrusion volume at maximum pressure from intrusion volume at zero

pressure. Sample bulk volume was assumed to be equal to the total penetrometer volume minus intrusion volume at zero pressure.

Table 3.4 Parameters used for MIP

Penetrometer volume	3.2825 mL
Penetrometer constant	10.790 µL/pF
Evacuation pressure	50 µmHg
Evacuation time	5 minutes
Mercury filling pressure	0.33 psia
Equilibration time	10 Secs

Three representative composite samples A,B and C detailed in table 3.5 were selected for MIP measurements to cover the widest range of the composition of fumed silica ranging from 80% (sample A) to 20% (sample C) employed in this study. In table 3.5 fumed silica, expanded perlite and polyester fibres are written as FS, EP and PF respectively.

The results of MIP of sample A, B and C are shown in table 3.5. These samples cover the broad range of mass% of both main constituent expanded perlite and fumed silica to ascertain the effect of both on pore size distribution. The total volume of mercury intruded was 13.232 $\times 10^{-6}$ m^3g^{-1}, 4.496 $\times 10^{-6}$ m^3g^{-1} and 3.790 $\times 10^{-6}$ m^3g^{-1} in samples A, B and C respectively. These results showed that with an increase in the mass proportion of expanded perlite in samples B and C the total intrusion volume decreased. This suggested that there is decrease in porosity of samples due to the presence of expanded perlite. Average pore diameter values are within the range of 150-300 nm and are comparable to that acquired by TEM, though TEM images are two dimensional.

Table 3.5 Total intrusion volume and average pore results of samples A,B and C obtained by MIP

Sample	**Ratios FS:EP:SiC:PF**	**Total intrusion volume (V) $\times 10^{-6}$ (m^3g^{-1})**	**Total Pore Area (A) (m^2g^{-1})**	**Average pore diameter (4V/A) (nm)**
A	80:0:12:8	13.232	182.4	290
B	50:30:12:8	4.946	128.0	155
C	20:60:12:8	3.790	77.27	196

Cumulative intrusion (%) of mercury in samples A,B and C over a range of pore size is shown in Fig 3.6. This figure shows that composite sample A which comprises of 80 mass% of fumed silica and no expanded perlite along with other constituents contained 81.84% of pore volume occupied by pores larger than 1 µm and remaining 18.16% by submicron pores (pores less than 1 µm). In composite samples B and C containing expanded perlite in mass ratios of 30% and 60% respectively along with other constituents, cumulative intrusion of mercury in submicron pore size range was found to be 33.28% and 21.75% respectively. This suggests that the presence of expanded perlite in composite samples B and C has led to increase in submicron size pores compared to sample A.

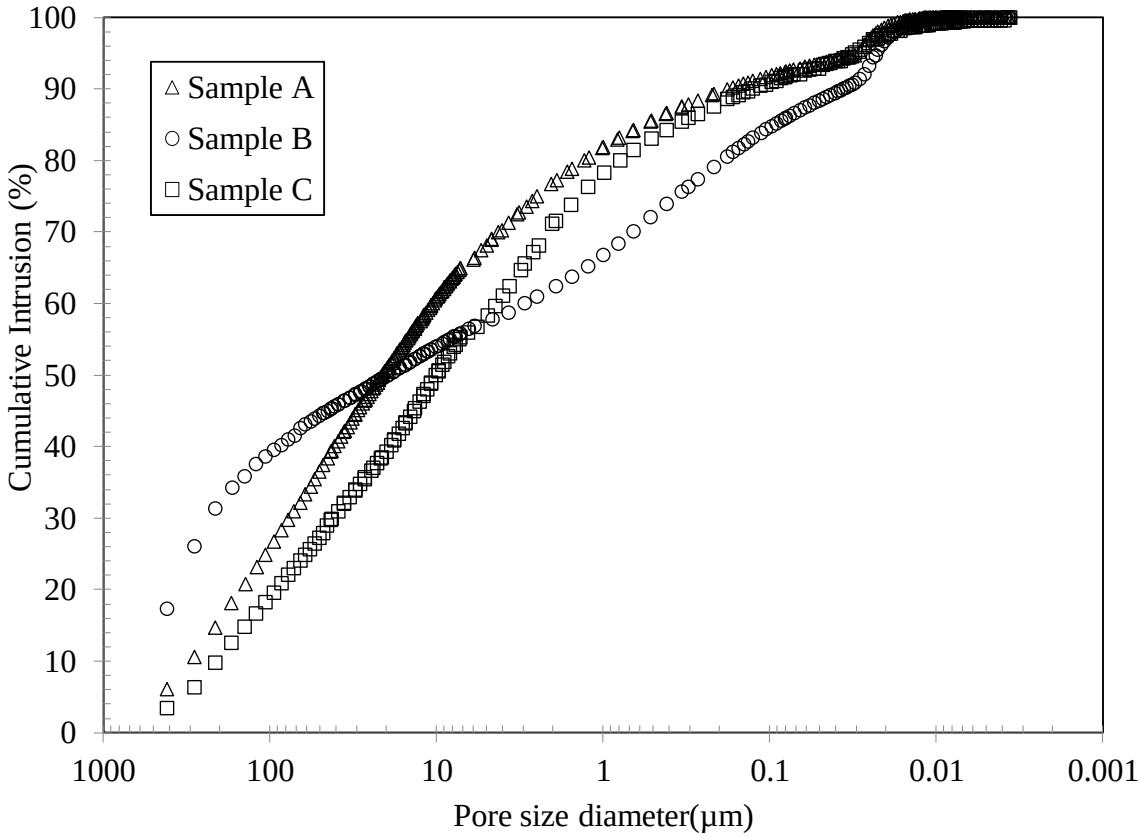

Figure 3.6 Measured distribution of cumulative intrusion (%) of fumed silica and expanded perlite composite samples A-C (Alam et al., 2014)

This increased submicron pore volume is 11.5% higher in composite sample B containing 30 mass% of expanded perlite compared to sample C containing 60 mass% of expanded perlite. This indicates that large amount of expanded perlite contains large pore volume of pores larger than 1 µm and only 20 mass% of fumed silica was not able to fill expanded perlite pores effectively. Hence, a balance needs to be achieved between the amounts of expanded

perlite and fumed silica in the composite material to obtain suitable volume of pores in submicron pore size range. Sample B containing 30 mass% expanded perlite and 50 mass% fumed silica appeared to be the best of all tested due to the availability of enough larger pores to be filled by a large amount of fumed silica. However, large intrusion volumes in pores with size >1 μm was observed for all samples which could be attributed to the compression of fumed silica and expanded perlite particles during the introduction of mercury. This is a major problem associated with MIP technique for materials such as fumed silica.

3.5 Fourier Transform Infrared (FTIR) Spectroscopy

Influence of opacifier on radiative heat transfer depends upon the extinction coefficient, which can be calculated from the transmission spectrum in the wavelength range of interest. The infrared spectrum of a sample is recorded by passing a beam of infrared light through the sample. This IR beam is transmitted, absorbed or reflected depending upon the molecular characteristics of the sample. FTIR is the technique used to acquire IR transmission spectrum by first collecting an interferogram of a sample signal and then performing a Fourier Transform (FT) on the interferogram to obtain the spectrum. In this research, FTIR technique has been employed to acquire the transmission spectrum of composite samples for quantifying the opacying effect and determining the optimum doping mass of opacifiers silicon SiC.

3.5.1 FTIR sample preparation

It was very difficult to obtain an optically thin film from the pure powders. Therefore, all samples were prepared after mixing with Potassium bromide (KBr) and then pressed into pellets. KBr powder becomes highly transparent to IR when pressed in pellet form due to its plasticity (Colthup et al., 1990). For this purpose KBr powder (150 mg) and composite sample powders (1 mg) were weighed using calibrated weighing balance (APX-60 readability 0.1 mg). These powders were grinded and mixed thoroughly in agate mortar quickly because the KBr tends to absorb moisture from the atmosphere. The powder mixture was placed in the die and pressed to compact the powders into pellets. Reference pellet containing only KBr were also prepared to measure the background absorption enabling to make correction for IR transmission losses due to KBr moisture absorption. Figure 3.7 shows the die components, die cross section and the press used for making pellets.

3.5.2 Spectrum acquisition and radiative conductivity

The transmission spectrum, an average of 100 scans, of each sample was acquired using FTIR spectrometer (Perkin Elmer Spectrum One) shown in figure 3.8. For this purpose, all samples were scanned at a room temperature of 22-24 ºC. Prior to obtaining the samples spectra, a background measurement on a pellet holder with a pellet of KBr only was used to account for the infrared light transmission losses in the KBr pellet and for moisture absorbed from atmosphere.

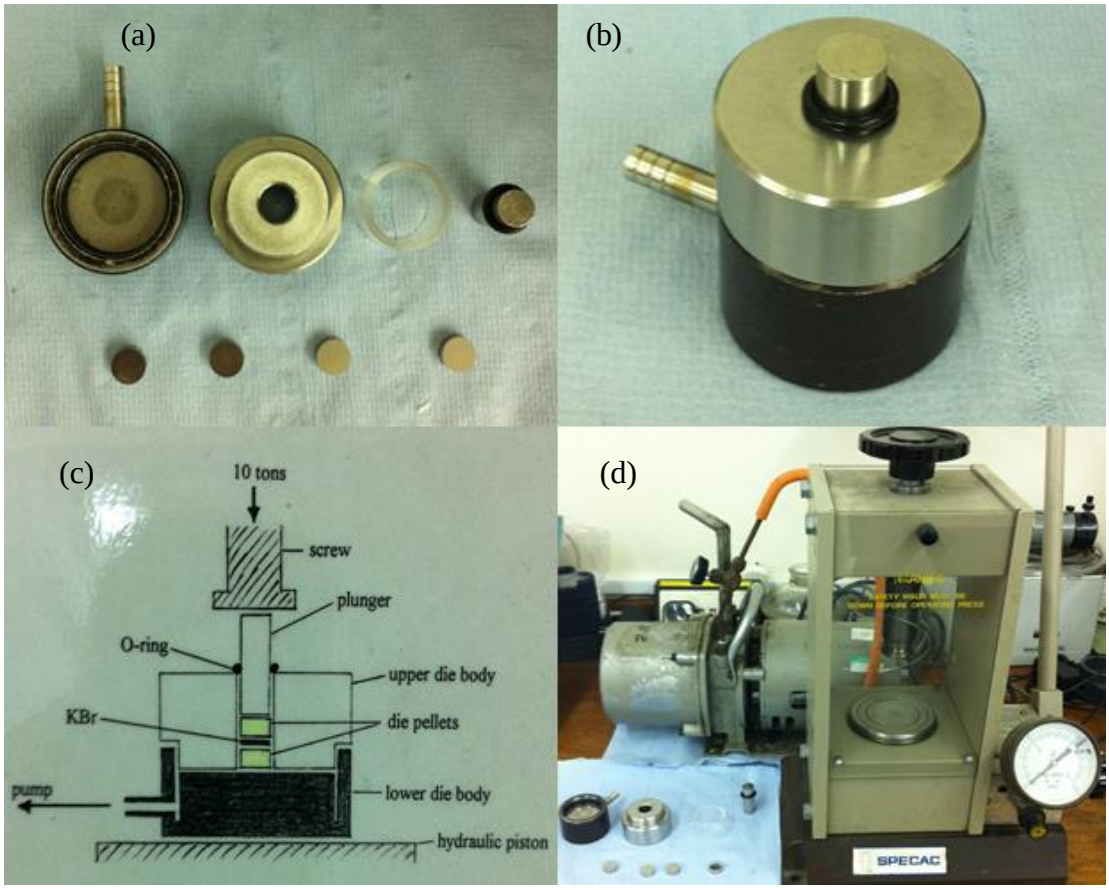

Figure 3.7 (a) die components (b) assembled die (c) die cross section (d) press machine for making pellets

Figure 3.8 FTIR spectrometer (Perkin Elmer Spectrum One)

Specific extinction,e^*, was calculated using equation (3.3) (Modest, 2003).

$$e^* = -\ln(\tau)/L \times \rho \quad (3.3)$$

where

τ is the transmission (%) obtained using FTIR

L the equivalent thickness (m)

ρ the density of sample (kgm^{-3})

The equivalent thickness (L) of sample in pellet corresponding to monolithic sample was calculated using equation (3.4) (Wei et al., 2011)

$$L = (M \times m_p)/(A \times \rho) \quad (3.4)$$

where

M is mass of KBr pellet (kg)

m_p is the mass fraction of sample in pellet (%)

A is the area of pellet (m^2)

E_c the extinction coefficient, was calculated using equation (3.5) (Fricke, 1993) .

$$E_c = e^* \times \rho \quad (3.5)$$

This extinction coefficient was used in Rosseland approximation equation to calculate radiative conductivity of samples at 300 K over the wavelength range of 2.5-22.2 µm for all opacifier samples.

3.6 VIP core board manufacturing

Core boards were made from loose powder mixture samples by uniaxial compressing using a Universal Testing Machine. For this purpose a special metallic die with the internal dimension of 100 mm × 100 mm was manufactured. The die was such that its parts were easily assembled and disassembled using steel screws. Side steel plates of die were assembled to each other and base plate with screws. A thin film of plastic film was placed on the base plate to avoid any sticking of core board with it during compaction. Die was filled with required amount of sample uniformly to achieve top even surface and a thin film of plastic was also placed on the top surface of sample powder. Pressure of 1.3 MPa was applied on the powder in the die using Universal Test Machine INSTRON 8501 shown in figure 3.9.

Figure 3.9 Compaction of core boards using INSTRON 8501 Test Machine

Pre-load was set at 10 N and speed for applying load was 10 mm/min for all samples. After applying the load, pressure was released slowly in 30 minutes to avoid any defects in compact due to sudden release of pressure. Core boards were ejected from the die by disassembling its side plates. Finally, thin plastic films were removed from the top and bottom surfaces of the core boards. Weight of each core board was measured and densities were calculated using the dimensions and mass of core boards. VIP core boards of sizes 100 mm × 100 mm × 12 ± 1 mm (using sample 1, 2, 4 and 5) and 100 mm × 100 mm × 15 ± 1 mm (using sample 3) were prepared to measure their thermal performance.

3.7 Thermal conductivity measurement of VIP core board

Thermal conductivity of core boards and VIP prototypes was measured by a guarded hot plate apparatus, shown in figure 3.10, at Empa (Swiss Federal Laboratories for Materials Testing) designed for small samples 100 mm×100 mm of low thermal conductivity values. This equipment was calibrated using conventional expanded polystyrene samples measured once in the standard test equipment and then cut into smaller pieces to be measured in a second run in this smaller apparatus (Stahl et al., 2012). Accuracy of this device was measured to be ±2 $mWm^{-1}K^{-1}$. Thermal conductivity was measured over a measuring zone of 25 mm × 25 mm. The mean temperature of the samples was equal to the room temperature of 22 ± 1 ºC with the cold side held at 14 ± 1 ºC and the warm, upper side, having measuring zone held at 30 ± 1ºC. Thermal conductivity was calculated from Fourier's Law using the temperatures of the plates, the heat input and the thickness of the samples.

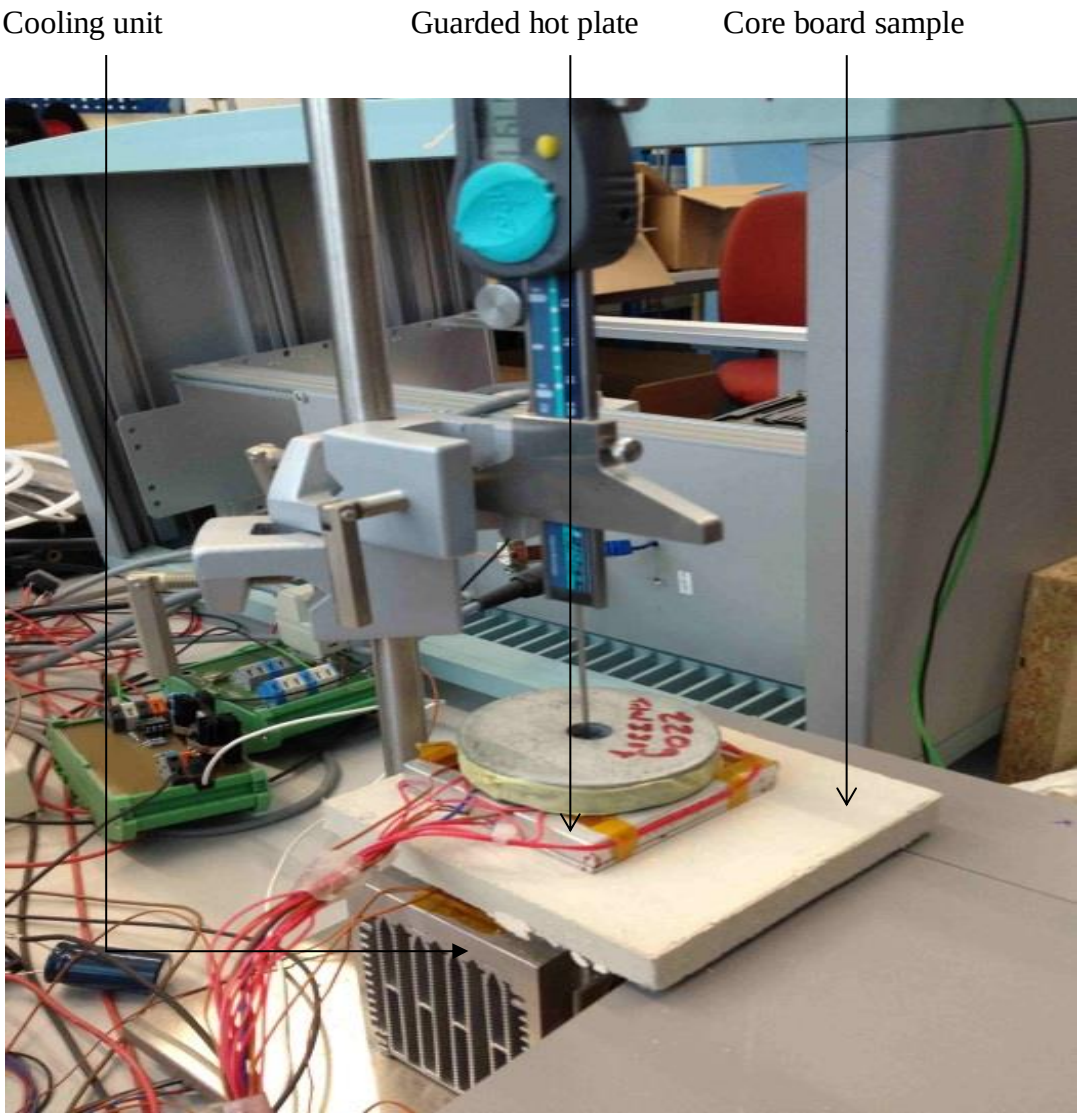

Figure 3.10 Thermal conductivity measurements of core boards using guarded hot plate apparatus

3.8 Conclusion

Pore size assessment, radiative conductivity and thermal conductivity data is critical to optimise the mass% of different constituents in composite to be used as effective core material for VIPs. In this chapter, materials and method to develop new composite material using low cost expanded perlite for VIP core along with the composition of the samples used for this research were presented. The samples were characterised for pore size, porosity and surface area using TEM, SEM, MIP and Gas adsorption methods. This pore size data is essential to investigate the influence of pore size and pressure on the gaseous conductivity of composite samples. Fumed silica aggregates material has been mixed with expanded perlite

to fill the pores of expanded perlite completely or partially reducing the pore size of composite samples. It was found that in composite samples fumed silica aggregates got into the larger pores of expanded perlite completely and partially which made the macropores of expanded perlite filled with fumed silica containing mesopores and micropores. Average pore diameters of composite samples were found to be in the range of 155-290 nm. IR transmission spectrums for evaluating the opacifying effect and optimising the critical doping mass of different opacifiers over a range of wavelength were acquired using FTIR spectrometer. FTIR method, experimental procedure for acquiring transmission spectrum and radiative conductivity calculation of composite samples were described. Thermal conductivity of core boards was measured using small size guarded hot plate apparatus. Methods of manufacturing core board from composite powder samples and measuring thermal conductivity of core boards along with the experimental conditions were presented.

Chapter 4

Thermo-Physical Analysis of Expanded Perlite- Fumed Silica Composite VIP Core Material

4.1 Introduction

Effectiveness of a material in a VIP core depends upon its thermo-physical properties such as porosity, pore size, density and thermal conductivity including gaseous and radiative conductivities. Generally, material with lower thermal conductivity and density, higher porosity and smaller pore size are suitable for use as VIP core. Evaluation of these thermo-physical properties of a material is required to assess its suitability as a VIP core. In this chapter, experimental results of thermo-physical properties of expanded perlite-fumed silica composite proposed in this research as low cost VIP core material are presented. Influence of addition of expanded perlite on different properties of low cost composite material is also investigated aiming at optimisation of this composite along with SiC opacifier and polyester fibres as an alternative material for the core of a VIP. Samples containing range of mass ratios of expanded perlite and fumed silica along with SiC opacifier and fibres have been investigated in order to identify optimum composition of composite material. Radiative conductivity of these composites was also calculated using the experimental transmission data obtained by FTIR spectroscopy. Centre of panel thermal conductivity of core boards made of composite samples was measured using guarded hot plate apparatus at atmospheric pressure to identify optimum composite for VIP core.

4.2 Effect of expanded perlite on gaseous thermal conductivity

Gaseous conductivity depends on the ratio of mean free path of gas molecules and the pore size of the material. Pore size of core material same order of size as mean free path of air are required to suppress the gaseous conductivity. Gaseous thermal conductivity of air at 25 °C can be calculated employed the following correlation, equation (4.1) (Kwon et al., 2009)

$$\lambda_G = \lambda_0/(1 + 0.032/P\Phi) \quad (4.1)$$

where

λ_G is the gaseous thermal conductivity ($Wm^{-1}K^{-1}$)

λ_0 is the thermal conductivity of air at atmospheric pressure ($Wm^{-1}K^{-1}$)

Φ is the pore size (m)

P is the pressure (Pa)

Gaseous conductivity does not fully develop even at atmospheric pressure in materials with pore size around 100 nm and can be suppressed at pressure of 10 mbar. However, Gaseous conductivity fully develops at higher pressures in materials containing micron size pores and requires a low pressure approximately in the range of 0.01 mbar to suppress the gaseous conductivity as shown in figure 4.1.

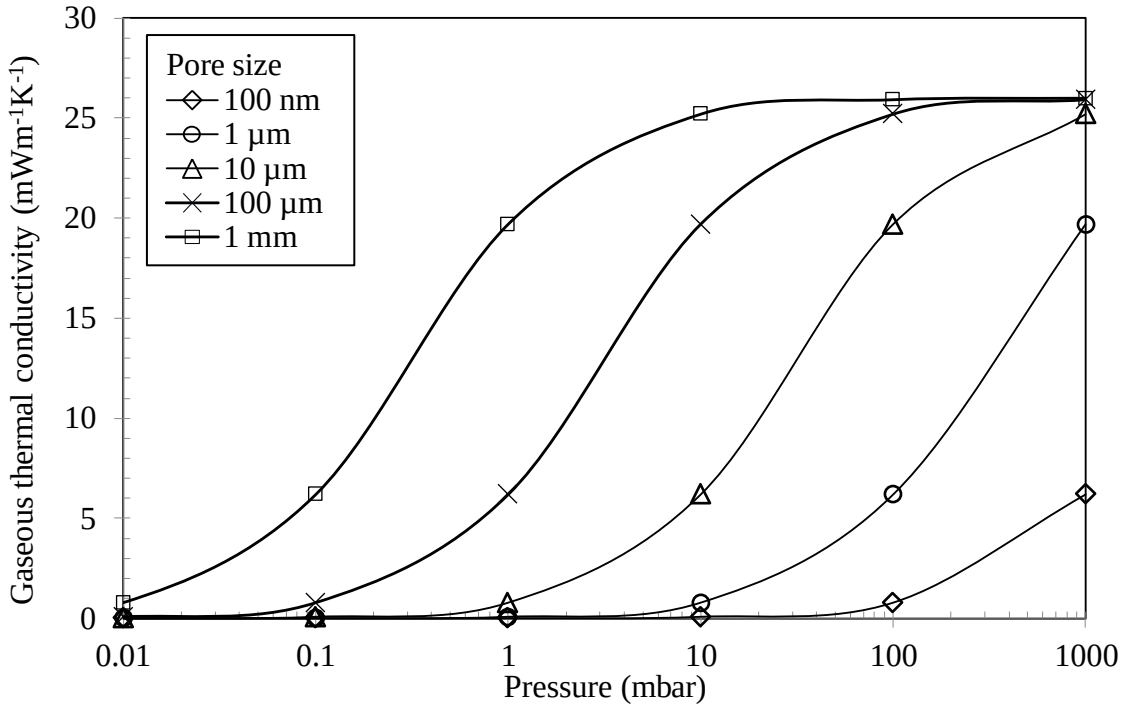

Figure 4.1 Variation of gaseous thermal conductivity with pore size and gas pressure

In the case of expanded perlite - fumed silica composite, filling the pores of expanded perlite with fumed silica aggregates containing micropores and mesopores helps in reducing the gaseous conductivity of expanded perlite even at higher pressures. Gaseous thermal conductivity (λ_G) of samples A, B and C (table 3.5) using the average pore diameter data and pore size range of expanded perlite between 3-10 µm, at different pressure levels was calculated using equation 4.1. Results are shown in figure 4.2. It is evident that for expanded perlite with a pore size range of 3-10 µm, a low pressure of approximately <0.1 mbar is required for gaseous thermal conductivity to become negligible. For composite samples A,B

and C having average pore size in the range of 150-300 nm relatively high pressure approximately 5 mbar was enough to suppress the gaseous thermal conductivity compared to a low pressure of <0.1 mbar required in case of pure expanded perlite. Gas pressure in VIPs will rise due to permeation through envelope surface, sealing flanges and out gassing of core material. This increase in gas pressure leads to rise in gaseous thermal conductivity. For larger pore size material the rise of gaseous conductivity will be higher compared to that in smaller pore size materials as shown in figure 4.1 and 4.2. For the largest pore size of expanded perlite (10 µm), the gaseous thermal conductivity at 100 mbar was calculated to be 19.6 $mWm^{-1}K^{-1}$. Three composite samples which have smaller average pore sizes gaseous conductivity was calculated to have a minimal rise in gaseous thermal conductivity to a value of 2.1 $mWm^{-1}K^{-1}$, 1.2 $mWm^{-1}K^{-1}$ and 1.5 $mWm^{-1}K^{-1}$ for sample A, B and C respectively.

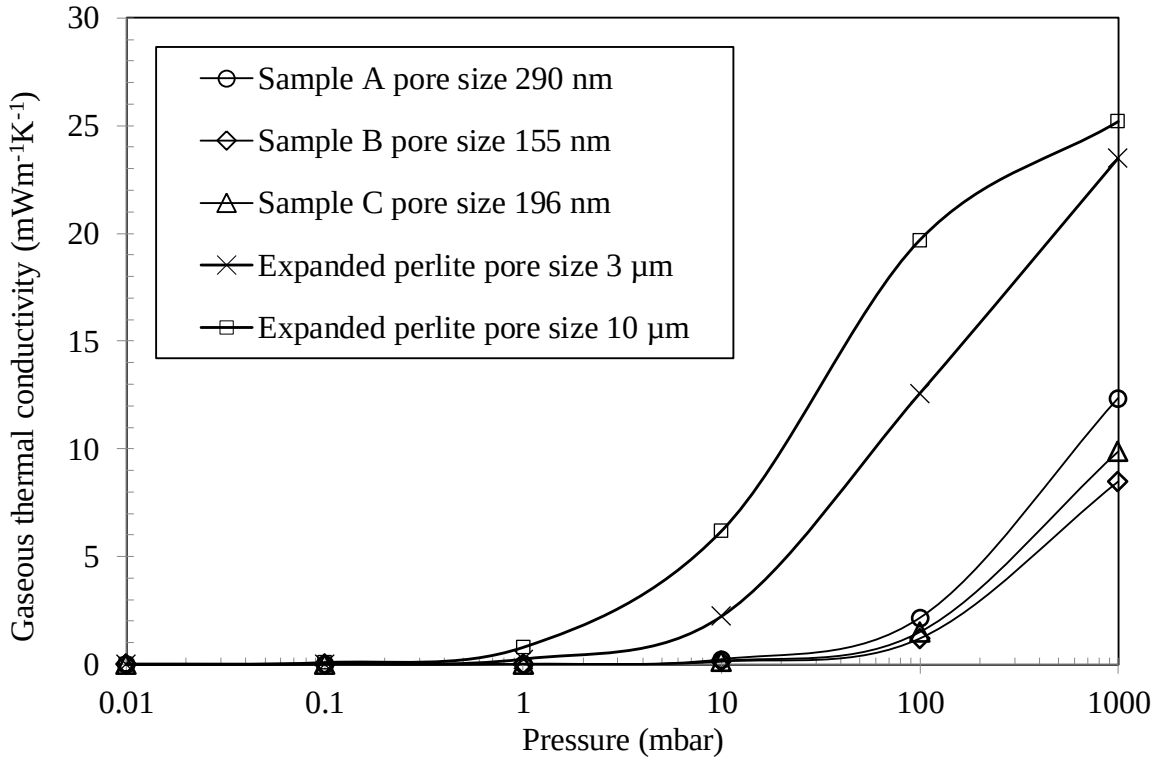

Figure 4.2 Variation of gaseous thermal conductivity of expanded perlite (pore size 3 -10 µm) and composite samples A, B and C as a function of gas pressure and pore size

Upon increasing the pressure from 100 mbar to atmospheric pressure gaseous thermal conductivity was further increased to 23.4-25.1 $mWm^{-1}K^{-1}$ for expanded perlite with pore size range of 3-10 µm. However, this increase in gaseous thermal conductivity at atmospheric pressure was 12.3 $mWm^{-1}K^{-1}$, 8.4 $mWm^{-1}K^{-1}$, 9.8 $mWm^{-1}K^{-1}$ for samples A, B and C respectively. Clearly, the composite samples A,B and C were less sensitive to increase in

thermal conductivity upon rise in pressure compared to pure expanded perlite at relatively high pressures (>1 mbar). Use of any of these samples will not affect the gaseous thermal conductivity below 10 mbar. However, sample with low expanded perlite mass% was preferred for VIP core due to a low density and correspondingly smaller gaseous thermal conductivity at ambient conditions. This combination of characteristics is expected to result in a low overall thermal conductivity under evacuated conditions.

4.3 Bulk density and porosity of fumed silica and expanded perlite composites

Results of bulk density and porosity obtained by MIP investigation are given in table 4.1. Using expanded perlite as a replacement of fumed silica in composite samples led to increase in density and decrease in porosity. Composite sample A was found to have a low density of 69 kgm^{-3} and this density values increased to 167 kgm^{-3} and 220 kgm^{-3} in composite sample B and C respectively. This increase in density is due to the presence of high density expanded perlite in composite sample B and C which contain 30 and 60 mass% of expanded perlite respectively.

Table 4.1 Bulk density and porosity results of composite samples A-C obtained by MIP

Sample	**Ratios FS:EP:SiC:PF**	**Porosity (%)**	**Bulk density (kgm^{-3})**
A	80:0:12:8	90	69
B	50:30:12:8	83	167
C	20:60:12:8	83	220

This rise in bulk density affects the solid conductivity and needs to be kept at minimum to obtain low solid thermal conductivity of VIP core. Porosity of all samples was calculated from bulk volume and pore volume using the equation (4.2) (Webb, 2001). Bulk volume and pore volume were measured using MIP.

$$Porosity\ (\%) = \left(V_{pore}/V_{Bulk}\right) \times 100 \qquad (4.2)$$

where

P % is the percent porosity

V_{pore} is volume of pores (m^3g^{-1})

V_{Bulk} is sample bulk volume (m^3g^{-1})

For samples A, B and C porosity was calculated to be 90%, 83% and 83% respectively. This indicated that with the addition of expanded perlite in the composite porosity decreased compared to sample A, for example; sample B and C with expanded perlite mass ratios of 30% and 60% respectively had porosity 7% lower than that of sample A with no expanded perlite at all. Composite sample B containing 30 mass% of expanded perlite was more suitable for VIP core due to its lower bulk density compared to that of sample C and is well within the range of 150-220 kgm^{-3} for VIPs reported by Simmler et al. (2005). However, porosity of sample B and C is less than that of sample A containing 80 mass% of highly porous fumed silica.

4.4 Effect of expanded perlite on thermal conductivity of core boards

Measurement of thermal conductivity at ambient conditions is the first step to optimise the core board composition with respect to thermal conductivity. Core board having the lowest overall thermal conductivity at ambient conditions is expected to exhibit lower thermal conductivity under vacuum conditions. To choose the optimal composition, samples were prepared to cover the widest range of the composition of fumed silica and expanded perlite, starting from no expanded perlite and gradually increasing the mass ratio of expanded perlite and decreasing the mass ration of fumed silica. For this purpose core boards 1-5 covering a wide range of mass ratios of both fumed silica and expanded perlite along with fibre (8 mass%) and opacifier (SiC 12 mass%) were prepared using the method described in chapter 3. The core boards manufactured are shown in figure 4.3. Mass ratios of both fumed silica and expanded perlite and experimentally measured values of thermal conductivity of core boards 1-5 at ambient conditions measured using guarded hot plate apparatus at Empa Laboratories Switzerland are also shown in figure 4.4. Sthal et al. (2012) has adopted the absolute error value for same device as ±2 $mWm^{-1}K^{-1}$ to have additional confidence on results. This assumption leads to a relative error of 3.8 to 8.3% and has no significant impact on results of thermal conductivity of core boards at ambient conditions. However, in evacuated conditions when thermal conductivity values are an order of magnitude lower than the error of ±2 $mWm^{-1}K^{-1}$ becomes significant. Core board 1 which had the highest mass ratio of fumed silica 80 mass% without any presence of expanded perlite had the lowest thermal conductivity of 23.9 $mWm^{-1}K^{-1}$. With the addition of expanded perlite mass ratio

from 0 mass% to 60 mass% the thermal conductivity of the core board increased from 23.9 $mWm^{-1}K^{-1}$ to 53.2 $mWm^{-1}K^{-1}$. An increase in expanded perlite mass ratio from 0% to 30% in composite led to minimal rise of 3.9 $mWm^{-1}K^{-1}$ in thermal conductivity from 23.9 $mWm^{-1}K^{-1}$ to 27.8 $mWm^{-1}K^{-1}$ respectively. However, a significant rise in thermal conductivity was measured when expanded perlite mass ratio was increased beyond this threshold value of 30 mass%. An increase in expanded perlite mass ratio from 30% to 60% led to a rise of 25.4 $mWm^{-1}K^{-1}$ in thermal conductivity from 27.8 $mWm^{-1}K^{-1}$ to 53.2 $mWm^{-1}K^{-1}$ respectively as shown in figure 4.5. Clearly, presence of low cost expanded perlite (compared to fumed silica) in the composite samples leads to increase in thermal conductivity. However, this rise in thermal conductivity needs to be minimum to achieve a cost reduction potential by displacing expensive fumed silica with comparatively cheaper expanded perlite. Core board 3 containing 30 mass% of expanded perlite appeared to be the optimal sample due to a 16.3% rise of thermal conductivity compared to the core board 1 containing 80 mass% of expensive fumed silica, at ambient conditions which could be decreased by an order of magnitude at lower pressure for use as core in VIPs depending upon the pore size. Thermal conductivity performance of core board 3 achieved under vacuum conditions has been discussed in chapter 5.

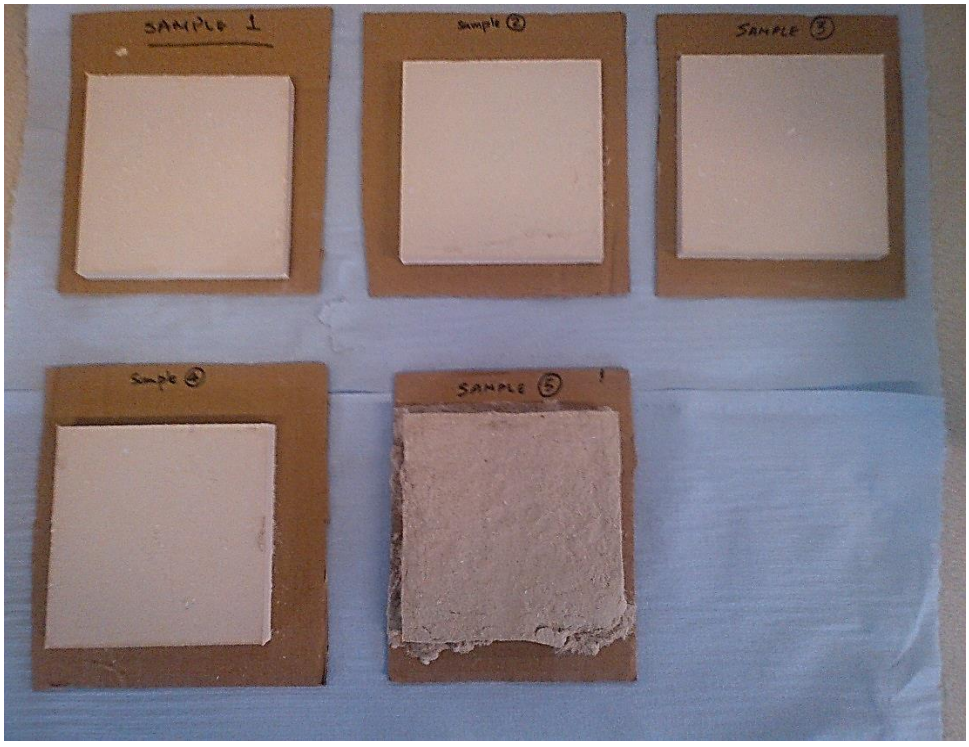

Figure 4.3 Core boards samples (100 mm × 100 mm) 1-3 (Top left to right) and 4-5 (Bottom left to right) placed on cardboard pieces

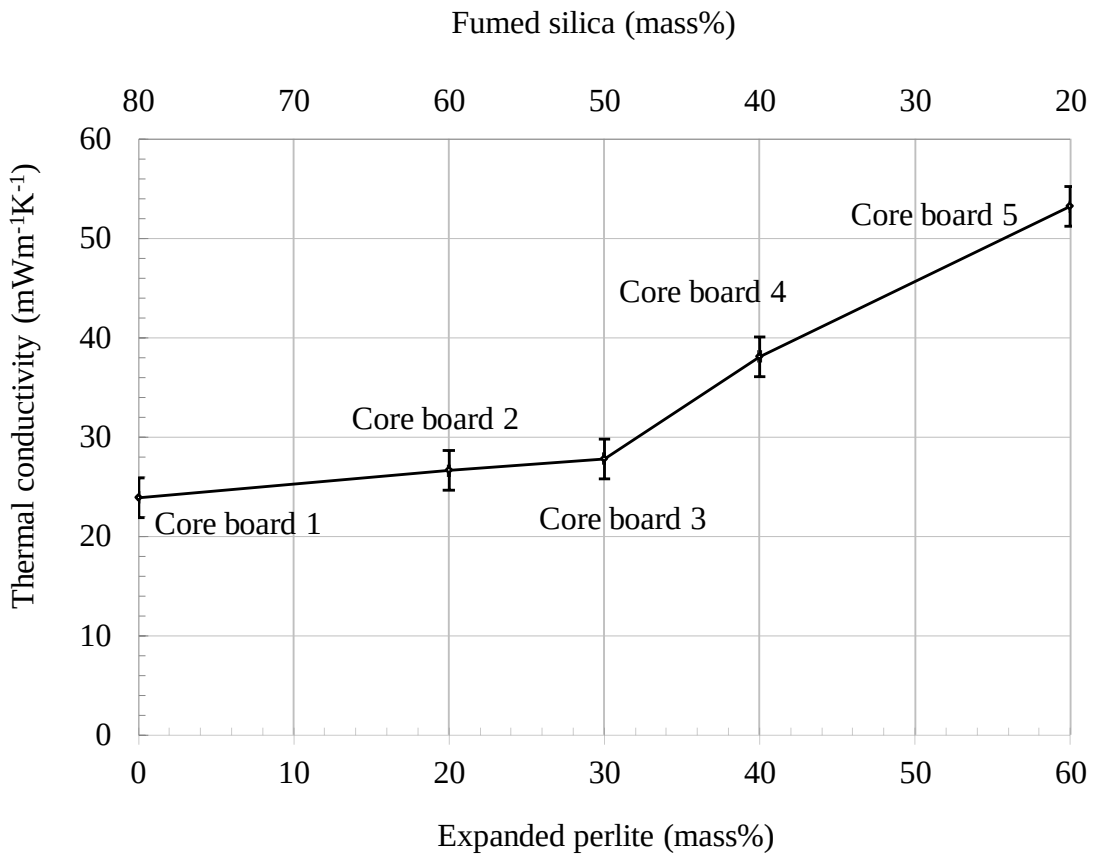

Figure 4.4 Thermal conductivity values of core boards at atmospheric conditions prepared with composite samples 1-5 with different mass ratios of expanded perlite and fumed silica along with SiC (12%) and fibre (8%)

4.5 Influence of expanded perlite on radiative conductivity

Results showed that expanded perlite has radiative exchange suppressing properties and acted as an opacifier in the composite samples leading to a lower radiative conductivity of core material employed. The advantage of this opacifying effect is a lower quantity of opacifier such as SiC will be required in order to achieve enhanced opacifying properties. Specific extinction (e^*) values for samples 1-5 over a wavelength range of 2.5-22.2 μm were calculated using the experimentally measured values of transmission shown in figure 4.5 in equations (4.3) and the parameters given in table 4.2.

$$e^* = -\ln(\tau)/L \times \rho \quad (4.3)$$

where

τ is the transmission (%) obtained using FTIR

L is the equivalent thickness (m)

ρ is the density of sample (kgm^{-3})

These specific extinction values were used for calculating the radiative conductivity of samples.

The radiative conductivity of samples was calculated using the equation (4.4) and parameters given in table 4.2.

$$\lambda_R = 16n^2\sigma T_r^3/3(e^* \times \rho) \quad (4.4)$$

where

n is the mean index of refraction

σ is the Stefan-Boltzmann constant (5.67×10^{-8} $Wm^{-2}K^{-4}$)

T_r is the average temperature within the insulation material (K)

$(e^* \times \rho)$ is the extinction coefficient of the insulating material

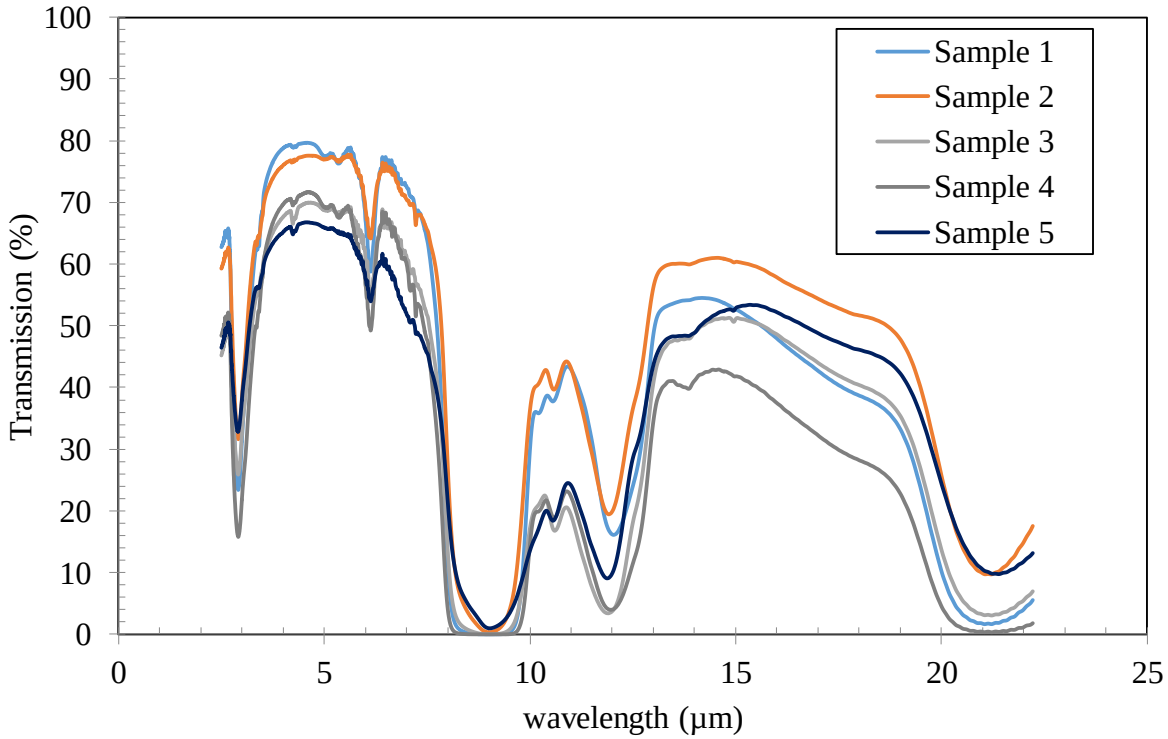

Figure 4.5 IR transmission (%) obtained using FTIR for samples 1-5

Table 4.2 Sample content and parameters used for radiative conductivity calculation of sample 1-5 at 300 K

Parameter	Sample 1	Sample 2	Sample 3	Sample 4	Sample 5
Composition	FS:EP:SiC:PF 80:0:12:08	FS:EP:SiC:PF 60:20:12:08	FS:EP:SiC:PF 50:30:12:08	FS:EP:SiC:PF 40:40:12:08	FS:EP:SiC:PF 20:60:12:08
Density (kgm^{-3})	235	281	332	342	421
Equivalent thickness (m)	3.19×10^{-5}	2.67×10^{-5}	2.26×10^{-5}	2.19×10^{-5}	1.78×10^{-5}
Mean index of refraction	1.5	1.5	1.5	1.5	1.5

Radiative conductivity values for wavelengths between 2.5 and 22.2 µm are shown in figure 4.6. It was found that with increasing mass ratio of expanded perlite average radiative conductivity of samples decreased.

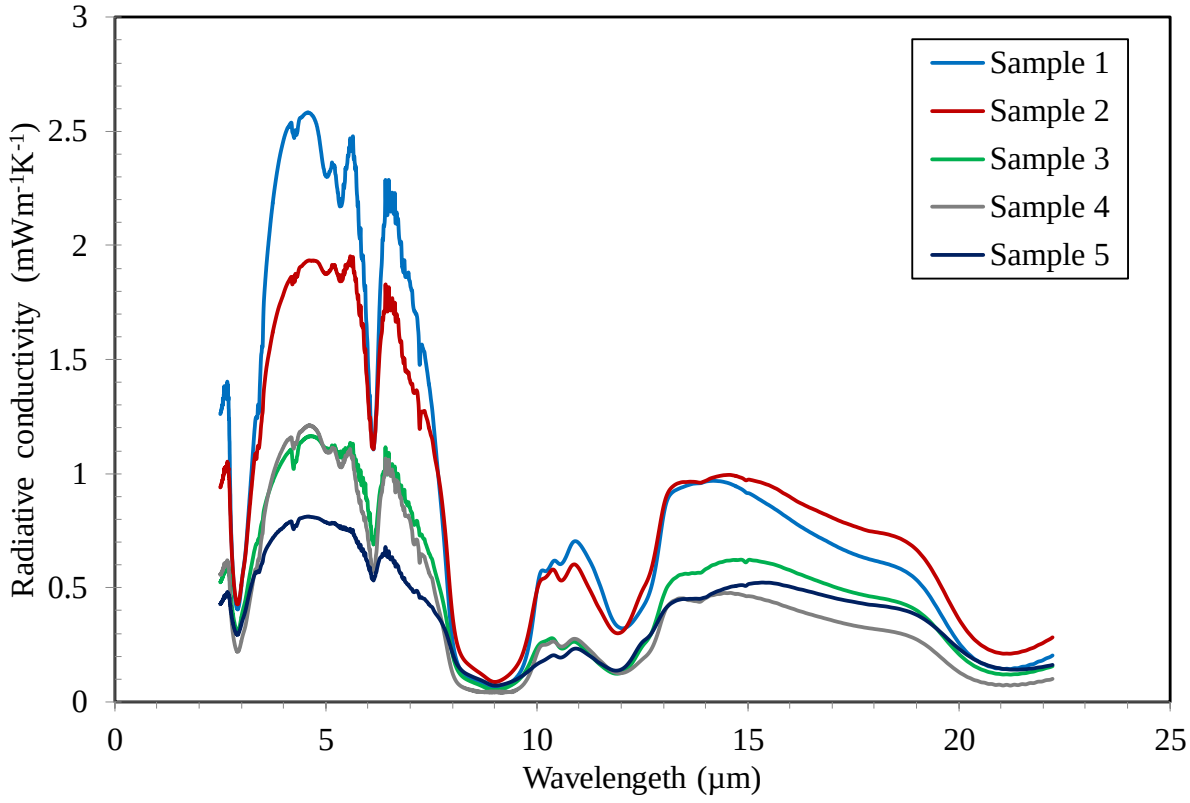

Figure 4.6 Comparison of radiative conductivity for composite samples 1 - 5

For sample 1 with fumed silica mass ratio of 80% and no expanded perlite, average radiative conductivity over a wavelength rang of 2.5 and 22.2 μm was calculated to be 1.37 $mWm^{-1}K^{-1}$, the highest of all samples. Sample 2 with mass ratio of expanded perlite 20%, radiative conductivity was calculated to be 1.12 $mWm^{-1}K^{-1}$. With increased mass ratios of 30%, 40% and 60% of expanded perlite in samples 3, 4 and 5 respectively, average radiative conductivity values decreased to 0.67 $mWm^{-1}K^{-1}$, 0.63 $mWm^{-1}K^{-1}$ and 0.50 $mWm^{-1}K^{-1}$ accordingly. This decrease in radiative conductivity can be due to the presence of large particles of expanded perlite (particle size 10-750 μm) and higher density compared to fumed silica in the composite. Radiative conductivity is inversely proportional to the density of sample and with increase in density of sample the radiative conductivity decreases. However, an increase in expanded perlite beyond 30 mass% to decrease in radiative conductivity will not be able to compensate the increase in the solid thermal conductivity and will lead to a higher centre of panel thermal conductivity for a VIP core. Effect of SiC on the radiative conductivity was similar in all samples as they contained the same amount of SiC opacifier. Mixing method used for preparing the samples was also similar and has not had any effect on the radiative conductivity of samples.

4.6 Opacifier (SiC) influence on radiative conductivity

Fumed silica offers low resistance to radiative heat transfer due to its small particle size and low bulk density and required to be doped with an opacifier to reduce the radiative heat transfer. Thermal conductivity of pure silica at room temperature is higher by 2-3 $mWm^{-1}K^{-1}$ than that of SiC opacified precipitated silica (Caps and Fricke, 2000). However, opacifiers typically have relatively high density and lead to a higher solid thermal conductivity. Higher content of opacifier in VIP core material leads to higher solid conductivity and may counterbalance any benefit of reduced radiative conductivity. Conversely, an inadequate mass content of opacifier in a VIP core will yield higher radiative conductivity. Therefore, an optimum content of an opacifier requires to be identified to achieve a minimum radiative conductivity in VIP cores. In the present study, expanded perlite and fumed silica composites samples 6-8 (shown in table 4.3) containing different mass ratios of SiC were prepared to analyse the influence of varying amounts of SiC on radiative conductivity (λ_R). Expanded perlite and polyester fibre mass ratios were fixed as 30% and 8% respectively in samples 6-8.

Table 4.3 Expanded perlite and fumed silica composites sample containing varying mass ratios of SiC

Sample 6	Sample 7	Sample 8
FS:EP:SiC:PF	FS:EP:SiC:PF	FS:EP:SiC:PF
57:30:05:08	52:30:10:08	47:30:15:08

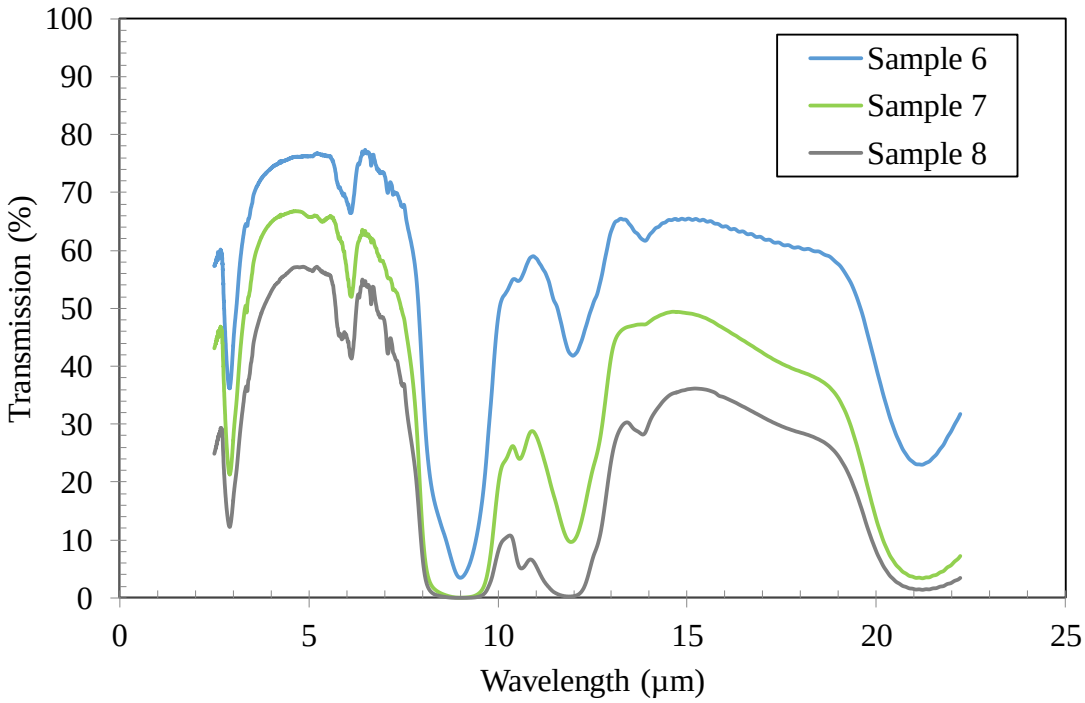

Figure 4.7 IR transmission (%) obtained using FTIR for samples 6-8

IR transmission spectrum through sample 6-8 was obtained using FTIR spectrometer and shown in figure 4.7. It is show that with increasing SiC mass ratio from 5% to 15% infrared transmission values decreased over the wavelength range of 2.5-22.2 µm. Radiative conductivity of samples 6-8 was calculated using equations (4.3) and (4.4) for temperature 300 K over the wavelength range 2.5-22.2 µm. Results of radiative conductivity of samples 6-8 are shown in figure 4.8. Average radiative conductivity of sample 6 (SiC 5%) was found to be 1.4 $mWm^{-1}K^{-1}$. Sample 7 (SiC 10%) had reduced average radiative conductivity of 0.9

$mWm^{-1}K^{-1}$ while radiative conductivity further decreased to 0.6 $mWm^{-1}K^{-1}$ for sample 8 (SiC 15%)

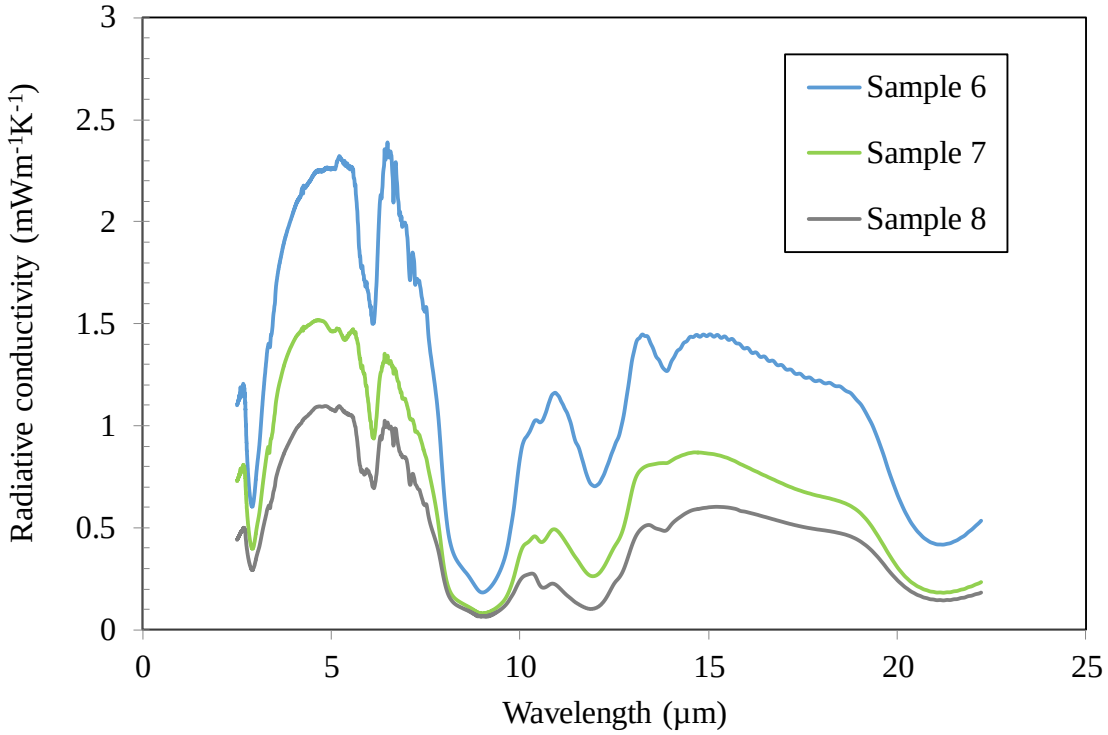

Figure 4.8 Comparison of radiative conductivity for composite samples 6 - 8

Based on these results, a composite containing mass ratio of 30% of expanded perlite and 10% to 15% of SiC has been identified as an optimum core material for VIPs due to its optimal density and radiative conductivity.

4.7 Conclusion

Expanded perlite a low cost material in the form of composite with fumed silica is evaluated for use in VIPs as core material in order to reduce the cost of VIP core material. Thermo-physical properties of composites samples containing range of mass ratios of expanded perlite, fumed silica along with SiC opacifier and fibre was determined. It was found that expanded perlite has pores ranging from 3-10 µm yielding gaseous conductivity in the range of 12.5-19.6 $mWm^{-1}K^{-1}$ at 100 mbar pressure. To reduce this higher gaseous conductivity its pore size needs to be reduced by incorporating materials of smaller size. Fumed silica

aggregates material has been mixed with expanded perlite to fill the pores of expanded perlite completely or partially reducing the pore size of composite samples yielding lower gaseous conductivity values of 1.2-2.1 $mWm^{-1}K^{-1}$ at 100mbar and became negligible upon further decreasing pressure below 10 mbar. Additional benefit of expanded perlite was its influence on reducing radiative conductivity owing to the large particles of expanded perlite (particle size 10-750 µm) and higher density compared to fumed silica in the composite samples. Expanded perlite mass ratio of 30% was identified as an optimum amount of expanded perlite in to decrease radiative conductivity through composite sample. Expanded perlite mass ratio beyond this threshold value will lead to high density and increase in the solid thermal conductivity of core board.

Thermal conductivity of composite materials in the form of core boards containing range of mass ratios of expanded perlite and fumed silica along with fibre (8 mass%) and opacifier (12 mass%) has been measured to assess the influence of expanded perlite on thermal conductivity. Thermal conductivity of core boards increased as the expanded perlite mass ratio was increased. An increase in expanded mass ratio from 0% to 30% led to rise of 3.9 $mWm^{-1}K^{-1}$ in thermal conductivity. However, increasing expanded perlite from 30 mass% to 60 mass% led to 25.4 $mWm^{-1}K^{-1}$ increase in thermal conductivity from 27.8 $mWm^{-1}K^{-1}$ to 53.2 $mWm^{-1}K^{-1}$. Based on these results, a composite containing mass ratio of 30% of expanded perlite and 50 mass% fumed silica along with fibre and opacifier has been identified as a potential core material for VIPs and its thermal performance in evacuated conditions has been further investigated in chapter 5 to evaluate its suitability as VIP core material.

Chapter 5

VIP Prototype Development and Thermal Performance Evaluation

5.1 Introduction

Generally, fumed silica is used as core material of VIP due to its low thermal conductivity, low density and smaller pore size. However, it is an expensive material and a contributing factor to higher cost of VIPs. For reducing the cost of VIPs alternative low cost materials are required to be developed to completely or partially replace the fumed silica. One of the main objectives of this research study was to develop low cost material with suitable properties and characterise its effectiveness as a core material for VIPs. This chapter provides the detailed information about the development of VIP prototype using core material consisting of 50 mass% of fumed silica, 30 mass% of expanded perlite along with 8 mass% of fibre and 12 mass% of SiC opacifier optimised in chapter 4. Thermal conductivity of VIP prototype manufactured with optimised core material at range of pressures was measured experimentally using guarded hot plate apparatus at Empa, the Swiss Federal Laboratories for Materials Science and Technology. Results of thermal conductivity of VIP prototypes at evacuated and atmospheric conditions were assessed to calculate solid, gaseous and coupling conductivities.

5.2 VIP Prototype development

5.2.1 Optimum composite core material

The composition of the composite used for core boards of VIP was 50 mass% of fumed silica (FS), 30 mass% of expanded perlite (EP), 8 mass% of polyester fibre (PF) and 12 mass% of SiC opacifier as identified in chapter 4. The VIP composite had optimum thermo-physical properties as listed in table 5.1.

Table 5.1 Thermo-physical properties of core material used for VIP prototypes

Property	Units	Value
Porosity	(%)	83
Average pore size	(nm)	155
Compact density	kgm^{-3}	332
Radiative conductivity (300 K)	$mWm^{-1}K^{-1}$	0.67

5.2.2 Core boards

Three core board specimens (S1,S2 and S3) were made at Brunel University London with optimised sample (50 mass% of fumed silica, 30 mass% of expanded perlite along with 8 mass% of fibre and 12 mass% of SiC) using the parameters as described in chapter 3. Size of the each core board was 100 mm×100 mm×15 mm. Core boards were dried at 105 °C for 24 hours prior to using for prototype manufacturing. Thickness, mass and density parameters of core board S1-S3 are given in the table 5.2.

Table 5.2 composition and parameters of core board specimens for VIP prototype

Specimen	Composition (mass%)	Thickness (mm)	Mass (g)	Density (kgm^{-3})	Weight loss after drying (%)
	FS : EP: SiC: PF				
S1	50 : 30 : 12 : 8	15	49.84	332.26	0.43
S2	50 : 30 : 12 : 8	15	49.69	331.26	0.45
S3	50 : 30 : 12 : 8	15	49.63	330.86	0.50

5.2.3 VIP Envelope

Envelope used for VIP prototype development was multilayer metallised polyethylene terephthalate (PET) and low density polyethylene (LDPE) laminate supplied by Hanita Coatings Limited (Israel). Water vapour transmission rate of envelope was ≤ 0.04 gm^{-2} per 24 hour as specified by the manufacturer. Envelope was prepared by heat sealing the two laminate together from three sides whilst the fourth side was kept open for placing the core board inside the envelope. VIP envelope sealed from three sides is shown in figure 5.1.

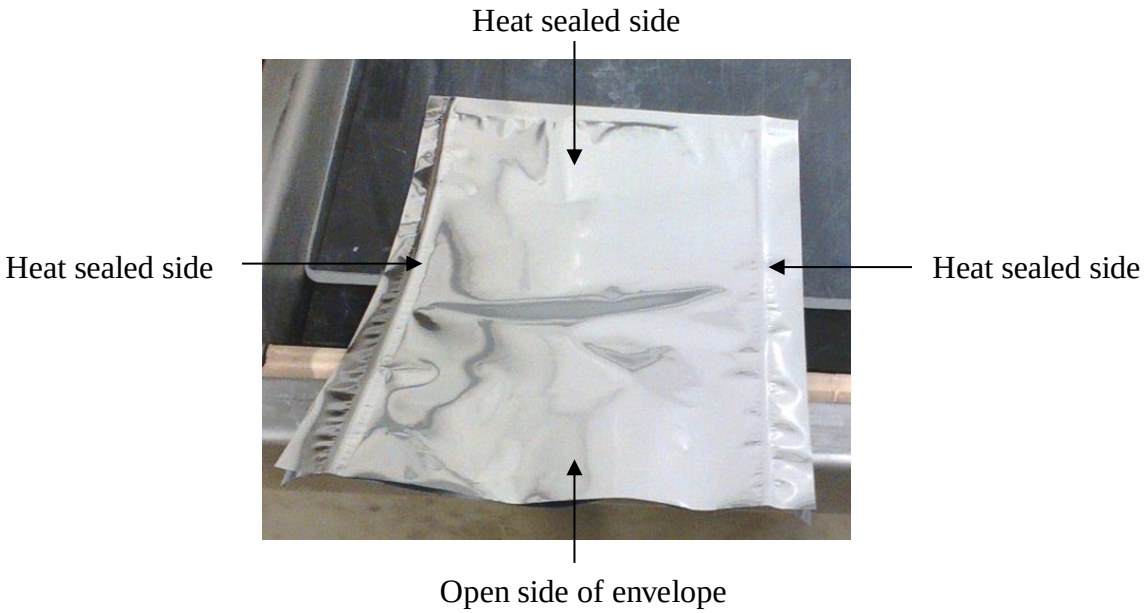

Figure 5.1 VIP envelope heat sealed from three side and open from fourth side for core insertion

5.2.4 VIP manufacturing process

VIP prototypes were manufactured using the vacuum sealing chamber at Empa, the Swiss Federal Laboratories for Materials Science and Technology. Core board was placed inside the envelope through the open side and placed inside the vacuum sealing chamber shown in figure 5.2 (a). The open side of the envelope was placed on the sealing bar of vacuum sealing chamber and envelop on the outside of seam was attached to the sealing bar with adhesive tape to prevent it from moving in the process of evacuation and sealing as shown in figure 5.2 (b). The chamber was evacuated to 0.5 mbar and vacuum was created inside the VIP envelope as shown in figure 5.2 (c). Once intended vacuum was reached the open side of envelop was sealed inside the vacuum sealing chamber as shown in figure 5.2 (d).

5.3 VIP core pressure measurement using the lift off method

The measurement of core pressure for the VIP is critical due to the depence of VIP thermal conductivity on internal perssure. The foil lift-off method was used for measuring the pressure inside a VIP which is used particularly for VIPs with flexible envelopes (Caps et al., 2008). The measurements were done at Empa, the Swiss Federal Laboratories for Materials Science and Technology at 25±1 °C and the set up is shown in figure 5.3..VIP prototypes were placed inside the vacuum chamber directly underneath the laser distance sensors to

measure theier internal perssures. Only two center laser distance meters readings were taken due to small size of the protoype samples. A diffuse reflective adhesive tape was placed on the middle of VIP prototype to detect the laser distance meter light.

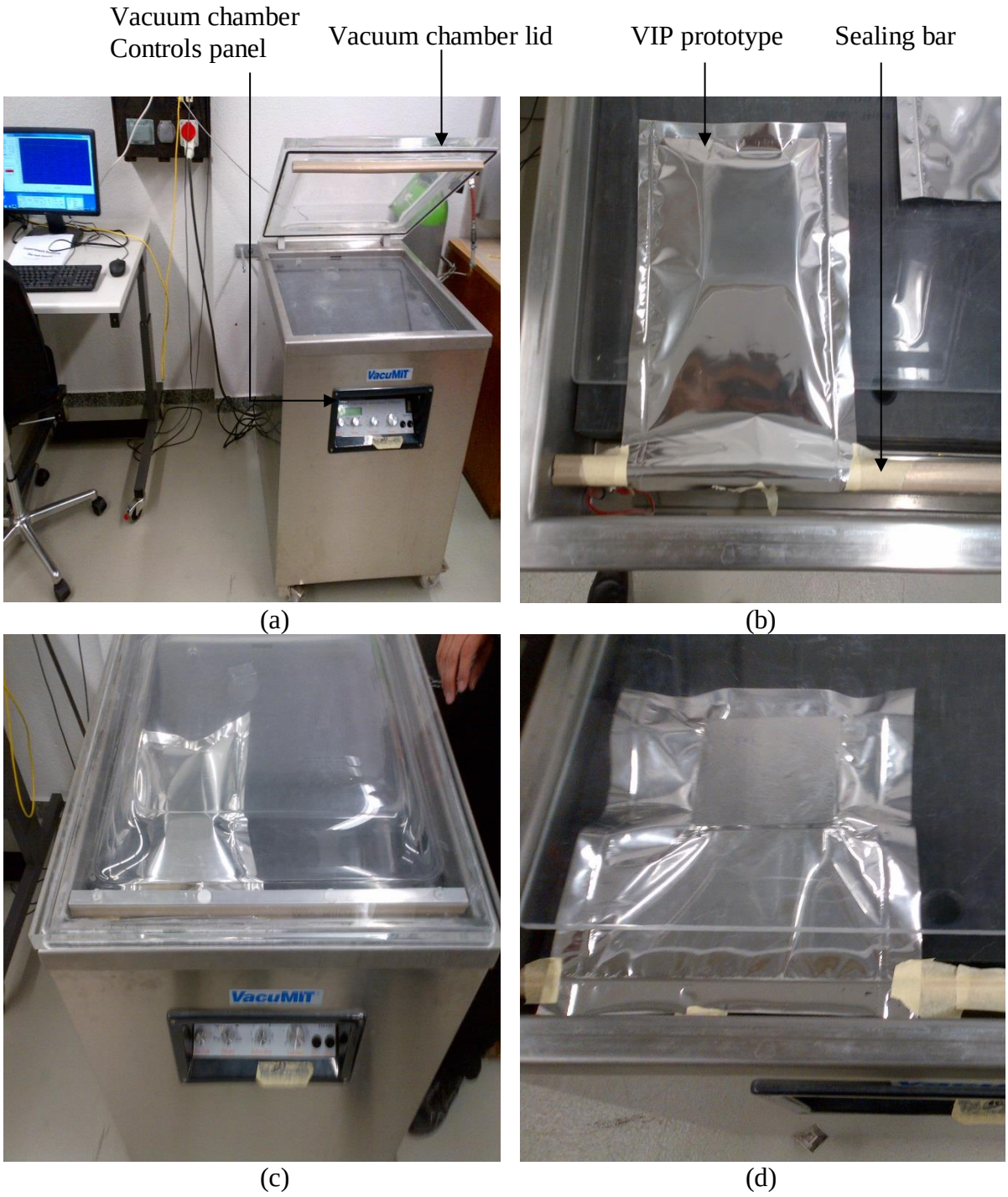

Figure 5.2 (a) Vacuum sealing chamber used for VIP prototype manufacturing (b) VIP prototype placed inside vacuum sealing chamber before evacuation (c) VIP prototype being

evacuated inside the vacuum sealing chamber (d) VIP prototype being sealed inside vacuum sealing chamber after evacuation

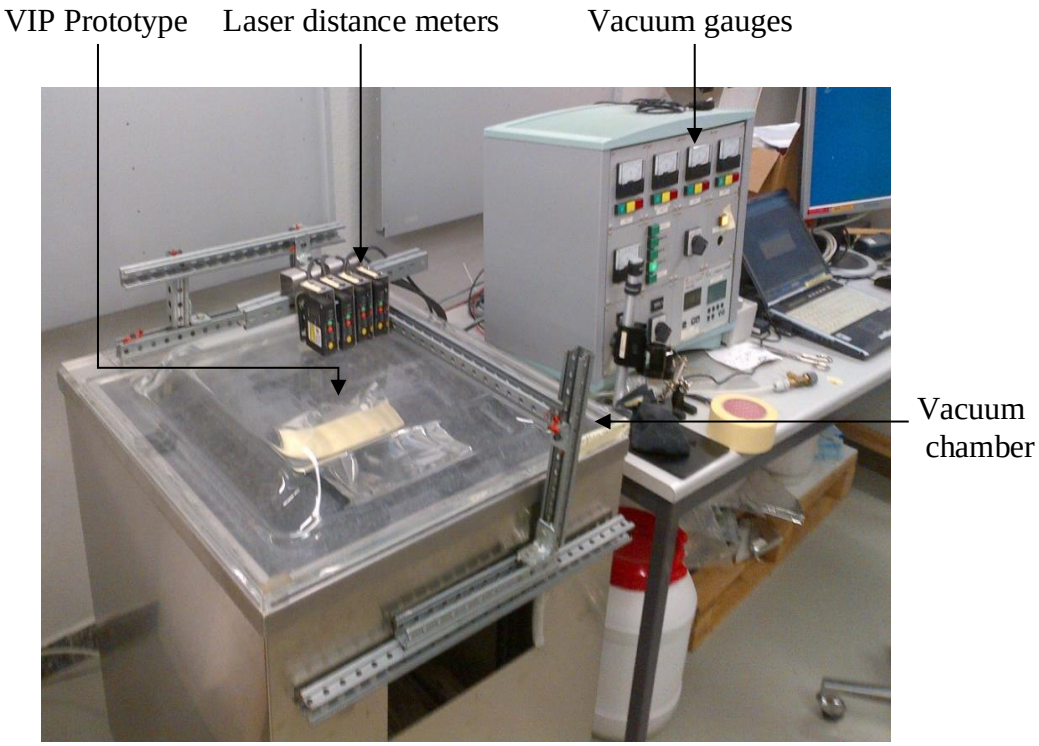

Figure 5.3 Envelope lift off method set up for measuring the perssure inside the VIP prototype

Pressure inside the chamber was lowered to allow the envelope to lift off. Envelope lift off was measured by laser distance sensor along with the chamber pressure. The data was analysed by drawing a graph of distance measurements and the chamber pressure. The start of enevelope lift off was approximated by two regression lines and the intersection of the lines were recorded. The results of the test are the average of two laser measuring points and absolute error of measurement was 0.1 mbar. VIP prototype internal perssure and corresponding thermal conductivity values are shown in section 5.4.

5.4 Thermal performance of VIP prototype

5.4.1 Centre of panel thermal conductivity

The centre of panel thermal conductivity of the VIP prototype specimens S1, S2 and S3 shown in figure 5.4,5.5 and 5.6 respectively was measured using small guarded hot plate

apparatus under room conditions at Empa, the Swiss Federal Laboratories for Materials Science and Technology as described in chapter 3. Centre of panel thermal conductivity of VIP specimens was measured at mean temperature of 22±1 °C for pressures varying from 0.5 mbar to 1000 mbar. The results obtained are shown in table 5.3. VIP S1, VIP S2 and VIP S3 were measured to have centre of panel thermal conductivities of 28.0 $mWm^{-1}K^{-1}$, 28.3 $mWm^{-1}K^{-1}$ and 28.0 $mWm^{-1}K^{-1}$ at atmospheric pressures respectively. As the pressure inside VIP prototypes was decreased the centre of panel thermal conductivity of VIP prototypes reduced as expected. For VIP S1 decreasing pressure from 1000 mbar to a pressure of 2.63 mbar resulted centre of panel thermal conductivity of 8.9 $mWm^{-1}K^{-1}$, for VIP S2 centre of panel thermal conductivity of 8.5 $mWm^{-1}K^{-1}$ was obtained at 2.35 mbar and for VIP S3 centre of panel thermal conductivity of 8.5 $mWm^{-1}K^{-1}$ was achieved at 2.35 mbar.

Figure 5.4 VIP prototype sample S1

Figure 5.5 VIP prototype sample S2

Figure 5.6 VIP prototype sample S3

Further, reducing the pressure to approximately 0.5-0.6 mbar led to decrease in the centre of panel thermal conductivity for all VIPs. For VIP prototype S1 at a core pressure of 0.64 mbar, centre of panel thermal conductivity was measured as 7.4 $mWm^{-1}K^{-1}$, for VIP prototype S2 centre of panel thermal conductivity of 7.6 $mWm^{-1}K^{-1}$ was obtained at 0.53 mbar pressure and for VIP prototype S3 centre of panel thermal conductivity of 7.6 $mWm^{-1}K^{-1}$ was achieved at 0.53 mbar pressure. This decrease in thermal conductivity at lower internal pressure was due to the reduction of gaseous thermal conductivity of core boards and reduction in coupling conductivity.

A graph of experimentally measured centre of panel thermal conductivities of all three VIP specimens (S1-S3) against corresponding internal pressures and a best fit line has been shown in figure 5.7. This best fit line has the characteristic "S" shape curve generally associated with change in thermal conductivity of small pore size materials due to variation in pressure. We used fumed silica and expanded perlite and average pore size of our sample was 155 nm, which is small enough to consider our sample as small pore size material. Part I of the best fit curve shows that the reduction of pressure for atmospheric pressure to around 10 mbar reduces the centre of panel thermal conductivity of VIP specimens exponentially due to the reduction of gaseous and coupling conductivity which are the two dominant modes of heat transfer in this region of curve. Further lowering the pressure to around 1 mbar led to the lower gaseous conductivity as shown by the region II of the curve. However, this decrease is not as large as part I of the curve due to the fact that in this region dominant mode of heat transfers is the gaseous conductivity. Part III of the best fit curve at lower pressures in figure 5.7 indicates that further reduction of internal pressure below 0.5 mbar will not have significant effect on reduction of centre of panel thermal conductivity of VIP prototypes. However, the initial centre of panel thermal conductivity values of 7.4-7.6 of VIP prototypes S1,S2 and S3 at 0.5-0.6 mbar pressure is lower than that of 9.2 $mWm^{-1}K^{-1}$ reported by Beikiricher and Demharter (2013) at an even lower core pressure of 0.08 mbar for evacuated perlite powder. This low centre of panel thermal conductivity in evacuated conditions in our VIP samples can be attributed to the suppression of gaseous and radiative thermal conductivities. Gaseous thermal conductivity was reduced because of the smaller pore size (155 nm) of composite samples and radiative conductivity due to the accumulative effect of SiC and expanded perlite on radiation extinction as described in chapter 4. However, initial centre of panel thermal conductivity values of 7.4-7.6 $mWm^{-1}K^{-1}$ for VIP specimen S1,S2 and S3 are comparatively higher than that of approximately 5 $mWm^{-1}K^{-1}$ claimed for commercially available silica VIP products at <5 mbar internal pressure such as va-Q-vip

(va-Q-tec AG, Germany) and Kevothermal VIP (Kevothermal Limited UK). This is due to the higher densities of VIP core material of specimens S1,S2 and S3 (341.13 - 341.56 kgm^{-3}) used in our VIPs compared to a density of 170-250 kgm^{-3} for commercial VIPs. This higher density led to a higher solid conductivity and consequently higher initial centre of panel thermal conductivity. The relationship of solid conductivity (λ_S) with density of the core material is shown in equation (5.1) (Fricke, 1993).

$$\lambda_S \approx \rho^{\alpha} \tag{5.1}$$

where ρ is density (kgm^{-3}) and the index α has a value of 1-2 depending upon the material structure. It is evident from equation (5.1) that the material with larger bulk densities will have a higher value of solid conductivity due to the decrease in volume ratio between pores and solid fraction. The effect of solid conductivity has been quantified on the centre of panel thermal conductivity of VIP prototype in section 5.4.2.

Table 5.3 Centre of panel thermal conductivity of VIP specimens at different core pressures

Specimen	Thermal conductivity ± 2 ($mWm^{-1}K^{-1}$)	Pressure ± 0.1(mbar)
VIP S1	28.0	1000
	21.7	380
	16.3	130
	11.5	20
	8.9	2.63
	7.4	0.64
VIP S2	28.3	1000
	24.5	430
	13.9	130
	11.8	18.4
	8.5	2.35
	7.6	0.53
VIP S3	28.0	1000
	25.9	520
	15.4	140
	12.3	24.9
	8.0	2.19
	7.6	0.53

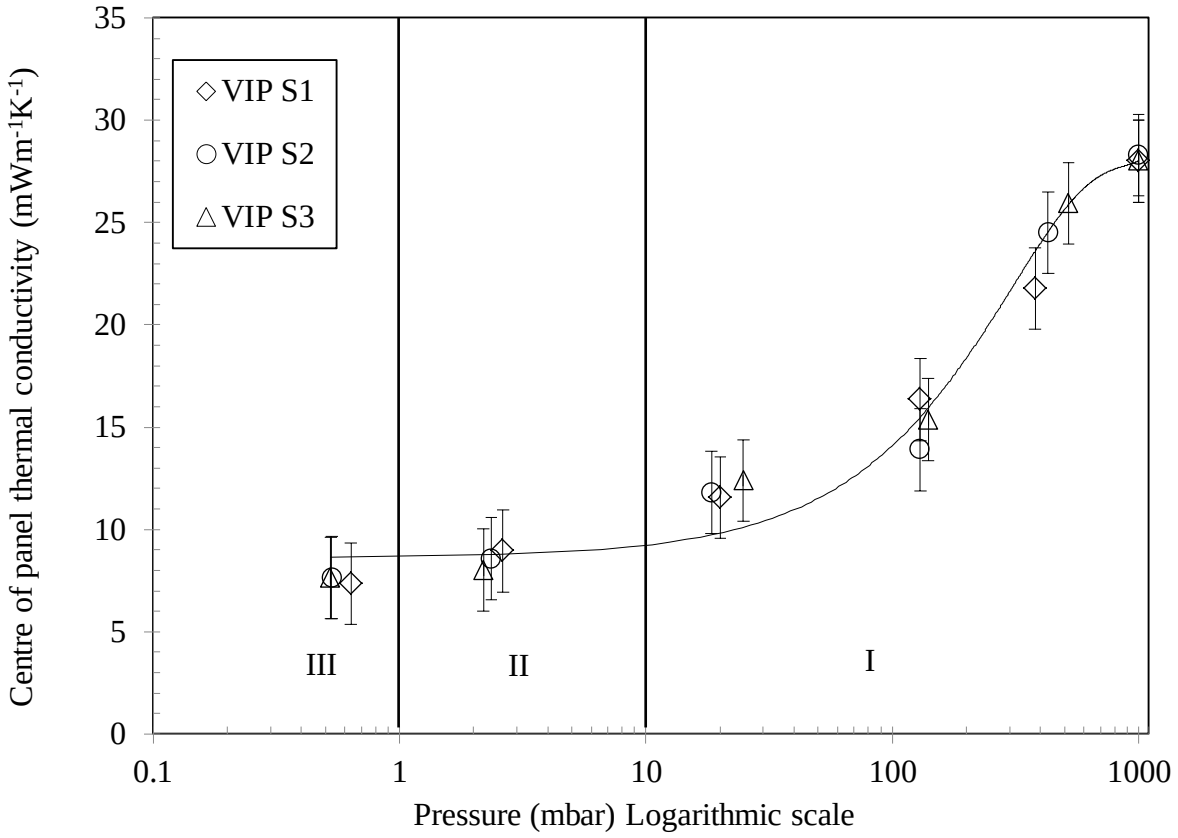

Figure 5.7 Variation of centre of panel thermal conductivity of VIP specimens with internal pressure

On the other hand, high density contributes in decreasing radiative conductivity of material. Radiative conductivity is attenuated with increasing density of sample and is also influenced by the material structure. Radiative conductivity measured for core sample used for prototype VIP S1-S3 is shown in figure 5.8. For VIP specimens S1,S2 and S3 with same core composition as listed in table 5.2, average λ_R at 300 K was measured in chapter 4 as 0.67 $mWm^{-1}K^{-1}$. Opacified silica core with density of 150 kgm^{-3} typically has radiative conductivity value of approximately 1 $mWm^{-1}K^{-1}$ at 300 K (Fricke et al. 2006). Radiative conductivity of VIP prototypes S1-S3 developed in this study is approximately 33% lower than that of typical radiative conductivity value of opacified silica core. This decrease can be attributed to the higher density of core composite and presence of large particles of expanded perlite and SiC in the core of VIP prototype.

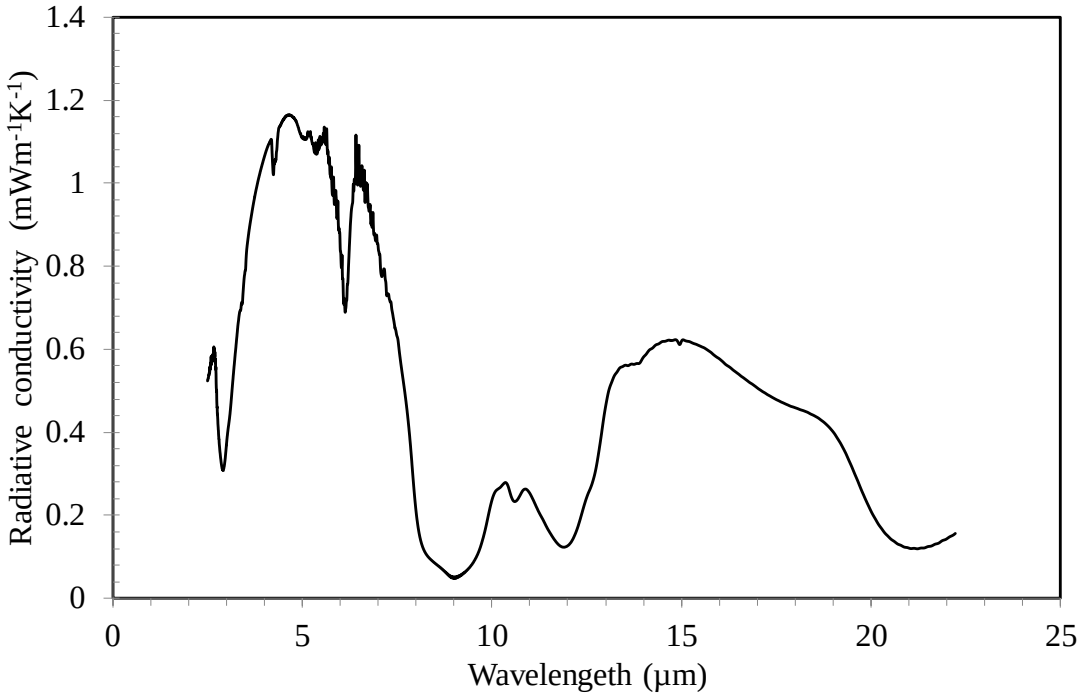

Figure 5.8 Radiative conductivity measured for composite core used for VIP prototypes S1,S2 and S3 at 300 K

5.4.2 Solid conductivity of VIP prototype

Solid conductivity (λ_S) is the major contributor to the overall thermal conductivity of VIPs and needs to be quantified. Solid conductivity was calculated from measured values of overall thermal conductivity for VIP and the radiative conductivity (λ_R). Centre of panel thermal conductivity in evacuated conditions is equal to the sum of λ_R at specified temperature and λ_S of a sample of given density and can be written as equation (5.2).

$$\lambda_{cop,evacuated} = \lambda_R + \lambda_S + \lambda_{G,evacuated} \quad (5.2)$$

In evacuated conditions gaseous conductivity ($\lambda_{G,evacuated}$) is very low compared to other modes of heat transfer and can be assumed negligible and equation (5.2) can be written as equation (5.3)

$$\lambda_{cop,evacuated} = \lambda_R + \lambda_S \quad (5.3)$$

Subsequently, the values of λ_S can be obtained by subtracting λ_R from the measured $\lambda_{cop,evacuated}$ for VIP specimens S1,S2 and S3. Values of λ_S for samples S1, S2 and S3 given in table 5.4 was finally calculated using the values of λ_R and $\lambda_{cop,evacuated}$ in equation (5.3).

Table 5.4 Solid conductivity values calculated for VIP specimens S1,S2 and S3

VIP samples	$\lambda_{cop,evacuated}$ ($mWm^{-1}K^{-1}$)	λ_R ($mWm^{-1}K^{-1}$)	λ_S ($mWm^{-1}K^{-1}$)	$\lambda_{G,evacuated}$ ($mWm^{-1}K^{-1}$)
S1	7.4	0.67	6.73	0.0125
S2	7.6	0.67	6.93	0.0125
S3	7.6	0.67	6.93	0.0125

These obtained values of λ_S for VIP specimens S1, S2 and S3 are 1.8-2 times higher compared to those of calculated by Frick et al. for 80 mass% precipitated silica and 20 mass% SiC (λ_S = 3.5-3.8 $mWm^{-1}K^{-1}$). This higher value of solid conductivity obtained in our experiments is due to the higher densities of VIP specimens (341 kgm^{-3}) compared to a density of 232 kgm^{-3} used by Fricke et al. This higher λ_S value is the main reason for higher values of $\lambda_{cop,evacuated}$ of VIP specimens S1,S2 and S3.

5.4.3 Gaseous and coupling conductivity of VIP prototype

Gaseous thermal conductivity refers to the conduction of gas inside pores of porous solids and depends upon the pore size of materials. Reducing the pore size and pressure inside the core material helps in reducing the gaseous conductivity. As VIP specimens S1,S2 and S3 have the same gaseous conductivity values shown as single curve in figure 5.6 due to their same core composition and measured average pore size of 155 nm. Gaseous conductivity becomes negligible below 1 mbar pressure and increases with pressure. At atmospheric pressure gaseous conductivity ($\lambda_{G,atm}$) value is 8.48 $mWm^{-1}K^{-1}$ as shown in figure 5.9. Along with gaseous conductivity there is another mode of heat conduction occurs due to the shortening of thermal resistances by gaseous conduction between powder particles and is called as coupling conductivity (K_c). This coupling effect at range of pressure between pressures 0.5 mbar and 1000 mbar can be estimated from $\lambda_{cop,evacuated}$, centre of panel thermal conductivity at atmospheric pressure ($\lambda_{cop,atm}$) and λ_G through the gas present in pores using equation (5.4).

$$K_c = \lambda_{cop,atm} - (\lambda_{G,atm} + \lambda_{cop,evacuated}) \quad (5.4)$$

The values of coupling conductivity for VIP specimen S1,S2 and S3 at ambient pressure are shown in table 5.5.

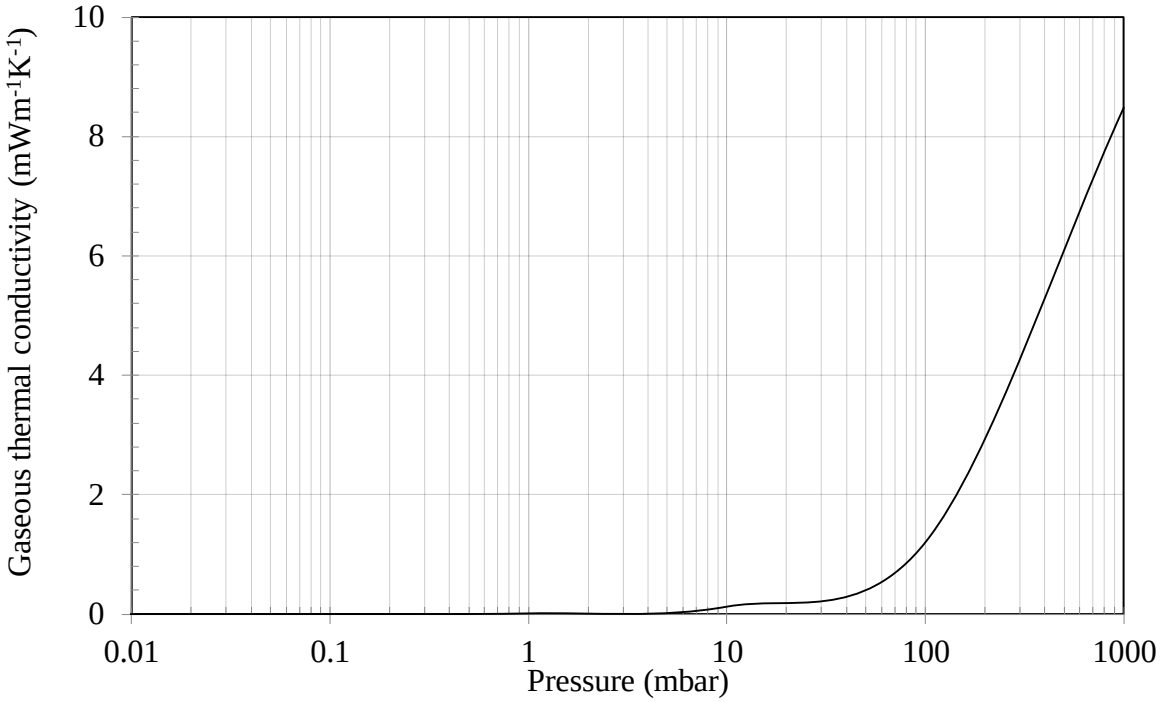

Figure 5.9 Gaseous conductivity of composite sample used for making VIP specimen S1,S2 and S3

Coupling effect values between 20 $mWm^{-1}K^{-1}$ and 30 $mWm^{-1}K^{-1}$ are likely for expanded perlite powders (Fricke et al., 2006). However, in the case of composite of expanded perlite and fumed silica gas conduction between particles has been reduced to between 11.8 $mWm^{-1}K^{-1}$ to 12.1 $mWm^{-1}K^{-1}$ in this study. The presence of fumed silica between and on the expanded perlite particles leading to reduced inter-particle gas conduction.

Table 5.5 Gaseous and coupling conductivities for VIP specimen S1,S2 and S3 at ambient pressure

VIP samples	$\lambda_{cop,atm}$ ($mWm^{-1}K^{-1}$)	$\lambda_{cop,evacuated}$ ($mWm^{-1}K^{-1}$)	$\lambda_{G,atm}$ ($mWm^{-1}K^{-1}$)	K_c ($mWm^{-1}K^{-1}$)
S1	28.0	7.4	8.48	12.1
S2	28.3	7.6	8.48	12.1
S3	28.0	7.6	8.48	11.8

5.5 VIP Service life

Service life of a VIP, time required for the thermal conductivity to reach a certain critical value, is an important criterion for predicting the effectiveness of a VIP core material. Internal pressure rises over time due to the diffusion of gases and water vapours through envelope surface or sealing flanges. This rise in pressure leads to increase in gaseous conductivity and reduction in service life of VIP. VIP thermal conductivity can be interpreted into a limiting pressure at which gaseous conductivity becomes equal to half of conductivity of still air and is called as critical pressure ($P_{critical}$) which can be approximated using equation (5.5) (Fricke et al., 2006).

$$P_{critical} \approx 230\ (mbar)/\Phi \tag{5.5}$$

where

Φ is the average pore size (µm)

Materials which exhibit lower $P_{critical}$ will have shorter service life and require evacuation to below 0.01 mbar pressure which will lead to a higher production cost. On the other hand, materials having higher $P_{critical}$ will yield a longer service life for VIP. Such VIPs will require core pressure to be maintained between 0.1-5 mbar. Using equation 5.3 and average pore size of 155 nm of expanded perlite and fumed silica composite used for VIP specimens developed in this study, $P_{critical}$ was obtained greater than 1000 mbar. This higher $P_{critical}$ indicates that gaseous conductivity in the VIP specimens was not fully developed even at atmospheric pressure leading to a longer service life. In case of using expanded perlite (Φ = 10 µm) as core material $P_{critical}$ will be approximately 23 mbar yielding shorter service life with metallised PET envelopes as barrier to hinder gaseous transmission.

5.6 Conclusions

In this chapter thermal performance of VIP prototypes made of low cost core materials consisting of 50 mass% of fumed silica, 30 mass % of expanded perlite along with 8 mass% of fibre and 12 mass% of SiC was experimentally evaluated. Initial centre of panel thermal conductivity of three VIP prototypes was measured to be 7.4-7.6 $mWm^{-1}K^{-1}$ at 0.5-0.6 mbar pressure which is lower than that of the evacuated perlite powder. However, centre of panel

thermal conductivity value of VIP prototypes is higher compared to a value of 4-5 $mWm^{-1}K^{-1}$ obtained for commercially available VIPs made of fumed silica core.

Higher solid conductivity of VIP prototypes is the main reason for higher initial centre of panel thermal conductivity. Solid conductivity in the range of 6.73-6.93 $mWm^{-1}K^{-1}$ for VIP prototypes was 1.8-2 times higher compared to that experience by fumed silica core VIPs. This behaviour can be attributed to the higher density of VIPs developed in this study. In the case of VIP prototypes, gaseous conductivity value was suppressed to 8.48 $mWm^{-1}K^{-1}$ due to the smaller average pore size and the coupling conductivity was calculated between 11.8-12.1 $mWm^{-1}K^{-1}$ which is much lower than that obtained of for powder such as expanded perlite (20-30 $mWm^{-1}K^{-1}$). Average radiative conductivity of VIP prototype was measured to be 0.67 $mWm^{-1}K^{-1}$ which is 33% lower compared to that of typical values of opacified silica core. Higher critical pressure of VIP prototypes (>1000 mbar) due to their smaller average pore size indicated a longer service life compared to VIPs made of core materials with larger pore size.

Chapter 6

Economic Analysis of Core Material and VIP

6.1 Introduction

VIPs offer an alternative to conventional insulation materials for buildings to achieve low or zero energy building status and to meet stringent building regulations whilst requiring minimum insulation thickness. Currently, use of VIPs is limited to retrofitting commercial and listed buildings where external facade cannot be altered to upgrade their thermal performance and at the same time minimum loss of high value internal floor area is required. VIPs can also be used as a component in thermal composite insulation system along with other insulation materials for achieving higher thermal resistance (Mandilaras et al., 2014; Mukhopadhyaya et al., 2014). However, high cost is the main obstacle for their large scale application in buildings. The aim of this study was to develop and characterise a low cost core material for VIPs. Fumed silica and expanded perlite composite was investigated as a potential low cost VIP core composite due to its favourable thermal characteristics such as lower gaseous and radiative conductivities. In this chapter, costs of core boards with varying mass proportions of fumed silica, expanded perlite, SiC and polyester fibres were calculated using their commercial prices. Typically the thermal performance and cost comparison of insulation material is expressed as cost of material to achieve unit thermal resistance (R-value) which is described as the ratio of thickness of the material to the thermal conductivity. Costs of core boards were linked with thermal performance of core boards to evaluate the cost per unit thermal resistance of developed core boards and VIP prototypes. Payback periods with and without considering the space saving potential, annual energy savings and annual emission savings were calculated for VIPs in different scenarios of insulating existing building and compared with those of conventional Expanded polystyrene (EPS) insulation in order to evaluate their cost effectiveness.

6.2 Core material cost calculating methodology

Cost reduction potential of core boards made of fumed silica and expanded composites was estimated using equation (6.1) (Alam et al., 2014):

$$C_{core} = C_{FS} \times m_{FS} + C_{EP} \times m_{EP} + C_{SiC} \times m_{SiC} + C_{PF} \times m_{PF} \quad (6.1)$$

where

C_{core} is the cost of core (£)

C_{FS}, C_{EP}, C_{SiC} and C_{PF} are costs of fumed silica, expanded perlite, SiC and polyester fibres per unit mass respectively and their units are £kg^{-1}.

m_{FS}, m_{EP}, m_{SiC} and m_{PF} are masses of fumed silica, expanded perlite, SiC and polyester fibre respectively in kg.

Prices of materials given in table 6.1 were used for calculating the cost of core board. These prices were commercial prices based on small quantities. Prices may vary based on large quantities; however, effect of bulk quantity prices will be similar for all materials.

Table 6.1 Commercial prices of materials used for VIP core cost estimation (Alam et al., 2014)

Material	**Price (£/kg)**
Fumed silica	3.50
Expanded perlite	0.27
SiC	1.58
Polyester fibre	4.60

6.3 Comparison of cost and thermal resistance of core boards at ambient pressure

Material cost of VIP core board samples 1-5 (detailed in chapter 4) was calculated using the methodology described in section 6.2. Increasing mass ratio of expanded perlite in the composite led to a lower cost of the core material. However, for fumed silica cost increases with its proportion in the composite as shown in table 6.2. The cost of core board 1 was calculated to be £11.08 m^{-2} due to the presence of the highest fumed silica content (80 mass%) of all the samples. For core board 3, with extra 3 mm thickness compared to other samples, cost was £11.90 m^{-2}. For core board 5 with 60 mass% of expanded perlite the cost reduction potential of 24.3% could be achieved compared to core board 1, but there was a disadvantage of increased thermal conductivity such that thermal conductivity was 2.2 times higher compared to that of the core board 1.

Comparison of cost per unit thermal resistance normalises the additional cost and thickness of core board 3 and has been shown in figure 6.1 for core boards 1-5. It has been shown that core board 1 had the cost of £24.07 m^{-2} per R-value of insulation.

Table 6.2 Comparison of material cost and R-value for core boards 1-5 at ambient pressure

Core boards	Material cost ($£m^{-2}$)	Thermal conductivity ($mWm^{-1}K^{-1}$)	Thickness (m)	R-value (m^2KW^{-1})
1	11.08	23.9	0.011	0.46
2	10.68	26.6	0.012	0.45
3	11.90	27.8	0.015	0.54
4	9.91	38.1	0.012	0.31
5	8.38	53.2	0.012	0.22

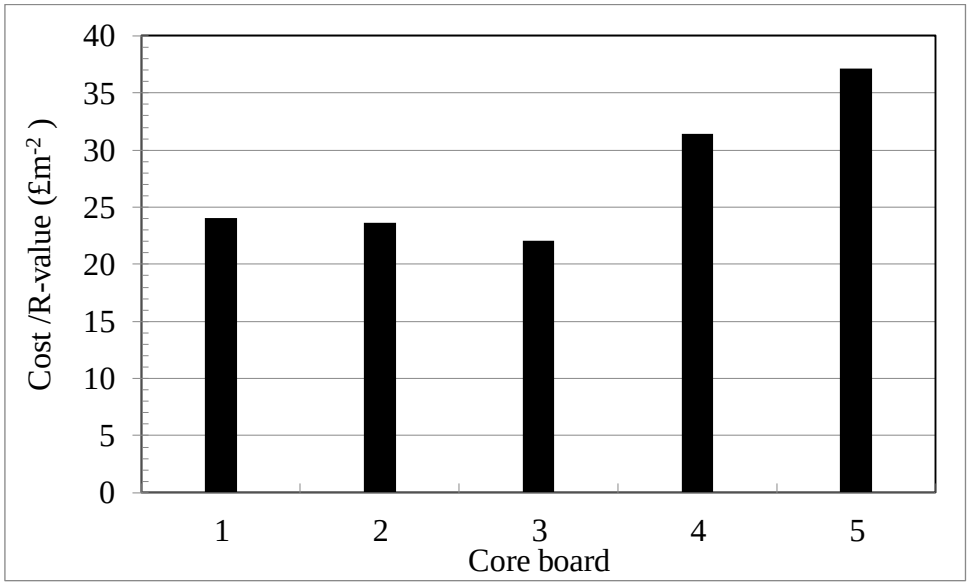

Figure 6.1 Comparison of cost/R-value of core boards 1-5 at ambient pressure

Core board 3 (having same composition as core board S1,S2 and S3 as described in chapter 5) had the cost of £22.05 m^{-2} per R-value of insulation and for core board 5 the cost was increased to £37.15 m^{-2} to achieve unit R-value of insulation. This shows that the core board 3 has the optimum sample content in terms of cost and insulation value to be used in VIP core. However, comparative economic performance comparison of VIP core materials in conjunction with thermal performance in evacuated conditions was also required to analyse the cost per R-value when used in VIPs and has been presented in section 6.4.

6.4 Cost and R-value comparison of core boards of VIP prototype

Centre of panel thermal conductivity of VIP core material decreases with reducing internal pressure as discussed in chapter 5 leading to higher R-values. Cost and R-value comparison of core materials when used as core of VIP prototypes has been presented in table 6.3. Total costs of core materials remained unchanged. The cost of core boards S1,S2 and S3 (detailed in chapter 5) was calculated to be £11.90 m^{-2} same as core board 3 presented in section 6.3.

Table 6.3 Comparison of material cost and R-value for core of VIP prototypes at lower internal pressure

Core boards of VIP	Core material cost (£m^{-2})	Thermal conductivity ($mWm^{-1}K^{-1}$)	Thickness (m)	R- value (m^2KW^{-1})
S1	11.90	7.4	0.015	2.027
S2	11.90	7.6	0.015	1.974
S3	11.90	7.6	0.015	1.974
Core board1	11.08	5	0.011	2.20
Core board1 (considering equivalent thickness)	15.10	5	0.015	3

However due to the low thermal conductivity of these boards at lower internal pressure their R-values increased leading to lower cost per unit thermal resistance. Cost per R-value of core boards of VIP S1-S3 and core board 1 has been shown in figure 6.2. Core boards of VIP S1-S3 had the cost of £5.87-6.02 m^{-2} per R-value of insulation which is 3.3 to 3.4 times less than that of core board 3 at ambient pressure and had the same material composition.

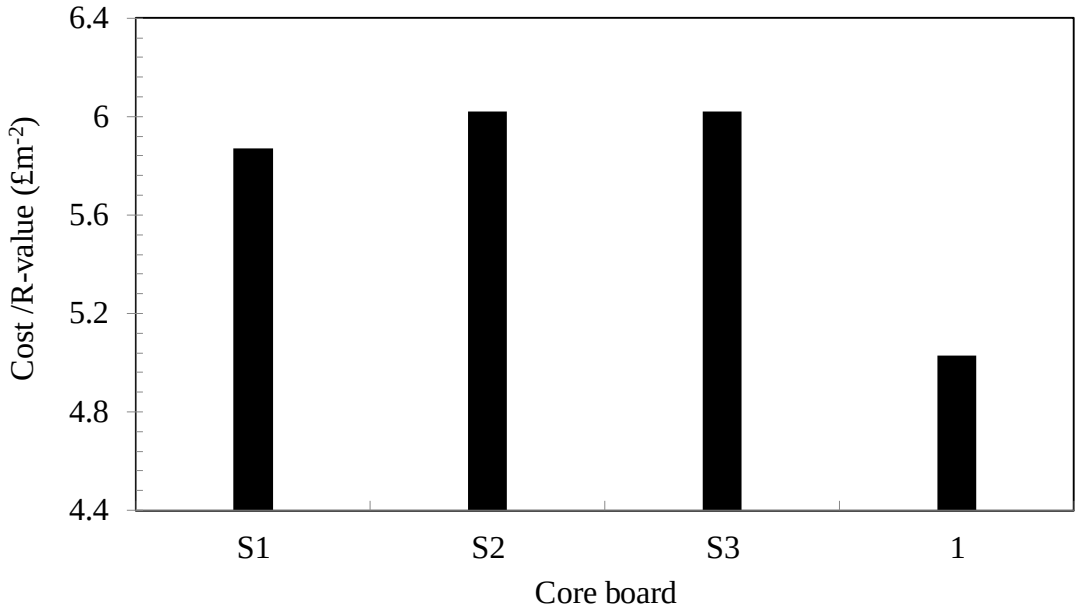

Figure 6.2 Comparison of cost per R-value of core boards of expanded perlite and fumed silica composite at lower pressure

However, the cost per unit R-value of core boards of VIP S1-S3 was comparatively higher than that of core board 1 which had 80 mass% of fumed silica as found in the commercially available VIPs with centre of thermal conductivity of approximately 5 $mWm^{-1}K^{-1}$. It is evident that increased expanded perlite content in core board resulted in a proportionately higher thermal conductivity and consequently lower R-value leading to comparatively higher cost per R-value. Thermal conductivity of expanded perlite and fumed silica cored boards needs to be decreased further to realise the potential of low cost expanded perlite in evacuated conditions. Low cost core made of expanded perlite and fumed silica can be employed in applications where R-value requirements are not stringent for fixed thickness of the VIP insulation. In case of considering the equivalent thickness of core board 1 as core boards of VIP S1-S3, it was found that cost of core board of VIP S1-S3 was lower than that of core board 1 as shown in table 6.3. Further potential of cost reduction of S1-S3 can be achieved by decreasing the solid thermal conductivity which is dominant mode of heat transfer in evacuated conditions. This could be realised by increasing the porosity of expanded perlite. Lower cost core materials with enhanced thermal performance will enable VIPs to be cost competitive with conventional insulation materials.

6.5 Comparison of payback period between VIP and EPS insulation

The payback period describes the time required to recover the cost of insulation through the reduced energy cost of heating/cooling a building and is a major deciding factor in choosing the type of insulation for buildings. It is defined as the ratio of the cost of insulation to the annual savings in heating energy cost. Insulation having smaller payback periods is desirable. In this study four different scenarios of applying VIP and EPS insulation on existing UK building with area weighted average U-value of 0.50 $Wm^{-2}K^{-1}$ (wall U-value 0.53 $Wm^{-2}K^{-1}$, floor U-value 0.30 $Wm^{-2}K^{-1}$, roof U-value 0.38 $Wm^{-2}K^{-1}$ and window U-value 1.4 $Wm^{-2}K^{-1}$) were assumed as detailed in table 6.4.

Table 6.4 Four different scenarios of existing UK building considered for calculating insulation payback periods

Scenario	Wall U-Value ($Wm^{-2}K^{-1}$)	Floor U-Value ($Wm^{-2}K^{-1}$)	Roof U-Value ($Wm^{-2}K^{-1}$)	Window U-Value ($Wm^{-2}K^{-1}$)	Area weighted U-Value ($Wm^{-2}K^{-1}$)
1	0.45	0.25	0.30	1.4	0.42
2	0.32	0.20	0.20	1.4	0.32
3	0.27	0.18	0.18	1.4	0.28
4	0.15	0.15	0.15	1.4	0.19

Payback periods for both insulations for all four building insulation scenarios were calculated and compared. Payback period was calculated using equations 6.2-6.4 (Dombayci et al., 2006) and parameters detailed in table 6.5.

$$PBP = C_{ins}/(C_{A,exis} - C_{A,imp}) \quad (6.2)$$

$$C_A = (86400 \times HDD \times C_f \times U_{avg} \times PWF)/(H_V \times \eta) \quad (6.3)$$

$$PWF = N / (1 + i) \quad (6.4)$$

where

PBP is the payback period (Year)

C_{ins} is the cost of insulation (£)

$C_{A,exis}$ is the annual heating cost with existing U-value (£m^{-2} per annum)

$C_{A,imp}$ is the annual heating cost with improved U-value (£m^{-2} per annum)

C_f is the cost of fuel (£m^{-3})

HDD is the heating degree days (°C days) which is a sum of the differences between the outdoor temperature and base temperature over a specified time period.

H_V is the heating value of fuel (Jm^{-3})

η is the thermal efficiency of heating system

PWF is the present worth factor if interest rate (i) is equal to inflation rate

N is the life time of insulation (Years)

U_{avg} is the area weighted average U-value which can be calculated using equation (6.5)

$$U_{avg} = [(U_1 \times A_1) + (U_2 \times A_2) + (U_3 \times A_3) + (U_4 \times A_4)]/[(A_1 + A_2 + A_3 + A_4)] \quad (6.5)$$

where

A_i is the insulated area of a building element '*i*'(m^2)

U_i is the U-value of a building element '*i*' ($Wm^{-2}K^{-1}$)

subscripts 1,2,3 and 4 denotes building elements wall, floor, roof and window respectively

Thermal conductivity values of 8 $mWm^{-1}K^{-1}$ and 35 $mWm^{-1}K^{-1}$ were used for VIP and EPS respectively for U-value calculations. Thermal conductivity value of 8 $mWm^{-1}K^{-1}$ was used as design value considering the edge effect and change in thermal conductivity due to pressure rise over the life time of VIP. Total thickness of insulation required for achieving average U-value for each scenarios of building insulation was calculated by adding the thicknesses required for unit area of all opaque building envelope elements. Thicknesses of VIP and EPS insulation for each element are shown in table 6.5. Window U-value was assumed to be 1.4 $Wm^{-2}K^{-1}$ for all scenarios. Four scenarios of applying VIP and EPS insulation on UK building with existing U_{avg} of 0.50 $Wm^{-2}K^{-1}$ along with annual heating costs, costs of insulation and other parameter used for payback period calculation are detailed in table 6.6. In case of scenario 1, average U-value of 0.42 $Wm^{-2}K^{-1}$ was attained using VIP thickness of 2.75 mm, 29.5 mm and 5.7 mm for wall, floor and roof respectively whereas, EPS thickness required was 12 mm, 129 mm and 25 mm for wall, floor and roof respectively as detailed in table 6.5. In scenario 2, VIP and EPS were employed for building insulation achieving average U-Value of 0.32 $Wm^{-2}K^{-1}$. Both scenarios 1 and 2 yielded long payback periods for

VIP insulation in comparison to those calculated for EPS as shown in figure 6.3. In scenario 3, payback period of EPS insulation to reach a building average U-value of 0.28 $Wm^{-2}K^{-1}$ was 10 times shorter than that for VIP for achieving similar U-value.

Table 6.5 U-values of building elements and thickness of VIP and EPS insulation to achieve different building insulation scenarios of existing UK building

Scenario		Wall	Floor	Roof	Window	U_{avg}
1	U-Value ($Wm^{-2}K^{-1}$)	0.45	0.25	0.30	1.4	0.42
	VIP Thickness (mm)	2.75	29.5	5.7	-	
	EPS Thickness (mm)	12	129	25	-	
2	U-Value ($Wm^{-2}K^{-1}$)	0.32	0.20	0.20	1.4	0.32
	VIP Thickness (mm)	10	37.5	19	-	
	EPS Thickness (mm)	43.5	165	83	-	
3	U-Value ($Wm^{-2}K^{-1}$)	0.27	0.18	0.18	1.4	0.28
	VIP Thickness (mm)	14.6	42	23.5	-	
	EPS Thickness (mm)	64	183	103	-	
4	U-Value ($Wm^{-2}K^{-1}$)	0.15	0.15	0.15	1.4	0.19
	VIP Thickness (mm)	38	50.8	32.2	-	
	EPS Thickness (mm)	167	222	141	-	

However, EPS insulation required 4.3 times large thickness on building elements compared to VIP. In scenario 4 the payback period of both insulations required to achieve an average building U-value of 0.19 $Wm^{-2}K^{-1}$ was found to be 5.28 years longer for VIP than that for EPS although former required smaller thicknesses of 38 mm, 50.8 mm and 32.2 mm for wall, floor and roof respectively than the later which required 167mm, 222mm and 141mm for wall, floor and roof respectively.

Table 6.6 Annual heating costs, costs of insulation and other parameter used for payback period calculation

Parameters	**Scenario 1**	**Scenario 2**	**Scenario 3**	**Scenario 4**
Fuel	Natural gas	Natural gas	Natural gas	Natural gas
HDD (°C days)	1931	1931	1931	1931
C_f (£m^{-3})	0.40	0.40	0.40	0.40
H_V (Jm^{-3})	39.5×10^6	39.5×10^6	39.5×10^6	39.5×10^6
η	0.90	0.90	0.90	0.90
N (Years)	25	25	25	25
i (%)	10	10	10	10
$C_{A,exis}$ (£m^{-2})	124.89	124.89	124.89	124.89
$C_{A,imp}$ (£m^{-2})	104.91	79.93	69.94	47.66
Total VIP C_{ins} (£m^{-2})	91.30	189	241.96	454.80
Total EPS C_{ins} (£m^{-2})	9.06	18.75	24.02	45.39

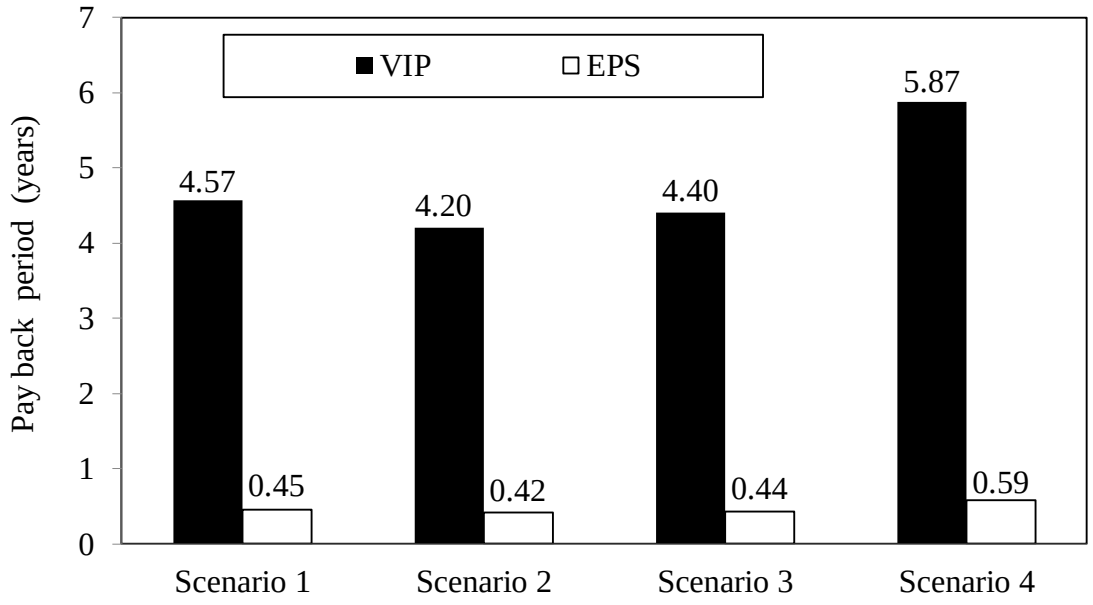

Figure 6.3 Payback periods for VIP and EPS employed as building insulation in scenarios 1-4 (table 6.4) of insulation applications

Such prohibitively large thickness of EPS insulation may not be feasible to apply on most of the existing buildings to insulate the wall and floor area. Clearly, VIP offers the advantage of

space saving due to the thinner sections required compared to EPS for achieving same U-value. However, cost effectiveness of VIP depends upon the annual rental value of building. Payback period for VIP insulation for average U-values of all four scenarios (detailed in table 6.4) was also calculated considering the economic value of space savings, interest rate of 10% and is shown in figure 6.4. Annual average rent of commercial buildings situated in central London range from £430 m^{-2}-£860 m^{-2} (Find a London office LLP, 2014). It is evident that for all four scenarios payback period for annual rent of £400m^{-2} is long and range between 2.02 to 4.4 years.

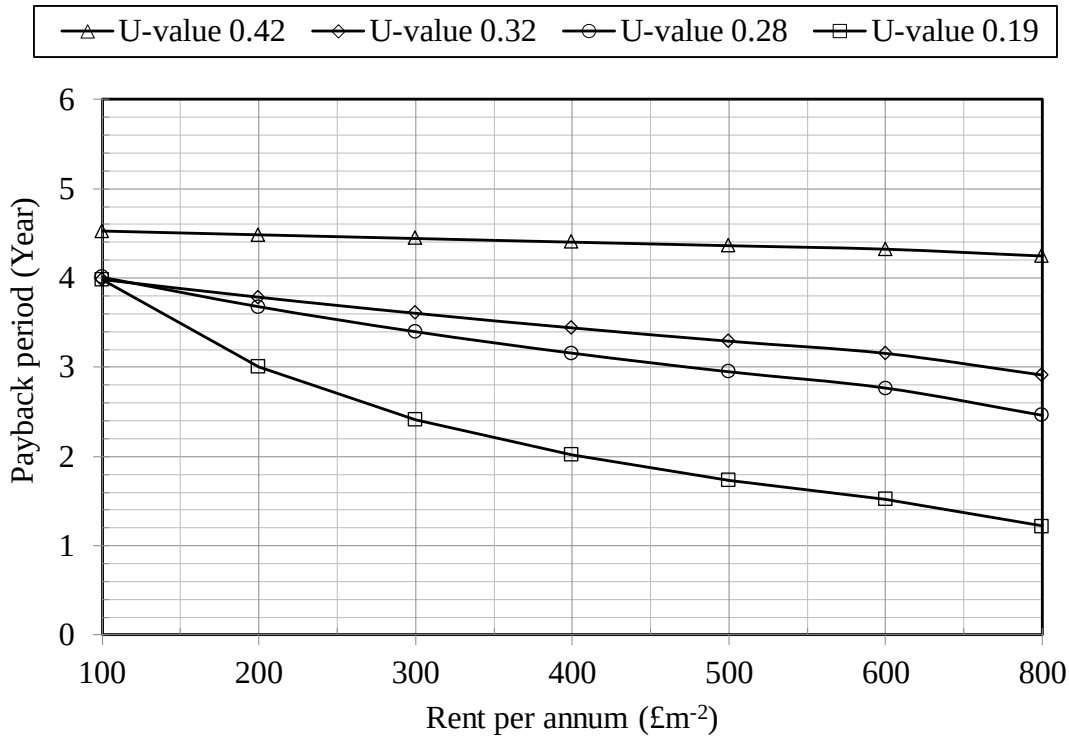

Figure 6.4 Payback periods considering economic value of space savings of VIP insulation for average U-values of four scenarios (detailed in table 6.4)

For scenario 4 (U-Value 0.19 $Wm^{-2}K^{-1}$) and annual rent of £800m^{-2}, payback period of 1.22 years was calculated. However, VIP still has longer payback compared to EPS insulation (0.59 years) and remains the costly option. High initial cost is the main reason for the longer payback period of VIP insulation in all scenarios and it must be reduced considerably if VIP is to be applied at a large scale in buildings. At present VIP is an attractive alternative to conventional insulation materials for existing commercial buildings, particularly those which cannot be insulated on the exterior such as listed buildings. High cost of VIPs is due to the higher cost of core and envelope materials used in VIPs. However, with time the prices of

materials used in VIPs may decrease due to the high volume production leading to lower VIP cost. In future, development of alternative low cost materials for VIPs may also lead to decrease in cost of VIPs making them attractive for building applications.

6.6 Energy savings calculation

In 2013, emissions from space heating energy use in UK buildings accounted for 98 million tonnes of CO_2 i.e. 17% of total UK greenhouse gas emissions (CCC, 2013). There is significant potential for reducing emissions from buildings by improving energy efficiency of buildings through applying insulation on building envelope. In this section space heating energy and emission savings potential for applying different thicknesses of EPS or VIP insulation required for different aveage U-values of building has been estimated. Heating energy annual consumption "E_A" ($kWhm^{-2}$) of building was calculated using equation (6.6).

$$E_A = [HDD \times (\sum(U_1 \times A_1)(U_2 \times A_2)(U_3 \times A_3)(U_4 \times A_4)) \times 24]/[(1000 \times \eta \times A_2)] \quad (6.6)$$

where

HDD is the heating degree days (°C days) which is a sum of the differences between the outdoor temperature and base temperature over a specified time period.

η is the thermal efficiency of heating system

U_i is the U-value of a building element '*i*' ($Wm^{-2}K^{-1}$)

A_i is the insulated area of a building element '*i*'(m^2)

Subscripts 1,2,3 and 4 denotes building elements wall, floor, roof and window respectively.

Average thickness of insulation was calculated by adding the insulation required for all building elements and divided by the total area of the building elements. Applying additional insulation either EPS or VIP to all opaque building elements to lower U_{avg} of existing English dwelling (U_{avg} of 0.50 $Wm^{-2}K^{-1}$ and annual space heating energy consumption of 153.14 $kWhm^{-}2$) resulted in decrease in annual space heating energy consumption. It is evident from figure 6.5 that space heating energy consumption decreased by applying increasing thickness of insulation either EPS or VIP to all opaque building elements to achieve U_{avg} for all building insulation scenarios (detailed in table 6.4).

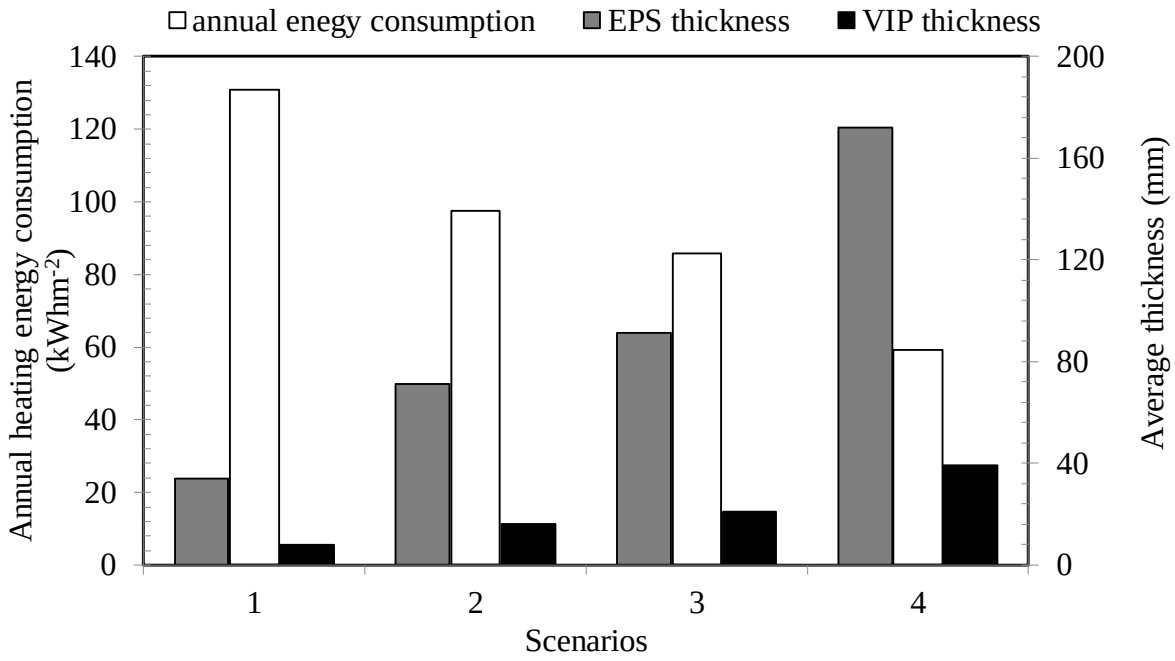

Figure 6.5 Space heating energy consumption for different thicknesses of EPS and VIP insulation required for unit area of building with different average U-values

In case of scenario 4, by applying EPS or VIP insulation annual space heating energy consumption was 59.22 $kWhm^{-2}$ and space heating energy savings amounted to 93.92 $kWhm^{-2}$ leading to annual emission savings of 17.28 $kgCO_2m^{-2}$ as shown in table 6.6. CO_2 emissions savings were calculated using fuel emission factor of 0.184 $kgCO_2/kWh$ (Energy Saving Trust, 2014). VIP insulation requires 4.3 times smaller thickness compared to EPS insulation

Table 6.7 Annual space heating energy consumption, heating energy savings and annual emission savings for unit area of building with different average U-values

U_{avg} ($Wm^{-2}K^{-1}$)	Annual heating energy consumption ($kWhm^{-2}$)	Annual heating energy savings ($kWhm^{-2}$)	Annual emission savings ($kgCO_2m^{-2}$)
0.50	153.14	-	-
0.42	130.79	22.35	4.11
0.32	97.63	55.51	10.21
0.28	85.79	67.35	12.39
0.19	59.22	93.92	17.28

English dwelling insulated to the level of scenario four with an average floor area of 91 m^2 yields space heating energy savings of 8546.7 kWh. In England there were an estimated 22.8 million dwellings as on March 2011 (DCLG, 2011). By achieving $U_{avg}$of 0.19 $Wm^{-2}K^{-1}$ for existing housing stock, there is a huge saving potential of annual heating energy of 194.87 TWh and 35.86 million metric tonnes of CO_2 emissions.

6.7 Conclusion

High cost of VIPs is a main barrier for their use in buildings application. In this study fumed silica, expanded perlite, SiC opacifier and polyester fibres composite as an alternative material for core of VIPs and their cost reduction potential was evaluated. It was shown that with increasing mass ratio of expanded perlite in composite the cost of core material decreased. Core board 3 containing fumed silica 50 mass %, expanded perlite 30 mass %, SiC opacifier 12 mass %, and polyester fibres 8 mass %, had the lowest cost of £20.07 m^{-2} per R-value of insulation compared to all core board samples in ambient conditions. In evacuated conditions R-value of core boards having similar composition as core board 3 had the cost per R-value of £5.87-6.02 m^{-2} which was 3.3 to 3.4 times lower than that at ambient conditions. However, the cost per R-value of core boards used for VIP S1-S3 was relatively higher than that of core board 1 which has the similar composition (80 mass% of fumed) which is used for commercially available VIPs. It was also found that cost of core board of VIP S1-S3 was lower than that of core board 1 and can be used in VIP applications where fixed thermal resistance in not required for set thickness of the VIP insulation. For an English dwelling with an average floor area of 91 m^2 space heating energy savings of 8546.7 kWh can be achieved. In England, by achieving average U-value of 0.19 $Wm^{-2}K^{-1}$ for existing housing stock there is a huge potential of 194.87 TWh and 35.86 million metric tonnes of annual heating energy saving and CO_2 emissions savings per annum respectively. Payback period for VIP in four scenarios of applying insulation on existing UK building with average U-value of 0.50 $Wm^{-2}K^{-1}$ was in the range of 4.2 to 5.87 years while for EPS it was calculated between 0.42 to 0.59 years. Considering the space saving potential offered by VIPs due to their small thickness, 4.8 times shorter payback period can be achieved for a building average U-value of 0.19 $Wm^{-2}K^{-1}$. However, VIP still remains a costly insulation material compared to conventional insulation due to its high initial cost which is to be reduced considerably to encourage large scale uptake in building applications.

Chapter 7

Conclusions and Future Recommendations

7.1 Introduction

Buildings contribute significantly to energy consumption and approximately half of that energy is used for space heating. Energy efficiency requirements for buildings are being continuously improved through building regulations. To meet these enhanced building regulations insulation standards conventional insulation materials require large thicknesses which may not be feasible in existing and new buildings. VIP, a high thermal resistance insulation with minimum thickness, has attracted substantial research as an alternative to conventional insulation materials for building applications over the last fifteen years. However, high cost of VIPs is the main barrier for their large scale application in buildings.

The main aim of this PhD project was to develop low cost VIP core material and evaluate its thermal performance for use in VIPs for building applications. This thesis examined the thermo-physical properties of expanded perlite and fumed silica composite as a low cost VIP core material and experimentally measured its thermal performance in VIP prototype samples. This work can be summarised as follows:

- Experimental investigation of pore size, density, and thermal conductivity of varying mass ratios of expanded perlite and fumed silica and their effect on gaseous and radiative conductivities of the core samples.

- IR transmission measurement of composite samples to ascertain the effect of expanded perlite on radiative conductivity of samples and identity the critical doping mass of SiC opacifier in optimal composite.

- Experimental evaluation of centre of panel thermal conductivity of VIP prototypes manufactured with optimised composition of low cost composite and assessment of the effect of expanded perlite on the coupling effect at a range of pressures.

- Payback period analysis of VIPs to achieve different building insulation scenarios and comparison with conventional EPS insulation to evaluate the cost effectiveness VIPs due to their advantage of high thermal resistance and space saving potential.

This chapter describes the conclusions arising from the research work and presents recommendations for future work.

7.2 Conclusions

1) An extensive review of studies related to VIPs for building applications has been presented. Most of the main studies looked into VIP properties and their measurements, service life prediction and thermal bridging evaluation arising due to different envelope materials. Majority of the research work considered expensive fumed silica based core material VIPs for building applications due to its suitable thermo-physical properties. However, cost of these VIPs is higher and needs to be reduced by employing alternative low cost core materials to make them price competitive with conventional insulation materials. Recently, use of alternative powders, foam and fibre materials as VIP core has also been researched and it was concluded that these materials will required lower pressure approximately 0.01 mbar to achieve thermal performance comparable to fumed silica due to their large pore sizes. These studies did not evaluate the cost effectiveness of these alternative materials for VIP cores. There are no studies in the literature considering the use of naturally occurring low cost porous expanded perlite mineral and fumed silica composite as VIP core material. The advantage of such composite will be that expanded perlite will partially replace the costly fumed silica and remaining fumed silica aggregates can partially or completely fill large pores of expanded perlite achieving high thermal performance at relatively higher pressures and lower material and production cost.

2) In the experimental work composite samples were prepared by dry mixing of low cost expanded perlite, fumed silica, SiC opacifier and polyester fibres in varying mass ratios to identify the optimal composite composition as low cost core material. Pore size analysis results showed that size of expanded perlite pores was between 3-10 μm yielding gaseous conductivity in the range of 12.5-19.6 $mWm^{-1}K^{-1}$ at 100 mbar pressures. Average pore diameter values of expanded perlite decreased with the partial filling of fumed silica aggregates and was found to be in the range of 150-300 nm

yielding lower gaseous conductivity values of 1.2-2.1 $mWm^{-1}K^{-1}$ at 100mbar and became negligible upon further decreasing pressures below 10 mbar.

3) Effect of expanded perlite on radiative conductivity of composite samples was identified. It was found that increased mass% of expanded perlite led to decrease in radiative conductivity of composite samples. For sample containing no expanded perlite, average radiative conductivity was calculated to be 1.4 $mWm^{-1}K^{-1}$ and radiative conductivity values decreased to 1.1 $mWm^{-1}K^{-1}$, 0.7 $mWm^{-1}K^{-1}$, 0.6 $mWm^{-1}K^{-1}$ and 0.5 $mWm^{-1}K^{-1}$ with mass ratio of expanded perlite 20%, 30%, 40% and 60% respectively. Expanded perlite mass ratio of 30% is an optimum amount of expanded perlite in composite and mass ratio beyond this threshold value will not be able to compensate the increase in the solid thermal conductivity.

4) Total thermal conductivity of composite materials in the form of core boards containing range of mass ratios of expanded perlite and fumed silica along with fibre and opacifier was measured to evaluate the influence of expanded perlite on thermal conductivity. Thermal conductivity of core boards increased as the expanded perlite mass ratio was increased. An increase in expanded mass ratio from 0% to 30% led to rise of 3.9 $mWm^{-1}K^{-1}$ in thermal conductivity. However, increasing expanded perlite from 30 mass% to 60 mass% in composite led to increase in thermal conductivity from 27.8 $mWm^{-1}K^{-1}$ to 53.2 $mWm^{-1}K^{-1}$ an increase of 25.4 $mWm^{-1}K^{-1}$. Based on these results, a composite containing mass ratio of 30 mass% of expanded perlite and 50 mass% fumed silica along with fibre (8 mass%) and opacifier has been identified as a potential core material for VIP.

5) According to the results of the thesis VIP prototypes consisting of core made with optimised composite consisting (50 mass% of fumed silica, 30 mass % of expanded perlite along with 8 mass% of fibre and 12 mass% of SiC) yielded centre of panel thermal conductivity of 7.4-7.6 $mWm^{-1}K^{-1}$ at 0.53-0.64 mbar pressure as shown in figure 7.1. However, commercially available VIPs made of fumed silica and opacifiers have centre of panel thermal conductivity of 4-5 $mWm^{-1}K^{-1}$. It was concluded that the solid conductivity of prototypes VIPs was 1.8-2 times higher compared to those of commercially available VIPs and is the main reason for higher centre of panel thermal conductivity.

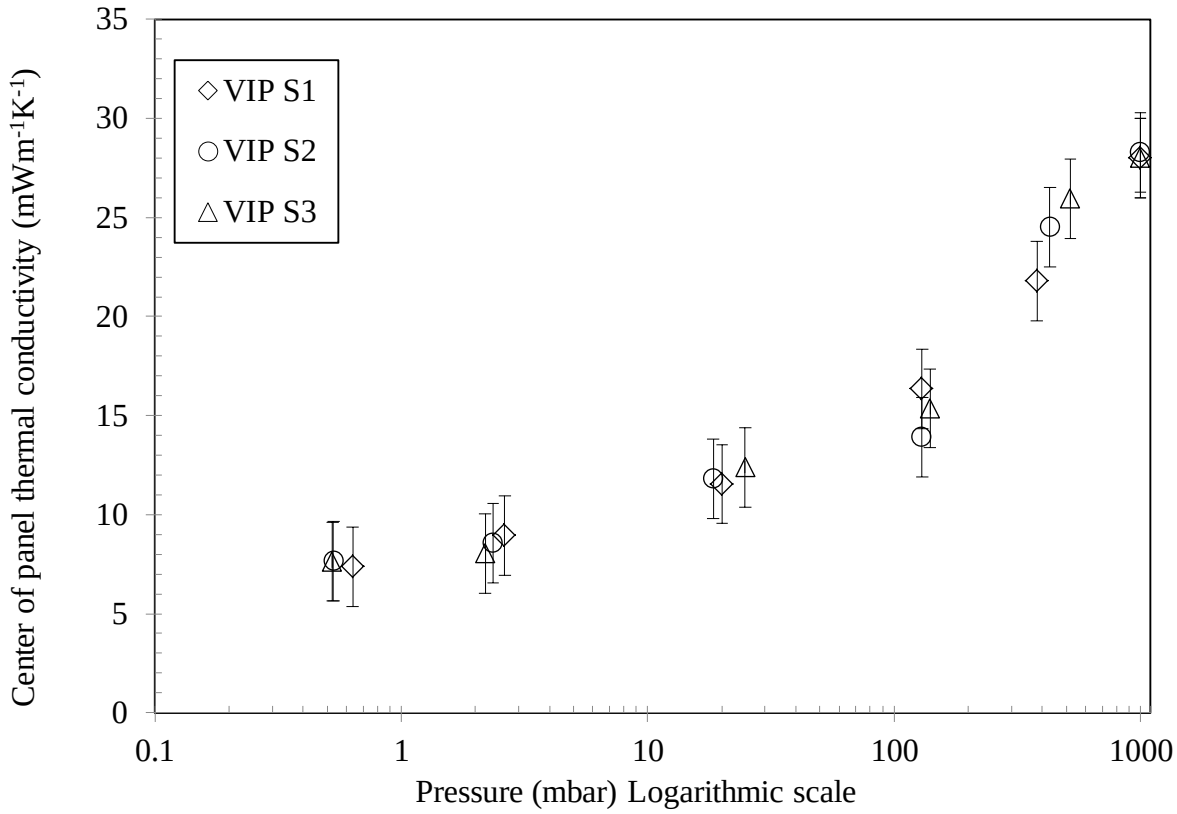

Figure 7.1 Centre of panel thermal conductivity of VIP prototypes at different pressures

6) Results of cost and thermal performance analysis revealed that cost of core material decreased with increasing expanded perlite content in the composite. Core board 3 containing fumed silica 50 mass %, expanded perlite 30 mass %, SiC opacifier 12 mass %, and polyester fibres 8 mass %, had the lowest cost of £20.07 m^{-2} per R-value of insulation compared to all core board samples in ambient conditions. In evacuated conditions R-value of core boards having similar composition as core board 3 had the cost per R-value of £5.87-6.02 m^{-2} which is 3.3 to 3.4 times less than that at ambient conditions. However, the cost per R-value of core boards used for VIP S1-S3 was relatively higher than that of core board 1 which has the similar composition (80 mass% of fumed silica) which is used for commercially available VIPs. It was also found that cost of core boards of VIP S1-S3 was lower than that of core board 1 and can be used in VIP applications where fixed thermal resistance in not required for set thickness of the VIP insulation.

7) VIP has longer payback compared to conventional EPS insulation due to its high initial cost. Payback period for VIP in four scenarios of applying insulation on existing UK

building with average U-value of 0.50 $Wm^{-2}K^{-1}$ was in the range of 4.2 to 5.87 years while for EPS it was calculated between 0.42 to 0.5 years. Considering economic benefit of the space saving potential offered by VIPs due to their small thickness, shorter payback period is possible. For building with achieving average U-value of 0.19 $Wm^{-2}K^{-1}$ and annual rent of £800m^{-2}, a shorter payback period of 1.22 years was possible for VIPs as shown in figure 7.2 and may become comparable to that of EPS in buildings with higher annual rents.

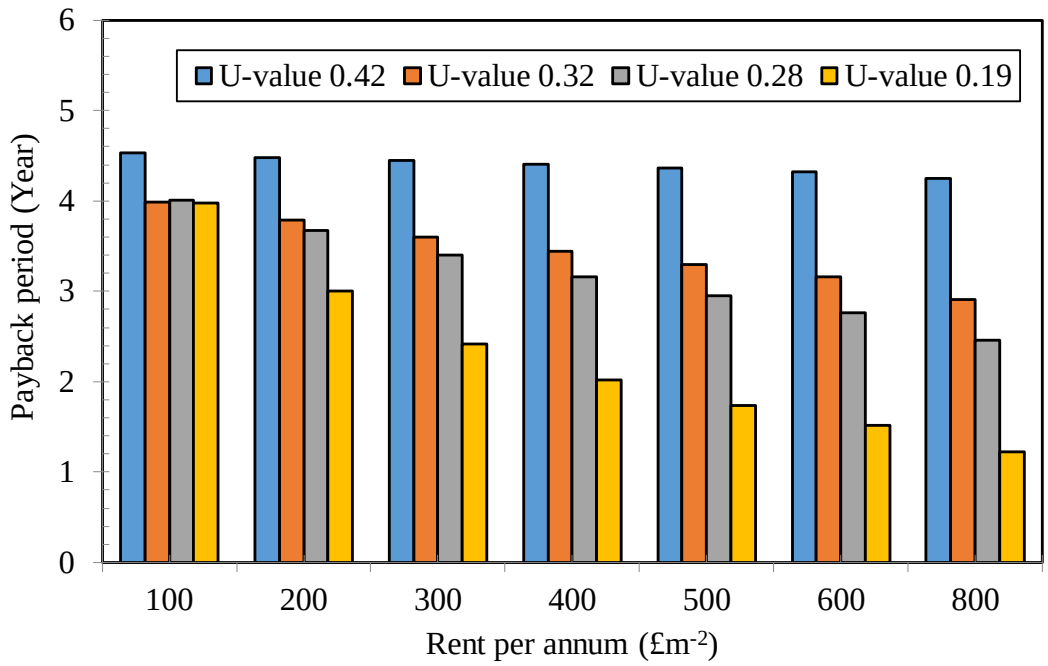

Figure 7.2 Payback period of VIPs for different U-values considering the space saving potential

7.3 Recommendations for future Work

- Collect experimental data of service life of prototype VIPs to ascertain the effect of climatic conditions and predict the service life of developed VIP prototypes.

- Development of expanded perlite with higher porosity and smaller pore size in the range of mean free path of air to completely replace the need of fumed silica in the composite material leading to further reduction of cost of the core material.

- Extend the research scope to other low cost minerals such as pumice and diatomite as VIP core materials with potential to achieve comparative or higher thermal performance with low cost to make VIPs price competitive with conventional insulation in building applications.

- Develop VIPs with these alternative materials and tests their thermal performance under room and accelerated ageing conditions for establishing their useful service life.

References

Abe H., Abe I., Sato K. and Naito M., (2005). Dry powder processing of fibrous fumed silica compacts for thermal insulation. Journal of the American Ceramic Society, 88, 1359-1361.

Alam M., Singh H. and Limbachiya M.C., (2011). Vacuum Insulation Panels (VIPs) for building construction industry - A review of the contemporary developments and future directions, Applied Energy, 88, 3592 - 3602.

Alam M., Singh H., Brunner S. and Naziris C., (2014). Experimental characterisation and evaluation of the thermo-physical properties of expanded perlite - fumed silica composite for effective vacuum insulation panel (VIP) core. Energy and Buildings, 69, 442- 450.

Alam M., Singh H. and Limbachiya M.C., (2011). Barrier performance of SiO_2 coated PET film for Vacuum Insulation Panel (VIP) envelope. In proceedings of 10th International Vacuum Insulation Symposium (IVIS) Ottawa, Canada.

Alotaibi S.S. and Riffat S. (2014). Vacuum insulated panels for sustainable buildings: a review of research and applications. International Journal of Energy Research, 38, 1-19.

Amrerg-Schwab S., Hoffmann M., Badera H. and Gessler M., (1998). Inorganic-organic polymers with barrier properties for water vapour, oxygen and flavours. Journal of Sol-Gel Science and Technology, 13, 141-146.

Araki K., Kamoto D. and Matsuoka S., (2009). Optimization about multilayer laminated film and getter device materials of vacuum insulation panel for using at high temperature, Journal of Materials Processing Technology, 209, 271-282.

ASTM C 1484 (2001), Standard Specification for Vacuum Insulation Panels, American Society for Testing and Materials (ASTM) International, West Conshohocken, US.

Augustynowicz S.D., Fesmire J.E. and Wikstrom J.P., (1999). Cyrogenic Insulation systems. In proceedings of 20th International congress of Refrigeration, IIR/IIF, Sydney.

Baetens R., Jelle B.P. and Gustavsen A., (2011). Aerogels for Building Applications: A State-of-the-Art Review. Energy and Buildings, 43, 761-769.

Baetens R., Jelle B.P., Thue J.V., Tenpierik M.J., Grynning S., Uvsløkk S. and Gustavsen A. (2010). Vacuum Insulation Panels for Building Applications: A Review and Beyond. Energy and Buildings, 42, 147-172.

Baltimore innovations Ltd. UK. Fumed silica SUPASIL^{TM} BIL-FS200, Technical Data Sheet.

Beck A., Binder M. and Frank O., (2009). Dynamic simulation of VIP moisture and heat transport. In: Proceedings of 9th international vacuum insulation symposium, London, UK.

Beikircher T. and Demharter M., (2013). Heat Transport in Evacuated Perlite Powders for Super-Insulated Long-Term storages up to 300 ºC. Journal of Heat Transfer, 135, 1-11.

Binz A., Moosmann A., Steinke G., Schonhardt U., Fregnan F., Simmler H., et al., (2005). Vacuum Insulation in the Building Sector. Systems and Applications (Subtask B), Final Report for the IEA/ECBCS Annex 39 HiPTI-project High performance thermal insulation for buildings and building systems.
Available from: http://www.ecbcs.org/docs/Annex_39_Report_Subtask-B.pdf [Accessed on 20 April 2012].

Boafo F.E., Chen Z., Li C., Li B. and Xu T., (2014). Structure of vacuum insulation panel in building system. Energy and Buildings, 85, 664-653.

Bolen W.P., (2012). U.S. Geological Survey Minerals Year Book, Perlite, 2012.

Bouquerel M., Duforestel T., Baillis D. and Rusaouen G., (2012). Mass transfer modeling in gas barrier envelopes for vacuum insulation panels: A review. Energy and Buildings, 55, 903-920.

Bovenkerk H.P., (1955). Insulating structure and method of forming same. US Patent 2700633.

Brown S.M. and Lard E.W., (1974). A comparison of nitrogen and mercury pore size distributions of silicas of varying pore volume. Powder Technology, 9, 187-190.

Brunner S., Gasser P., Simmler H. and Wakili K.G., (2006). Investigation of multi-layered aluminium-coated polymer laminates by focused ion beam (FIB) etching, Surface and Coatings Technology, 200, 5908-5914.

Brunner S., Wakili K.G., Stahl T. and Binder B., (2014). Energy and Buildings Vacuum insulation panels for building applications - continuous challenges and developments, 85, 592-596.

Brunner S. and Simmler H., (2008). In situ performance assessment of vacuum insulation panels in a flat roof construction. Vacuum, 82, 700-707.

BS EN 12086:1997. Thermal insulating products for building applications-Determination of water vapour transmission properties.

BS EN 12667:2001. Thermal performance of building materials and products - Determination of thermal resistance by means of guarded hot plate and heat flow meter methods - Products of high and medium thermal resistance.

BS ISO 15901-2:2006. Pore size distribution and porosity of solid materials by mercury porosimetry and gasadsorption -Part 2: Analysis of mesopores and macropores by gas adsorption.

Building Performance Institute Europe (BIPE), (2011). Europe's Buildings Under the Microscope.http://bpie.eu/uploads/lib/document/attachment/20/HR_EU_B_under_microscope_study.pdf [Accessed on 12 December 2014].

Caps R. and Beyrichen H., (2005). Monitoring gas pressure in vacuum insulation panels. In: Zimmermann M, Editor, Proceedings of the 7th international vacuum insulation symposium, Duebendorf, Switzerland, 57-66.

Caps R., Beyrichen H., Kraus D. and Weismann S., (2008). Quality control of vacuum insulation panels: methods of measuring gas pressure. Vacuum, 82, 691-699.

Caps R., Fricke J. and Reiss H., (1983). Improving the extinction properties of an evacuated high-temperature powder insulation. High Temperatures-High Pressures, 15, 225-232.

Caps R. and Fricke J., (2000). Thermal conductivity of opacified powder filler materials for vacuum insulations. International Journal of Thermophysics, 21, 445-452.

Cho K., Hong Y. and Seo J., (2014). Assessment of the economic performance of vacuum insulation panels for housing projects. Energy and Buildings, 70, 45-41.

Climate Change Act (2008), Crown copyright. http://www.opsi.gov.uk/acts/acts2008/pdf/ukpga20080027_en.pdf [Accessed on 19 June 2012].

Colthup N.P., Daly L.H. and Wiberley S.E., (1990). Introduction to Infrared and Raman Spectroscopy. Third Edition, Academic Press London.

Committee on Climate Change (CCC), (2013). Fact sheet: Buildings http://www.theccc.org.uk/wp-content/uploads/2014/08/Factsheetbuildings2014_Final1.pdf [Accessed on 19 October 2014].

Demirboğa R. and Gül R., (2003). The effects of expanded perlite aggregate, silica fume and fly ash on the thermal conductivity of lightweight concrete. Cement and Concrete Research, 33, 723-727.

Department of Energy and Climate Change (DECC), (2010). Energy Trends – June 2010.

Department for Communities and Local Government (DCLG), (2007). Building a Greener Future:policy statement. http://www.communities.Gov.uk/documents/planningandbuilding/pdf/building-greener.pdf [Accessed on 01 July 2012].

Department for Communities and Local Government (DCLG), (2014). Code for Sustainable Homes Technical Guide Code Addendum England. https://www.gov.uk/government/uploads/system/uploads/attachment_data/file/315504/250414__Code_Addedum_2014_Combined_Final_V10.pdf [Accessed on 27 October 2014].

Department for communities and local Government (DCLG), (2009). Zero carbon for new non domestic buildings consultation policy options. Available from: http// www. Communities.gov.uk/documents/planningandbuilding/pdf/13991110.pdf. [Accessed on 17 April 2012].

Department for communities and local Government (DCLG), (2011). Dwelling stock estimates: 2011, England.
https://www.gov.uk/government/systems/uploads/attachement_data/file/6868/2039750.pdf [Accessed on 30 April 2012].

Di X., Gao Y., Bao C., Hu Y. and Xie Z., (2013). Optimization of glass fiber based core materials for vacuum insulation panels with laminated aluminum foils as envelopes. Vacuum, 97, 55-59.

Di X., Gao Y., Bao C. and Ma S., (2014). Thermal insulation property and service life of vacuum insulation panels with glass fiber chopped strand as core materials Energy and Buildings, 73, 176-183.

Dombayci Ö. A., Gölcü M. and Y Pancar., (2006). Optimization of insulation thickness for external walls using different energy-sources. Applied Energy, 83, 921-928.

Dubé W.P., Sparks L.L. and Slifka A.J., (1991). Thermal conductivity of evacuated perlite at low temperatures as a function of load and load history. Cryogenics, 31, 3-6.

European Commission, (2010). Directive 2010/31/EU of the European Parliament and Council on the Energy Performance of Buildings 19 May 2010 (EPBD Recast).
http://eurlex.europa.eu/legalcontent/en/all/;elx_sessionid=7ljljb0dy8bgd582q22psd9jppbxz1vcgjndyvj5xrhk1jsjmqsj!-663730610?uri=celex:32010l0031 [Accessed on 6 December 2014]

Energy Saving Trust, (2014). http://www.energysavingtrust.org.uk/content/our-calculations [accessed on 29 September 2014].

Evonik Industries (2006), Basic properties and characteristics of Aerosil® products, Technical bulletin Fine Particles, Number 11.

Fahlteich J., Schönberger W., Fahland M. and Schiller N., (2011). Characterization of reactively sputtered permeation barrier materials on polymer substrates. Surface and Coatings Technology, 205, 141-144.

Feng J., Yan Y., Chen, D. Ni W., Yang J., Ma S. and Mo W., (2011). Study of thermal stability of fumed silica based thermal insulating composites at high temperatures, Composites Part B: Engineering, 42, 1821-1825.

Find a London Office LLP, (2014). http://www.findalondonoffice.co.uk/toolbox/rental-guide/ [Accessed on 29 October 2014].

Fricke J., (1993). Materials research for the optimization of thermal insulations. High Temperatures-High Pressures, 25, 379-390.

Fricke J., Schwab H. and Heinemann U., (2006). Vacuum Insulation Panel-Exciting Thermal Properties and Most Challenging Applications. International Journal of Thermophysics, 27, 1123-1139.

Gervais P.P. and Goumy D., (1979). Insulating material with low thermal conductivity formed of a compacted granular structure. US Patent 4159359.

Groezinger J., Boermans T., John A., Seehusen J., Wehringer F. and Scherberich M., (2014). Overview of Member States Information on NZEBs-Working version of the progress report - final report.
https://ec.europa.eu/energy/sites/ener/files/documents/Updated%20progress%20report%20NZEB.pdf [Accessed on 19 June 2015].

Hall M.R., (2010). Materials for energy efficiency and thermal comfort in buildings, Woodhead Publishing Limited.

Henry B.M., Erlat A.G., McGuiga A., Grovenor C.R.M., Briggs G.A.D., Tsukahara Y., Miyamoto T., Noguchi N. and Niijima T., (2001). Characterization of transparent aluminium oxide and indium tin oxide layers on polymer substrates. Thin Solid Films, 382, 194-201.

Howells D.G., Henry B.M., Laterrier Y., Manson J.A.E., Madocks J. and Assender H.E., (2008). Mechanical properties of SiO_x gas barrier coatings on polyester films. Surface and Coating Technologies, 208, 3529-3537.

Hull T.R. and Stec A.A., (2011). Assessment of the fire toxicity of building insulation materials. Energy and Buildings, 43, 498-506.

Johansson P., Geving S., Hagentoft C.E., Jelle B.P., Rognvikc E., Kalagasidisa A.S. and Timec B., (2014). Interior insulation retrofit of a historical brick wall using vacuum insulation panels: Hygrothermal numerical simulations and laboratory investigations. Building and Environment, 79, 31-45.

Jung H., Yeo I. and Song T.H., (2014). Al-foil-bonded enveloping and double enveloping for application to vacuum insulation panels. Energy and Buildings, 84, 595-606.

Kaganer M.G., (1969). Thermal insulation in cryogenic engineering, translated by A. Moscona, Israel programme for scientific translation Ltd.

Kalnaes S.E. and Jelle B.P. (2014). Vacuum insulation panel products: A state-of-the-art review and future research pathways. Applied Energy, 116, 355-375.

Karami P., Afriyie E.T., Norberg P. and Gudmundsson K., (2014). A study of the thermal conductivity of granular silica materials for VIPs at different levels of gaseous pressure and external loads. Energy and Buildings, 85, 199-211.

Kim J., Lee J.H. and Song T.H., (2012). Vacuum insulation properties of phenolic foam. International Journal of Heat and Mass Transfer, 55, 5343-5349.

Kistler S.S., and Caldwell A.G., (1934). Thermal conductivity of silica aerogel. Industrial and Engineering Chemistry, 26, 658-662.

Kwon J.S., Jang C.H., Jung H., Song T.H., (2009). Effective thermal conductivity of various filling materials for vacuum insulation panels. International Journal of Heat Mass Transfer, 52, 5525-5532.

Kwon J.S., Jang C.H., Jung H. and Song T.H., (2010). Vacuum maintenance in vacuum insulation panels exemplified with a staggered beam VIP. Energy and Buildings, 42, 590-597.

Kuhn J., Korder S., Arduini-Schuster M.C., Caps R., and Fricke J., (1993). Infrared-optical transmission and reflection measurements on loose powders. Review of Scientific Instruments, 64, 2523-2530.

Lange J. and Wyser Y., (2003). Recent innovations in barrier technologies for plastic packaging – a review. Packaging Technology and Science, 16, 149-158.

Li C.D., Duan Z.C., Chen Q., Chen Z.F., Boafo F.W., Wu W.P. and Zhou J.M., (2013). The effect of drying condition of glassfibre core material on the thermal conductivity of vacuum insulation panel. Materials and Design, 50, 1030-1037.

Lim H.S., Baek J.H., Park K., Shin H.S., Kim J. and Cho J.H., (2010). Multifunctional hybrid fabrics with thermally stable super hydrophobicity. Advanced Materials, 22, 2138-2141.

Malsen J.V., Tenpierik M.J., Looman R.H.J. and Cauberg J.J.M., (2008). Heat seal strength of barrier film used in vacuum insulation panels at room temperature and at – 130°C. Journal of Plastic Film and Sheeting, 24, 35-52.

Mandilaras I., Atsonios I., Zannis G. and Founti M. (2014). Thermal performance of a building envelope incorporating ETICS with vacuum insulation panels and EPS. Energy and Buildings, 85, 654-665.

Marouani S., (2012). Investigation of the resistance welding of multilayers aluminum-coated polymer complexes used as envelopes of vacuum insulation panels. Materials and Design, 36, 546-556.

Miesbauer O., Kucukpinar E., Kiese S.,Carmi Y., Noller K. and Langowski H.C. (2014). Studies on the barrier performance and adhesion strength of novel barrier films for vacuum insulation panels. Energy and Buildings, 85, 597-603.

Modest M. F., (2003). Radiative Heat Transfer, Second Edition. Academic Press London.

Mukhopadhyaya P., Kumaran K., Normadin N., and Reen D.V., (2009). Fibre-powder composite as core material for Vacuum Insulation Panel. In Proceedings of 9th international vacuum insulation symposium, London, UK.

Mukhopadhyaya P., MacLean D., Korn J., van Reenen D. and Molletia S., (2014). Building application and thermal performance of vacuum insulation panels (VIPs) in Canadian subarctic climate. Energy and Buildings, 85, 672-680.

Nemanič V. and Žumer M., (2015). New organic fiber-based core material for vacuum thermal insulation. Energy and Buildings, 90, 137-141.

Nemanič V., Zajec B., Žumer M., Figar N., Kavšek M. and Mihelič I., (2014). Synthesis and characterization of melamine-formaldehyde rigid foams for vacuum thermal insulation, Applied Energy, 114, 320-326.

Nemoto T., Takagi J. and Ohshima M., (2008). Control of bubble size and location in Nano-/Microcellular Poly(propylene)/Rubber Blend Foams. Macromolecular Materials and Engineering, 293, 574-580.

NORNER Industrial Polymer Institute, OTR and WVTR calculator, www.norner.no/projects/packaging-industries/otr-and-wvtr-barrier-calculator [accessed on 14 March 2013].

Nowobiliski J.J., Acharya A. and Kather K.C., (1988). Vacuum Insulation Panel, US patent 4726974. http://www.freepatentsonline.com/4726974.pdf [Accessed on 20 November 2011]

Palmer J. and Cooper I., (2012). United Kingdom Housing Energy fact file 2012 https://www.gov.uk/government/.../uk_housing_fact_file_pdf. [Accessed on 19 June 2014]

Perlite Institute USA, (1983). "Perlite" Techninal Data Sheet / No. 2-4. Available from: www.schundler.com/TD2-4.pdf [Accessed on 13 May 2012].

Perlite Institute USA. “Evacuated Perlite” Available from: www.pdfport.com/view/535638-evacuated-perlite.html [Accessed on 24 May 2012].

Pfundstein M., Gellert R., Spitzner M.H. and Rudolphi A., (2008). Detail Practice: Insulating Materials: Principles, Materials and Applications. ISBN 9783764386542.

Potter F.J., (2001). Nanogel Production, properties, applications. In: Zimmermann M, Bertschinger H. Editors, Proceedings of the international conference and workshop on high performance thermal insulation, Duebendorf, Switzerland.

Quenard D. and Sallee H. (2005). From VIP’s to building facades: three levels of thermal bridges. In proceedings of the 7th international vacuum insulation symposium, Duebendorf, Switzerland.

Rouquerol F., Rouquerol J. and Sing K. (1999). Adsorption by powders and porous solids: principles, methodology and applications. San Diego: Academic Press; 439 - 467.

Rusek S.J., (2009). Gen3 Long Life High Performance Vacuum Insulation Panel for Construction Applications. In Proceedings of 9th international vacuum insulation symposium, London, UK.

Sari A. and Karaipekli A., (2008). Preparation, thermal properties and thermal reliability of capric acid/expanded Expanded Perlite composite for thermal energy storage. Materials Chemistry and Physics, 109, 459-464.

Sass J.P., Fesmire J.E., Nagy Z.F., Sojourner S.J., Morris D.L. and Augustynowicz SD., (2008). Thermal Performance Comparison of Glass Microsphere and Perlite Insulation Systems for Liquid Hydrogen Storage Tanks. In: American Institute of Physics Conference Proceedings, 985, 1375-1382.

Schwab H., Heinemann U., Beck A., Ebert H.P. and Fricke J., (2005). Prediction of useful life time for vacuum insulation panels with fumed silica kernel and foil cover. Journal of Building Physics, 28, 357-374.

Sengul O., Azizi S., Karaosmanoglu F. and Tasdemir M. A., (2011). Effect of expanded perlite on the mechanical properties and thermal conductivity of lightweight concrete. Energy and Buildings, 43, 671-676.

Simmler H. and Brunner S., (2005). Vacuum insulation panels for building application: Basic properties, aging mechanisms and service life. Energy and Buildings, 37, 1122-1131.

Simmler H., Brunner S., Heinemann U., Schwab H., Kumaran K., Mukhopadhyaya P., Quénard D., Sallée H., Noller K., Kücükpinar-Niarchos E., Stramm C., Tenpierik M., Cauberg H., Binz A., Steinke G., Moosmann A., (2005). Vacuum Insulation - Panel Properties and Building Applications (Subtask A). A Report for the IEA/ECBCS Annex 39 High Performance Thermal Insulation for Buildings and Building Systems 2005, Available from: http://www.ecbcs.org/docs/Annex_39_Report_Subtask-A.pdf [Accessed on 26.04.2012].

Sing K.S.W., Everett D.H., Haul R.A.W., Moscou L., Pierotti R.A., Rouquerol J. and Siemieniewska T., (1985). Reporting physisorption data for gas/solid systems with special reference to the determination of surface area and porosity. Pure and Applied Chemistry, 57, 603-619.

Sprengard C. and Holm H.A., (2014). Numerical examination of thermal bridging effects at the edges of vacuum-insulation-panels (VIP) in various constructions. Energy and Buildings, 85, 638-643.

Stahl Th., Brunner S., Zimmermann M. and Wakili K.G., (2012). Thermo-hygric properties of a newly developed aerogel based insulation rendering for both exterior and interior applications. Energy and Buildings, 44, 114-117.

Swimm K., Reichenauer G., Vidi S. and Ebert H.P., (2009). Gas pressure dependence of the heat transport in porous solids with pores smaller than 10 μm. International Journal of Thermophysics, 30, 1329-1342.

Temmerman P.D., Doren E.V., Stede Y.V., Francisco M.A.D. and Mast J., (2012). Quantitative characterization of agglomerates and aggregates of pyrogenic and precipitated

amorphous silica nanomaterials by transmission electron microscopy. Journal of Nanobiotechnology, 10:24 doi:10.1186/1477-3155-10-24

Tekin N., Kadinci E., Demirbaş Ö., Alkan M., Kara A. and Doğan M., (2006). Surface properties of poly(vinylimidazole)-adsorbed expanded perlite. Microporous and Mesoporous Materials, 93, 125-133.

Teniers C., (2009). How laminates with EVAL^{TM} EVOH film improve the performance of VIPs. In proceedings of 9th international vacuum insulation symposium, London, UK.

Tenpierik M.J., (2009). Vacuum insulation panels applied in building constructions (VIP ABC). Ph.D. Thesis, Delft University of Technology, Delft, Netherlands.

Tenpierik M. and Cauberg H., (2007). Analytical models for calculating thermal bridge effects caused by thin high barrier envelopes around vacuum insulation panels. Journal of Building Physics, 30, 185-215.

Tenpierik M. and Cauberg H., (2006). Vacuum Insulation Panel: friend or foe? In: Proceeding of 23rd Conference on passive and low energy architecture, Geneva, Switzerland.

Tenpierik M., van Der Spoel W. and Cauberg H., (2007). Simplified analytical model for useful life time prediction of a vacuum insulation panel. In proceedings of 8th international vacuum insulation symposium, Würzburg, Germany.

Tenpierik M.J. and Cauberg J.J.M., (2010). Encapsulated vacuum insulation panel: theoretical thermal optimization. Building Research and Information, 38, 660-669.

Thorsell T. and Kallebrink I., (2005). Edge loss minimization in vacuum insulation panels. In proceedings of 7th symposium on building physics in the Nordic countries, Reykjavik, Iceland.

Tseng P.C. and Chu H.S., (2009). The effects of PE additive on the performance of polystyrene vacuum insulation panels. International Journal of Heat and Mass Transfer, 52, 3084-3090.

Wakili K.G., Bundi R. and Binder B., (2004). Effective thermal conductivity of vacuum insulation panels, Building Research and Information, 32, 293-299.
Wang X., Walliman N., Ogden R. and Kendrick C., (2007). VIP and their applications in buildings: a review. Construction Materials, 160, 145-153.

Wang Z., Tu H., Gao J., Qian G., Fan X. and Wang Z., (2011). A Novel Building Thermal Insulation Material: Expanded Perlite Modified by Aerogel. Advanced Materials Research, 250-253, 507-512.

Webb P.A., (2001). An introduction to the physical characterization of materials by mercury intrusion porosimetry with emphasis on reduction and presentation of experimental data. Micrometrics Instrument Corp. Pages 1-9.

Wei G., Liu Y., Zhang X. and Du X., (2013). Radiative heat transfer study on silica aerogel and its composite insulation materials. Journal of Non-Crystalline Solids, 362, 231-236.

Wei G., Liu Y., Zhang X. and Du X., (2011). Thermal Radiation in Silica Aerogel and its Composite Insulation Materials. In proceeding of the 9th International Mechanical Engineering Congress and Exposition IMECE, Denver, Colorado, USA.

Willems W.M. and Schild K., (2005a). The Next Generation of Insulating Materials: Vacuum Insulation. In proceedings of the 7th symposium of building physics in the Nordic countries, Reyjhavik, Iceland.

Willems W.M., Schild K. and Hellinger G., (2005b). Numerical investigation on thermal bridge effects in vacuum insulating elements. In proceedings of the 7th international vacuum insulation symposium, Duebendorf, Switzerlan, 145-152.

William Sinclair Ltd. UK. Expanded perlite Techical Data Sheet.

Wolf R., Wandel K. and Boeffel C., (2007). Moisture barrier films deposited on PET by ICPECVD of SiN. Plasma Process and Polymers, 4, 185-189.

Wong C. and Hung M., (2008). Polystyrene Foams as Core Materials Used in Vacuum Insulation Panel.Journal of Cellular Plastics, 44, 239-259.

Yang C.G., Xu L., Wang J. and Shi F.L., (2007). Outgassing of Rigid Open-celled Polyurethane Foam Used in Vacuum Insulation Panels under Vacuum Condition. Journal of Cellular Plastics 2007, 43, 17-29.

Young J.R. and Schreck R.M., (1984). Vacuum Thermal Insulation Panel, US patent 4444821. http://www.freepatentsonline.com/4444821.pdf [Accessed on 14 October 2011].

Yun-Jin S., Ya-Bo F., Qiang C., Chun-Mei Z., Li-Jun S. and Yue-Fei Z., (2008). Silicon Dioxide Coating Deposited by PDPs on PET Films and Influence on Oxygen Transmission Rate. Chinese Physics Letters, 25, 1753-1756.

Zhang D., Tian S. and Xiao D., (2007). Experimental study on the phase change behaviour of phase change material confined in pores. Solar Energy, 81, 653-660.

Appendix I Journal Publications

Energy and Buildings 69 (2014) 442–450

Contents lists available at ScienceDirect

Energy and Buildings

journal homepage: www.elsevier.com/locate/enbuild

Experimental characterisation and evaluation of the thermo-physical properties of expanded perlite—Fumed silica composite for effective vacuum insulation panel (VIP) core

M. Alam [a], H. Singh [a,*], S. Brunner [b], C. Naziris [a]

[a] School of Engineering and Design, Brunel University, Uxbridge UB8 3PH, UK
[b] Empa, Swiss Federal Laboratories for Materials Testing, Research Laboratory for Building Technologies, CH-8600 Duebendorf, Switzerland

ARTICLE INFO

Article history:
Received 24 October 2012
Received in revised form 25 October 2013
Accepted 6 November 2013

Keywords:
Vacuum insulation panel
Expanded perlite
Fumed silica
Pore size distribution
Thermal conductivity
Radiative conductivity

ABSTRACT

The thermo-physical properties of expanded perlite-fumed silica composites were experimentally investigated as an alternative lower cost material for vacuum insulation panel (VIP) core using expanded perlite as a cheaper substitute of fumed silica. Pore size analysis was carried out using nitrogen sorption technique, mercury intrusion porosimetry and transmission electron microscopy and average pore size was estimated to be in the range of 50–150 nm. VIP core board samples measuring 100 mm × 100 mm and consisting of varying proportions of expanded perlite, fumed silica, silicon carbide and polyester fibre in the composite were prepared. The centre of panel thermal conductivity of the core board containing expanded perlite mass proportion of 60% was measured as 53 mW m^{-1} K^{-1} at atmospheric pressure and 28 mW m^{-1} K^{-1} when expanded perlite content was reduced to 30%. The centre of panel thermal conductivity with 30% expanded perlite content was measured as 7.6 mW m^{-1} K^{-1} at 0.5 mbar pressure. Radiative conductivity of the composite with expanded perlite mass of 30% was measured to be 0.3–1 mW m^{-1} K^{-1} at 300 K and gaseous thermal conductivity 0.016 mW m^{-1} K^{-1} at 1 mbar, a reduction of 8.3 mW m^{-1} K^{-1} from the value of gaseous thermal conductivity at 1 atm pressure. Opacifying properties of expanded perlite were quantified and are reported. A VIP core cost reduction potential of 20% was calculated through the use of expanded perlite in VIP core.

1. Introduction

Energy use in buildings accounts for approximately around half of the UK's total energy consumption and is responsible for almost 50% of the UK's total carbon dioxide (CO_2) emissions [1]. Use of high thermal resistance insulation in buildings is critical to save the substantial amounts of space heating energy lost through the building fabric. Vacuum insulation panel (VIP) with a high thermal resistance (centre of panel thermal conductivity 0.004 W m^{-1} K^{-1} and overall thermal conductivity of 0.008 W m^{-1} K^{-1}) is an energy efficient alternative to conventional building insulation. It has a huge potential to help in reducing the carbon foot prints of buildings and in conforming to stringent energy standards such as Building Regulations (2010) [2], Code for sustainable Homes (2006) [3], Passivhaus (1991) [4] and Minergie-P® (2012) [5], while using minimal existing space. VIPs are produced as a rigid panel comprising inner core board laminated in an outer high barrier envelope under evacuated conditions (less than 3 mbar). Heat transfer across VIPs occurs mainly by solid conduction, gaseous conduction and radiation. Gaseous conduction is suppressed by creating vacuum in nano/micro porous core material, solid conduction by using low density material and radiative heat transfer by using opacifiers [6,7]. The VIP core is fabricated as rigid board from materials such as open porous foams, powders and fibres. Currently, fumed silica (FS) is widely used as the core of VIPs for longer service life required for building applications [8,9]. It is relatively expensive and a major contributing factor to the current high cost of VIPs. The cost of VIPs must be reduced to encourage their widespread application in the built environment. Cost reduction can be achieved by replacing or reducing the proportion of FS with low cost alternative materials. Mukhopadhyaya et al. [9] reported the use of powder fibre composite of mineral oxide fibre/high density glass fibre and pumice powder composites as low cost alternative core material for VIPs. Expanded perlite (EP) is another potential candidate as a more economically viable material for incorporation in core of a VIP in the form of composite with FS [10]. Perlite is a low cost glassy amorphous mineral rock and can be expanded on heating at temperature of 760–1100 °C [11]. It has been used for different construction applications such as lightweight cement aggregate, insulation and ceiling tiles [12] due to its low density

* Corresponding author. Tel.: +44 1895265468.
E-mail address: harjit.singh@brunel.ac.uk (H. Singh).

0378-7788/$ – see front matter © 2013 Elsevier B.V. All rights reserved.
http://dx.doi.org/10.1016/j.enbuild.2013.11.027

(35–120 kg m^{-3}), porous nature, low thermal conductivity, ease of handling and non-flammability [13]. However, the thermal resistance of EP is rather limited; its thermal conductivity is between 0.045 and 0.070 W m^{-1} K^{-1} at 300 K [14]. Due to its porous nature it is well suited for use under vacuum conditions [15] and has been used in cryogenic insulation systems at a temperature range of 20–90 K [16] and liquid hydrogen storage tanks [17]. Fricke et al. [18] showed that at 0.1 mbar pressure, thermal conductivity values of EP are comparable to that of micro silica powders. However, pore size of EP is relativity large in micrometric range (approximately 3 μm) [19] and requires a high level of vacuum (0.01 mbar) to limit its gaseous thermal conductivity. Larger pores of EP can be partly filled by aggregates of FS powder (mean aggregate size 0.2–0.3 μm), thus limiting the gaseous conductivity under vacuum conditions. Several studies investigating the use of FS in VIP cores have been reported, but there is no study reporting the use of EP for VIP core to date.

The aim of the present study is to develop and experimentally characterise a lower cost composite of EP, FS, opacifier silicon carbide (SiC) and reinforcing polyester fibres (PF) to evaluate its viability as a VIP core. Based on the commercial prices obtained from [20] and [21], it has been found that EP is approximately 12 times cheaper than FS, making it an attractive substitute for expensive FS. In order to achieve a minimal thermal conductivity of a VIP at minimum cost, the mass proportions of FS, EP, SiC and PF must be optimised in the composite. For this purpose composites with variable mass ratios of these constituents were prepared and their porosity, pore size distribution, and densities were measured. Gaseous thermal conductivity at different vacuum levels was estimated from the pore size data measured and verified using nitrogen (N_2) sorption, mercury intrusion porosimetry (MIP) and transmission electron microscopy (TEM). Centre of panel thermal conductivity of core boards (100 mm × 100 mm) made of composite samples at atmospheric pressure was measured by using a small guarded hot plate device with an accuracy of ±2 mW m^{-1} K^{-1} and radiative conductivity of composite samples was measured using Fourier transform infrared (FT-IR). The effects of addition of EP in VIP core composite on thermal conductivity, density, porosity, and radiative conductivity have been measured and discussed.

2. Preparation of composites

FS powder, SupaSil™ BIL-FS200-10S, sourced from Baltimore Innovations Ltd. [23] and EP powder sourced from Silvaperl Ltd. [22] were used as the main core material. EP used was an aluminium silicate with its composition detailed in Table 1. Its particle size ranged between 10 and 750 μm with a free moisture content of 0.5%, specific heat of 837 J kg^{-1} K^{-1}, thermal conductivity of 0.05 W m^{-1} K^{-1} and density of 180–200 kg m^{-3} as specified by the supplier. Brunauer, Emmett and Teller (BET) specific surface area of FS powder was 200 ± 25 m^2 g^{-1} as specified by the supplier. Polyester fibres (PF) with diameter of 12 μm, length of 1.6 mm and melting point >230 °C were mixed into FS and EP powder matrix to increase mechanical strength of the core board. SiC with a mean particle size of 0.1–1 μm was used as an opacifier to reduce the radiative heat transfer by inducing a low infrared transmittance. A range of composite samples were prepared by mechanically mixing FS, EP, SiC and PF together in different mass ratios at low speed (~1200 rpm) to avoid the breaking up of fibres in a 4 bladed conventional mixer for 5 min. Table 2 shows the different composite samples prepared with respective proportions of different constituents. VIP core boards of different composite samples detailed in Table 2 were prepared. Powder samples were uniaxially compacted in a square cross-section die at an applied pressure of 1.3 MPa at room temperature to make VIP core boards of size 100 mm × 100 mm × 12 ± 1 mm (sample 1, 2, 4 and 5) and 100 mm × 100 mm × 15 ± 1 mm (sample 3).

Table 1
Composition of commercial expanded perlite.

Chemical constituent	Mass ratio (%)
Silica (SiO_2)	73
Aluminium (Al_2O_3)	15
Potassium (K_2O)	5
Sodium (Na_2O)	3
Calcium and magnesium (CaO + MgO)	1
Iron (Fe_2O_3)	2
Others	1

Table 2
Composite samples and respective ratios of different constituents.

Sample	Composition (mass %)			
	Fumed silica (FS)	Expanded perlite (EP)	Silicon carbide (SiC)	Polyester fibre (PF)
1	80	0	12	8
2	60	20	12	8
3	50	30	12	8
4	40	40	12	8
5	20	60	12	8
6	58	30	12	0
7	57	30	5	8
8	52	30	10	8
9	47	30	15	8
10	57	20	15	8
11	46	46	0	8
12	62	30	0	8

The morphology of the composites was characterised by using TEM. TEM image in Fig. 1 clearly shows the submicron-sized particles of FS powder fused into short chains arranged in pseudo circular shape forming nanometre size pores. These pores appear to be random in shape and size ranging from approximately 50 to 150 nm. The size of these pores is in the same order as the mean free path of free air (70 nm), which helps in reducing the gaseous thermal conductivity.

3. Pore size measurement

Porosity, pore volume, pore size distribution and surface area was measured using MIP and N_2 sorption and TEM. Four representative composite samples 1, 3, 5 and 6, detailed in Table 2, were selected for MIP measurements and samples 1 and 3 for N_2 sorption to cover the widest range of the composition of EP ranging from 0% (sample 1) to 60% (sample 5) employed in this study using Micromeritics Autopore IV mercury porosimeter. MIP was

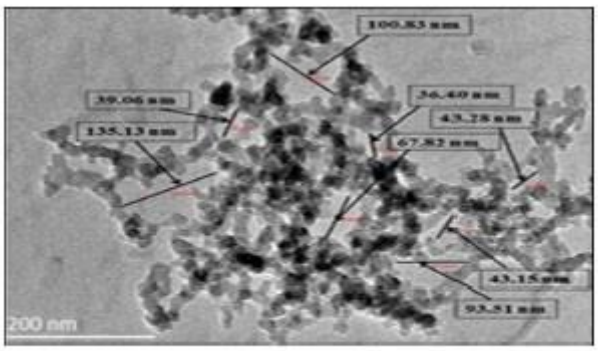

Fig. 1. TEM image of FS and EP composite showing the nanometre size pores.

Table 3
Pore size and bulk density results of composite samples 1, 3, 5 and 6 using MIP.

Sample	Total intrusion volume (V) $\times 10^{-6}$ ($m^3 g^{-1}$)	Total pore area (A) ($m^2 g^{-1}$)	Average pore diameter(4 V/A) $\times 10^{-6}$ (m)	Porosity (%)	Bulk density ($kg m^{-3}$)
1	13.232	182.404	0.290	90	69
3	4.946	128.008	0.155	83	167
5	3.790	77.271	0.196	83	220
6	5.199	149.852	0.139	85	164

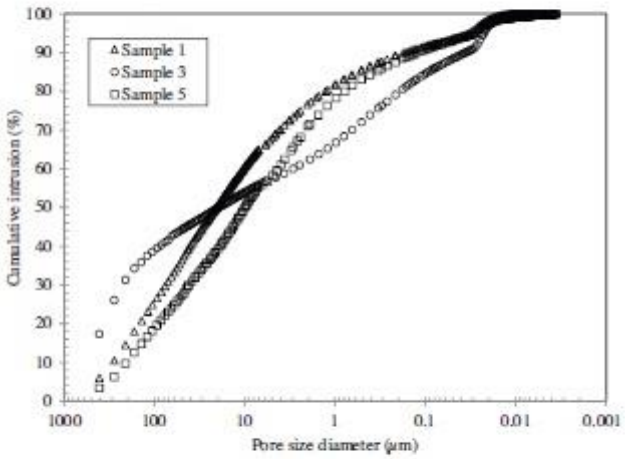

Fig. 2. Distribution of cumulative intrusion (%) in samples 1, 3 and 5 containing EP content of 0%, 30% and 60% respectively.

performed over a pressure range of 0–413.6 MPa and total intrusion volume was measured over this range, Figs. 2 and 3. The surface tension of 0.48 N m^{-1} and a contact angle of 140° were used for mercury. Total pore volume was calculated by software package Autopore IV 9500 V 1.09 by subtracting intrusion volume at maximum pressure from intrusion volume at zero pressure. MIP technique is limited by the concomitant compression of material due to pressure applied for intrusion of mercury into pores. Still Simmler et al. [23] have reported the use of MIP for similar materials for VIP applications.

Sample porosity, defined as the ratio of the volume of voids plus the volume of open pores to the total volume occupied by the powder, was calculated from bulk volume and pore volume using Eq. (1).

$$P(\%) = \frac{V_{pore}}{V_{Bulk}} \times 100 \quad (1)$$

where P is the porosity (%), V_{pore} the volume of pores ($cm^3 g^{-1}$) and V_{Bulk} the sample bulk volume ($cm^3 g^{-1}$).

For sample 1, 3 and 5 sample porosity was calculated to be 90%, 83% and 83% respectively using Eq. (1) as shown in Table 3. This showed that with the addition of EP content in the composite the porosity decreased, for example sample 5 with EP mass ratio of 60% had porosity 7% lower than that of sample 1 which had no EP at all. The Bulk density of the composite was found to increase with an increased proportion of EP in the matrix as shown in Table 3, the bulk density increased from 167 to 220 kg m^{-3} as the EP mass content increased from 30% to 60% between sample 3 and 5.

The density range of the core composites detailed in Table 3 falls well within the range of 150–220 kg m^{-3} reported by Simmler et al. [23]. It can be seen in Fig. 2 that sample 3 with EP mass ratio of 30% was found to have approximately 38% pore volume occupied by pores with diameter of >100 μm, sample 1 approximately 22% and sample 5 approximately 18%.

A shift of approximately 20% in pore volume from >100 μm to <100 μm was observed in the sample 5 compared to the sample 3. This was due to an apparent migration of nanometric size FS particles into the larger pores of EP resulting in increasing the proportion of pore size <100 μm. MIP based pore size distribution shows that sample 3 had approximately 33% of pore volume occupied by submicron pores (<1 μm) while sample 5 had 18%. This behaviour is expected to result from the availability of high number of FS particles to migrate into the large diameter pores of EP leading to a higher proportion of submicron size pores in sample 3. Sample 5 despite of having lesser pore volume occupied by pores of size >100 μm and submicron pores is expected to have a higher solid conductivity due to the high content of EP when compared to sample 3. Clearly, sample 3 is a better composite with respect to pore size distribution, 33% of pore volume occupied by submicron pores (less than 1 μm), and a lower solid conductivity due to a lower content of EP. To evaluate the effect of PF on the composite porosity and density, sample 6 with no PF content was prepared with FS, EP and SiC in the mass proportions of respectively 58%, 30% and 12%.

Measured pore size data for sample 6 was compared to that of the sample 3 as shown in Fig. 3. It is clear that the addition of fibres for increasing the mechanical strength of core for manufacturing purpose had negligible effect on pore size distribution in submicron range and a shift of less than 2.5% from submicron to micron size was observed. The composite bulk density was still well within the range of 160–180 kg m^{-3}. However, a significantly lower pore volume distribution in the range of equal to or greater than 100 μm was measured for sample 6 indicating simultaneous fibre-fibre and fibre-powder particles interactions which resulted into a higher number of pores sized >100 μm. TEM observations (Fig. 1) clearly showed the presence of submicron and nanometre size pores in all samples whose presence was separately confirmed by MIP and N_2

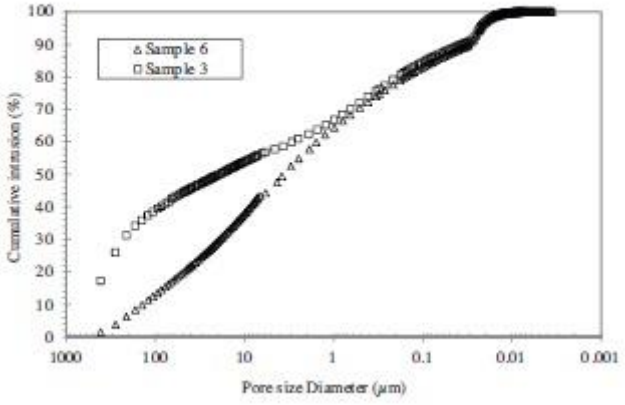

Fig. 3. Distribution of cumulative intrusion (%) of samples with and without PF.

Table 4
Pore volume, surface area and pore radius results of sample 1 and 3 from N_2 sorption method.

	Sample 1	Sample 3
Pore volume ($cm^3 g^{-1}$)	0.731	0.393
BJH surface area ($m^2 g^{-1}$)	152.116	76.765
Pore radius (Å)	17.012	15.262

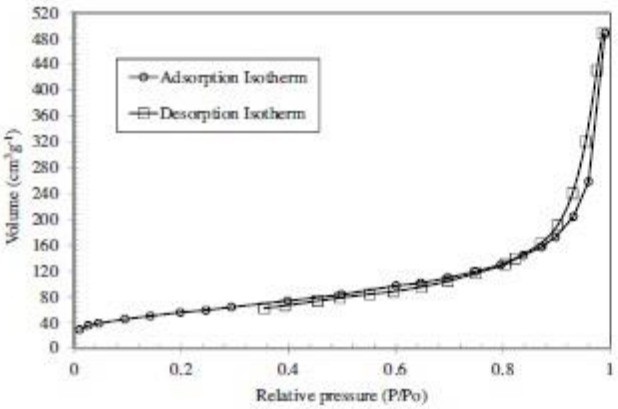

Fig. 4. Nitrogen adsorption and desorption isotherms for sample 1.

sorption. However, MIP technique, that covers the whole range of mesopores (2–50 nm) and macropores (>50 nm), when employed for fine silica powders has a drawback in possible deformation of powder particles caused by the high pressures involved. To verify the pore size data obtained from MIP technique samples 1 and 3 were further tested using N_2 sorption. The nitrogen adsorption measurements were performed at 77 K. Prior to N_2 sorption, both samples were degassed at 250 °C for 24 h. The pressure programme comprised 21 adsorption and 17 desorption points measured at equilibrium with a maximum relative pressure of 0.999. The total pore volume, pore radius and surface area given in Table 4 were calculated using BJH method. Isotherms for both samples as shown in Figs. 4 and 5 indicate that the pore size distribution continues in macropores region (>50 nm), but the bigger pores could not be resolved by N_2 sorption. This development is also supported by the evolution of the pore size distribution that is indicated by MIP and TEM. This also suggests that the average pore size of these samples was >50 nm and ranges between 50 and 150 nm. Further, it is argued that the effect of average pore size values in the range of 50–150 nm have a negligible effect on gaseous conductivity for VIP

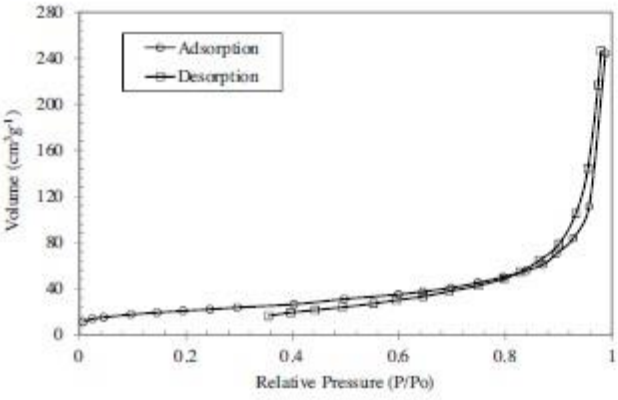

Fig. 5. Nitrogen adsorption and desorption isotherms for sample 3.

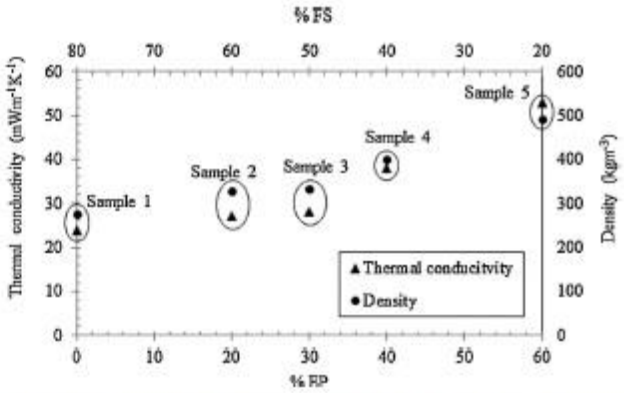

Fig. 6. Variations of total thermal conductivity at atmospheric pressure of core boards made with different mass ratios of FS and EP composite along with SiC (12%) and PF (8%).

core at vacuum pressure of 0.1–10 mbar. That means one can adopt any pore size between this range without affecting the gaseous conductivity values for VIP under vacuum. This behaviour is illustrated in Section 8.

4. Thermal conductivity measurement

Centre of panel thermal conductivity (λ_{cop} of a VIP core is a summation of the solid conductivity, gaseous conductivity and radiative conductivity and can be expressed using Eq. (2) [24].

$$\lambda_{cop} = \lambda_S + \lambda_R + \lambda_G + \lambda_{coup} \quad (2)$$

where λ_s is the solid thermal conductivity, λ_R the radiative thermal conductivity and λ_G the gaseous conductivity. Here λ_{coup} is the thermal conductivity caused by a complex interaction between gas and solid particles of EP and PF in the composite. This term, λ_{coup}, rises exponentially at higher pressures. However, at low pressure this term can be negligible. Solid conduction takes place through the structure of core material where heat is transmitted through the physical contact of particles of core material. Solid conductivity is the material property and its value depends upon material structure, density and external pressure on the core. Materials with low density are preferred for achieving low solid conduction. Thermal conductivity in VIP core can be lowered by restricting the gaseous and radiative conductivities. Thermal conductivities of core boards of samples 1, 2, 3, 4 and 5 were measured by a small guarded hot plate apparatus at Swiss Federal Laboratories for Materials Testing (Empa) designed for small samples of low thermal conductivity values. Thermal conductivity was measured over an area of 25 mm × 25 mm at a mean sample temperature of 21 °C with the cold and warm sides held at 12 °C and 30 °C respectively. The measuring zone was located on the warm upper side of the samples under measurement.

5. Influence of expanded perlite on total thermal conductivity

Experimentally measured value of thermal conductivity and the density of core board samples are shown in Figs. 6 and 7. Sample 1 containing FS mass ratio of 80% had the lowest thermal conductivity of 24 mW m^{-1} K^{-1} and with increasing mass ratio of EP from 0% to 60% the thermal conductivity of the composites increased from 24 to 53 mW m^{-1} K^{-1}. An increase in EP mass ratio from 40% to 60% in the samples led to a rise in thermal conductivity from 38 to 53 mW m^{-1} K^{-1} respectively. However, the measurements indicated that the addition of EP up to mass ratio of 30% led to a

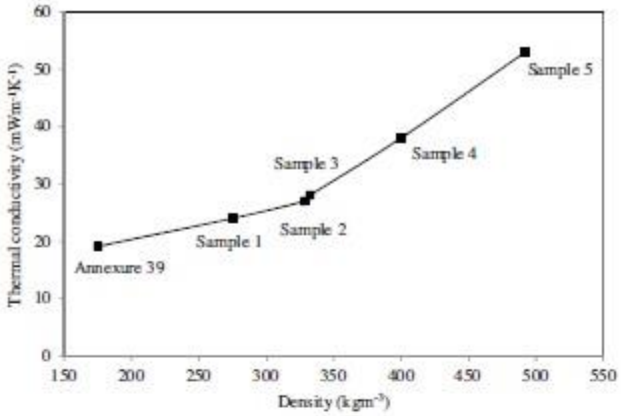

Fig. 7. Comparison of centre of panel thermal conductivity at atmospheric pressure and density of core boards made of samples 1, 2, 3, 4, 5 and commercial pyrogenic silica.

very small increase in thermal conductivity of 4 mW m^{-1} K^{-1} compared to FS board of sample 1. Rate of thermal conductivity rise was measured to be minimal for EP mass ratio ranging from 0% to 30%, with a significant rise recorded when EP mass ratio was increased beyond this threshold value of 30%. Density and thermal conductivity of compacted board made of sample 3 was measured to be 332 kg m^{-3}and 28 mW m^{-1} K^{-1} respectively. Thermal conductivity value was higher by approximately 17% compared to board made of sample 1. Commercially available pyrogenic silica cores as described in the IEA Annexure 39 [23] were reported to have thermal conductivity of 19.1–20.8 mW m^{-1} K^{-1} and bulk density of 162–192 kg m^{-3}. Clearly, the presence of EP in the composite causes thermal conductivity and density to rise as shown in Fig. 7, but a cost reduction potential is foreseen by displacing FS with comparatively cheaper EP.

VIP core cost reduction potential was estimated using equation (3) and the prices for the materials specified in Table 5.

$$C_{core} = C_{FS} \times m_{FS} + C_{EP} \times m_{EP} + C_{SiC} \times m_{SiC} + C_{PF} \times m_{PF} \quad (3)$$

where C_{core} is the cost of core, C_{FS}, C_{EP}, C_{SiC} and C_{PF} are the costs of FS, EP, SiC and PF per unit mass respectively, m_{FS}, m_{EP}, m_{SiC} and m_{PF} are the masses of FS, EP, SiC and PF respectively.

In Fig. 8 costs of VIP core for samples 1–5 has been compared with increasing EP content or decreasing FS content; a decreasing FS content reduced the cost. The cost of sample 1 was calculated to be highest (£9.30 m^{-2}) due to the presence of the highest (80 mass%) FS of all the samples studied. For the sample 3, with extra 3 mm thickness compared to other samples, cost was £8.7 m^{-2}; however, when assumed the thickness of sample 3 to be same as that of other samples the cost reduction potential of up to 20% for the sample 3 was calculated. For sample 5 with 60 mass% of EP the cost reduction potential of 54% can be achieved, but the resulting thermal conductivity became approximately twice as high as compared to that of the sample 3. Sample 3 was selected for further investigation into thermal conductivity variation over a range of pressures and the results are presented in Section 8.

Table 5
Market prices of various materials used for cost estimation.

Material	Price (£/kg)
FS	3.50
EP	0.27
SiC	1.58
PF	4.60

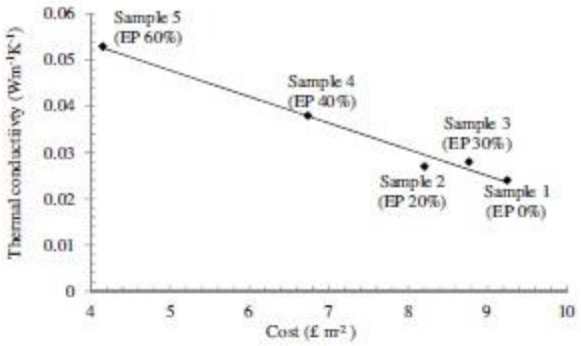

Fig. 8. Variation of core cost for composite samples 1–5 with different EP mass ratios and thermal conductivity at 1 atm pressure.

6. Effect of opacifier (SiC) on radiative conductivity

Fumed silica, owing to its very small particle size and low bulk density has a low solid conduction, but suffers from a lower resistance to radiative heat transfer [25]. Caps and Fricke [8] reported that at room temperature thermal conductivity of pure silica is higher by 0.002–0.003 W m^{-1} K^{-1} than that of SiC opacified precipitated silica. Nonetheless, caution has to be exercised when using opacifiers as these typically have high solid thermal conductivity which means higher content of opacifier will lead to a higher solid thermal conductivity offsetting any benefit it provides by reducing the radiative conductivity; on the other hand, an insufficient amount of opacifier in a VIP core will lead to a higher radiative conductivity. Hence, an optimum mass proportion of a given opacifier needs to be identified to achieve a minimum radiative conductivity in VIP cores. The effect of opacifier on radiative heat transfer is described by the specific extinction (e^*), which can be calculated from the transmission spectrum in the wavelength range of interest. In the present study a range of EP-FS composites, see Table 1, containing varying mass proportions of SiC were prepared to evaluate the effect of varying amounts of SiC on radiative conductivity (λ_R).

The transmission spectrum, an average of 100 scans, of each sample was acquired using FT-IR spectroscopy equipment (Perkin Elmer Spectrum One). For this purpose, all samples were scanned at room temperature of 22–24 °C. It was very difficult to obtain an optically thin film from the pure powders, therefore all samples were prepared after mixing with potassium bromide (KBr) and then pressed into pellets. Specific extinction, e^*, was calculated using Eq. (4) [26].

$$e^* = \frac{-\ln(\tau)}{L \times \rho} \quad (4)$$

where τ is the transmission (%), L the equivalent thickness (m), ρ the density of monolithic sample (kg m^{-3}).

The equivalent thickness (L) of sample in pellet corresponding to monolithic sample was calculated using Eq. (5) [27]

$$L = \frac{M \times m_p}{A \times \rho} \quad (5)$$

where M is mass of KBr pellet (kg), m_p the % mass of sample in pellet (%) and A section area of pellet (m^2).

The specific extinction measured for samples with increasing SiC content in the composite is shown in Fig. 9. It can be seen that with increasing SiC mass ratio from 5% to 15% specific extinction values improved by factor of two. For example, sample 7 with 5% SiC had a specific extinction of 37 m^2 kg^{-1} in the wavelength range of 4.5–5.5 μm compared to the values of 55 m^2 kg^{-1} and 77 m^2 kg^{-1} respectively for samples 8 and 9 for the same range of wavelength.

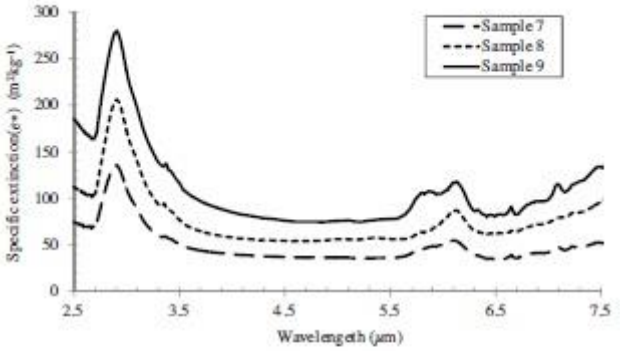

Fig. 9. Comparison of specific extinction for samples 7 (SiC 5%), 8 (SiC 10%), and 9 (SiC 15%) over the wavelength range of 2.5–7.5 μm.

The specific extinction value of 55 $m^2\,kg^{-1}$ measured for sample 8 in the present study matches with that of reported by Feng et al. [28] for a sample of FS powder containing 25% SiC. This suggests that the presence of EP enhanced the specific extinction values of the core composite in the present study. Thus, in sample 8 a 10% mass ratio of SiC was sufficient to achieve a similar specific extinction due to the presence of EP. The effect of addition of EP in samples on radiative conductivity is further discussed in Section 8. The radiative conductivities of VIP core samples with EP and SiC providing opacifying properties was calculated using Eq. (6) [25].

$$\lambda_R = \frac{16n^2\sigma T^3}{3E(T)} \tag{6}$$

where n is the refractive index, σ the Stefan–Boltzmann constant ($5.67 \times 10^{-8}\,W\,m^{-2}\,K^{-4}$), T the medium local temperature (K) and E the extinction coefficient, which was calculated using Eq. (7) [24].

$$E = e^* \times \rho \tag{7}$$

Radiative conductivity calculated using Eq. (6) for temperature 300 K and the specific extinction values obtained using Eq. (4) over the wavelength range 2.5–7.5 μm is shown in Fig. 10. Of samples 7, 8, 9, sample 9 (SiC 15%) exhibited the lowest radiative conductivity range of 0.0003 $W\,m^{-1}\,K^{-1}$ to 0.0010 $W\,m^{-1}\,K^{-1}$. Sample 8 (SiC 10%) yielded a range of 0.0004 $W\,m^{-1}\,K^{-1}$ to 0.0014 $W\,m^{-1}\,K^{-1}$.

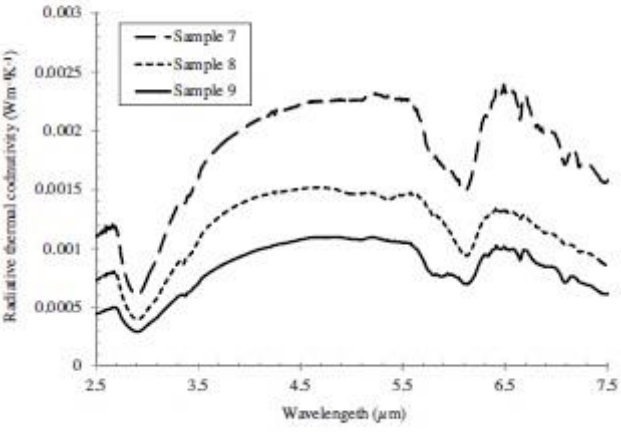

Fig. 10. Variation of radiative conductivity at 300 K for composite samples 7 (SiC 5%), 8 (SiC 10%), and 9 (SiC 15%) over the wavelength range of 2.5–7.5 μm.

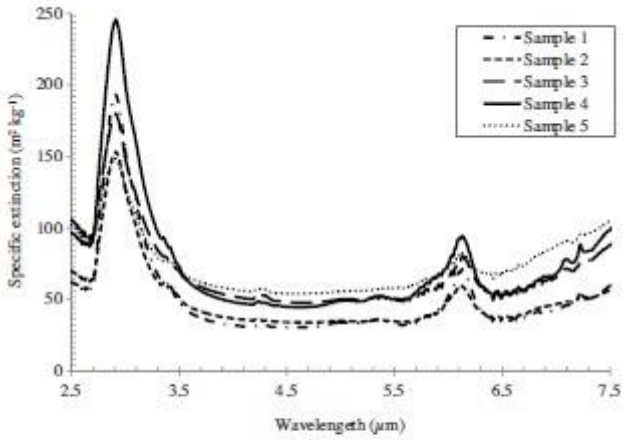

Fig. 11. Specific extinction comparison of samples 1, 2, 3, 4 and 5.

7. Effect of expanded perlite (EP) on radiative conductivity

The results explained in Section 6 clearly indicate that EP acted as an opacifier in the EP-FS composite, hence a lower proportion of SiC in the composite was required to achieve similar or better specific extinction as published by other researchers such as Feng et al. [28]. The effect of EP on the specific extinction and radiative conductivity is shown in Figs. 11 and 12. By comparing the measured specific extinction and radiative conductivity values for samples with different mass ratios of FS, EP, SiC and PF, it was observed that an increasing mass ratio of EP increased the specific extinction and reduced radiative conductivity. The values of specific extinction and radiative conductivity for wavelengths between 4 and 6 μm for samples 1 and 2 with mass ratio of EP in the range of 0 and 20% was found to be between 30–40 $m^2\,kg^{-1}$ and 0.002–0.0025 $W\,m^{-1}\,K^{-1}$ respectively. With increased mass ratios of 30%, 40% and 60% of EP in samples 3, 4 and 5 respectively, specific extinction increased to 50–60 $m^2\,kg^{-1}$ and radiative conductivity decreased to 0.0010–0.0012 $W\,m^{-1}\,K^{-1}$. This decrease in radiative conductivity can be attributed to the presence of EP with a coarser (10–750 μm) particle size and a higher density compared to FS in the composite. A similar effect was observed by Hümmer et al. [29] for composites containing silica aerogels and carbon soot. Samples 9 and 10 had a slightly higher SiC content of 15% compared to 12% of samples 1–5. Radiative conductivity of samples 9 and 10 with EP mass ratios of 30% and 20% respectively is shown in Fig. 13. Clearly the presence of extra 10% of EP in sample 9 led to decrease of 47%

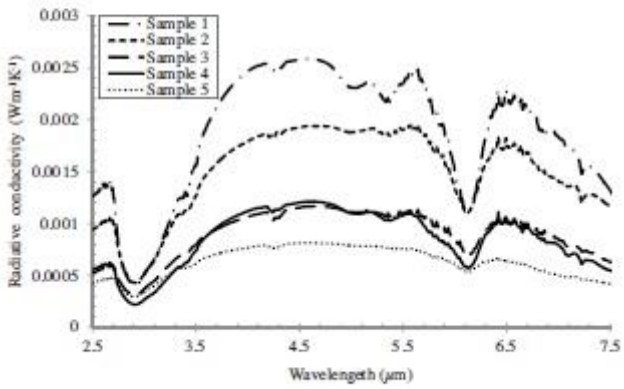

Fig. 12. Variation of radiative conductivity at 300 K for composite samples 1, 2, 3, 4 and 5.

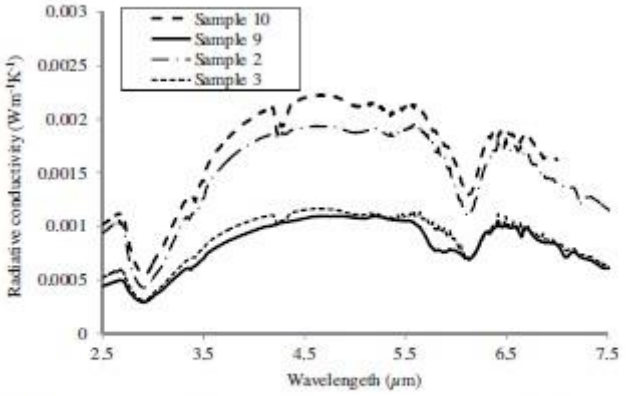

Fig. 13. Comparison of radiative conductivity at 300 K of sample 2 and 3 containing EP mass ratios of 15% and 9 and 10 containing EP mass ratios of 30% and 20% respectively.

in radiative conductivity, from 0.0021 to 0.0011 W m^{-1} K^{-1}. However, a decrease in radiative conductivity achieved through further addition of EP will not be able to compensate the increase in the solid thermal conductivity, EP and SiC have higher solid conductivities which will cause a higher centre of panel thermal conductivity for a VIP core. To evaluate the opacifying effect of EP, raditive conductivity of sample 3 with 12% SiC has been compared with those for samples 11 and 12 which contained no SiC and the results are shown in Fig. 14. It is shown that sample 12 with 0% SiC and 46% EP had a lower radiative conductivity (0.00044–0.00085 W m^{-1} K^{-1}) compared to that of sample 3 (0.0088–0.0011 W m^{-1} K^{-1}) for wavelengths ranging between 3.5 μm and 6 μm.

Based on this study, a composite containing mass ratio of 30% of EP and 10% to 15% of SiC has been identified as an optimum core material for VIPs. Nevertheless, to realise a lower density core composite it will be pertinent to use a greater quantity of EP as an opacifier than SiC due to the low density of former (35–120 kg m^{-3}) compared to that of the later (3200 kg m^{-3}).

8. Effect of pore size on gaseous thermal conductivity

Heat transfer occurs by convection and conduction processes in gases. Its intensity depends on the ratio of mean free path of gas molecules and the pore size of the material i.e., Knudsen Number. The gaseous thermal conductivity (λ_G of samples 1, 3 and 5, using the average pore diameter data presented in Table 1 at different

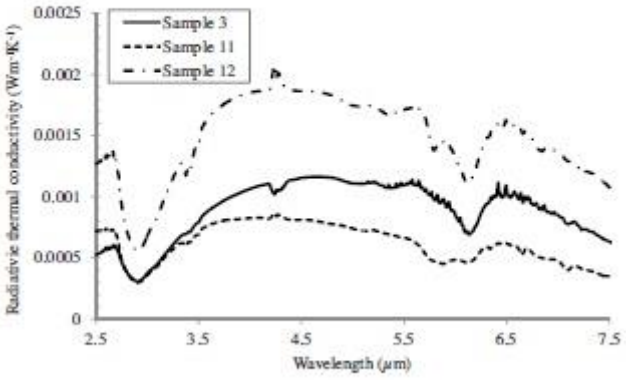

Fig. 14. Variation of radiative conductivity at 300 K for composite samples 3 (SiC 5%, EP 30%), sample 11 (SiC 0%, EP 46%) and sample 12 (SiC 0%, EP 30%).

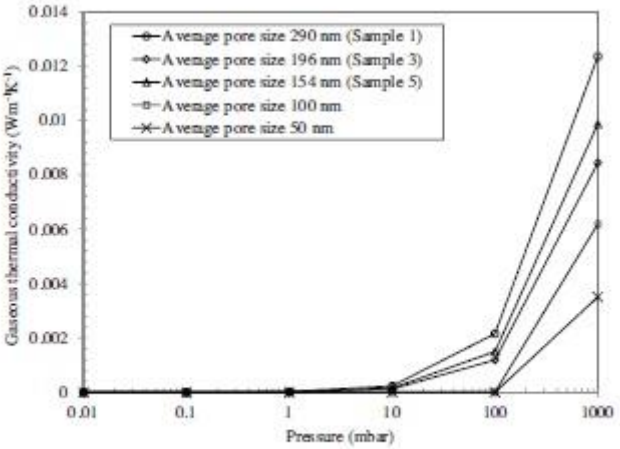

Fig. 15. Gaseous thermal conductivity of composite samples 1, 3 and 5 as a function of gas pressure and pore size.

pressure level was calculated using Eq. (8) [30]. The results are shown in Fig. 15.

$$\lambda_G = \frac{\lambda_0}{1 + (0.032/P\Phi)} \tag{8}$$

where (λ_0) is the thermal conductivity of air at atmospheric pressure (W m^{-1} K^{-1}) at 25 °C, P the pressure (Pa) and Φ the pore width of the porous insulation material (m).

It is shown that gaseous thermal conductivity for all three samples at gas pressures below 10 mbar is negligible. However, in real life the inner gas pressure in VIPs will rise due to permeation through envelope surface, sealing flanges and outgassing of core material. This rise in gas pressure increases the gaseous thermal conductivity. For the samples considered, at 10 mbar the gaseous thermal conductivity was calculated to be 0.1 mW m^{-1} K^{-1} (Fig. 15). Of the three samples, sample 3 was calculated to have minimal rise in gaseous thermal conductivity to a value of 1 mW m^{-1} K^{-1} when the pressure was raised from 10 mbar to 100 mbar. Further, the gaseous thermal conductivity for sample 3 at the atmospheric pressure was calculated to be 8.3 mW m^{-1} K^{-1}. This gaseous thermal conductivity for sample 3 at atmospheric pressure was lower than 18.9 mW m^{-1} K^{-1} measured by Caps et al. [31]. The combined thermal conductivity, λ_C, the sum of λ_S and λ_{coup}, of sample 1, 3 and 5 was calculated by using Eq. (9)

$$\lambda_C = \lambda_{cop} - (\lambda_R + \lambda_G) \tag{9}$$

For sample 1, 3 and 5 the values of λ_C were 0.0103 W m^{-1} K^{-1}, 0.0190 W m^{-1} K^{-1} and 0.0431 W m^{-1} K^{-1} respectively at a pressure of 1 atm. Centre of panel thermal conductivity of sample 3 was calculated for a gas pressure of 1 mbar using Eqs. (2) and (8) with the values of radiative conductivity measured at 300 K shown in Fig. 16. The centre of panel thermal conductivity for the sample 3 is higher than those usually quoted by VIP developers due to a higher value of λ_C coming from equation (9); under vacuum conditions λ_{cop} is expected to be much smaller because of lower values of the coupling term. VIPs are often manufactured with a low gas pressure, <3 mbar, maintained in the core.

Three cores of the composition same as sample 3 were prepared to experimentally measure the variation of thermal conductivity at a range of vacuum pressure. Tests were conducted using guarded hot plate apparatus for pressures varying from 0.5 mbar to 1 atm and results are shown in Fig. 17. A best fit curve to experimentally measured values is also shown. The results shown in Fig. 17 clearly validate the assertion presented above that under vacuum conditions λ_{cop} is much lower than that at atmospheric pressure, the λ_{cop}

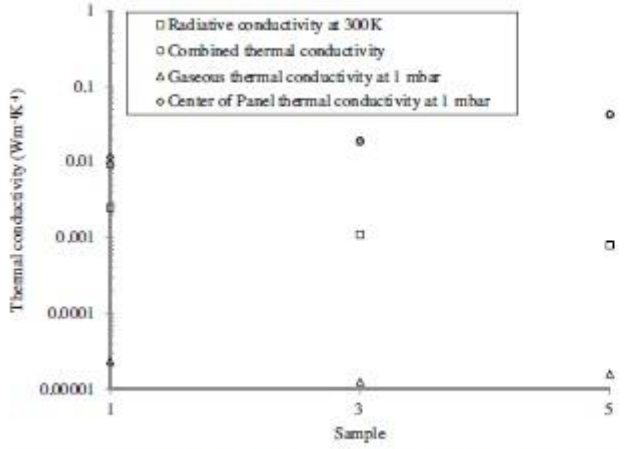

Fig. 16. Variation of centre of panel thermal conductivity, combined thermal conductivity at atmospheric pressure, radiative conductivity at 300 K and gaseous thermal conductivity at 1 mbar pressure for samples 1, 3 and 5.

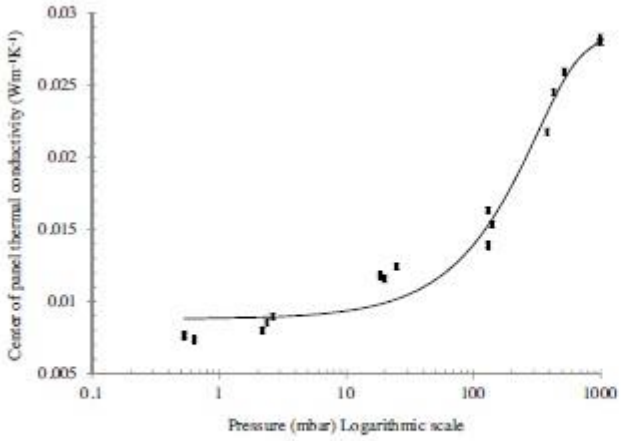

Fig. 17. Variation of centre of panel thermal conductivity of composite samples 3 with pressure.

for EP-FS composite at 0.5 mbar is 0.0076 W m^{-1} K^{-1}. One advantage that the EP-FS composite offers is its lower cost and this can be used to produce alternative core material for VIPs making these economically viable.

9. Conclusions

An alternative lower cost composite material for core of VIPs consisting of fumed silica, expanded perlite, SiC and polyester fibres has been developed and tested for its thermal performance. Core boards made of composite sample 3 containing 30% EP and 50% FS along with SiC and polyester fibres were found to achieve a centre of panel thermal conductivity of 28 mW m^{-1} K^{-1} at atmospheric pressure and 7.6 mW m^{-1} K^{-1} at 0.5 mbar. The radiative conductivity was measured to be 0.3–1 mW m^{-1} K^{-1} at 300 K with the gaseous thermal conductivity at 1 mbar being 0.012 mW m^{-1} K^{-1}–0.04 × 10^{-3} mW m^{-1} K^{-1} for an average pore size of 50–150 nm. This composite is proposed to be used for producing lower cost VIP cores. The opacifying properties of expanded perlite were observed and quantified. Expanded perlite reduced the radiative conductivity of the composite requiring smaller quantities of high density opacifiers such as SiC. Using the current commercial prices for FS, EP, SiC and PF, a cost reduction of up to 20% has been predicted for sample 3 against sample 1. The effectiveness of expanded perlite-fumed silica composite to replace the currently used pure fumed silica for VIP cores has been evidently demonstrated.

Acknowledgement

We would like to acknowledge Mr Pär Johansson for his help with experimental measurement of thermal conductivity.

References

[1] Department of Energy and Climate Change – DECC, Digest of United Kingdom Energy Statistics 2011, National Statistics Publications, London, 2011, Available from: http://www.decc.gov.uk/assets/decc/11/stats/publications/dukes/2312-dukes-2011-full-document-excluding-cover-pages.pdf (accessed 27.02.12).
[2] The Building Regulations, 2010, Available from: http://www.planningportal.gov.uk/buildingregulations/approveddocuments/partl/approved#ApprovedDocumentL1A:ConservationoffuelandpowerNewdwellings2010edition (accessed 27.09.12).
[3] Code for sustainable Homes, 2006, Available from: www.planningportal.gov.uk/uploads/code_for_sust_homes.pdf (accessed 27.09.11).
[4] Passivhaus, 1991, Available from: http://www.passivhaus.org.uk/standard.jsp?id=122 (accessed 15.09.11).
[5] Minergie®, 2012, Available from: http://www.minergie.ch/publications.478.html (accessed 29.09.12).
[6] H. Simmler, S. Brunner, Vacuum insulation panels for building application basic properties, aging mechanisms and service life, Energy and Buildings 37 (2005) 1122–1131.
[7] R. Baetens, B.P. Jelle, J.V. Thue, M.J. Tenpierik, S. Grynning, S. Uvsløkk, et al., Vacuum insulation panels for building applications: a review and beyond, Energy and Buildings 42 (2010) 147–172.
[8] R. Caps, J. Fricke, Thermal conductivity of opacified powder filler materials for vacuum insulations, International Journal of Thermophysics 21 (2000) 445–452.
[9] P. Mukhopadhyaya, K. Kumaran, N. Normadin, D.V. Reen, Fibre-powder composite as core material for vacuum insulation panel, in: 9th International Vacuum Insulation Symposium, London, UK, 2009.
[10] M. Alam, H. Singh, M.C. Limbachiya, Vacuum insulation panels (VIPs) for building construction industry – a review of the contemporary developments and future directions, Applied Energy 88 (2011) 3592–3602.
[11] N. Tekin, E. Kadinci, Ö. Demirbaş, M. Alkan, A. Kara, M. Doğan, Surface properties of poly(vinylimidazole)-adsorbed expanded perlite, Microporous and Mesoporous Materials 93 (2006) 125–133.
[12] A. Sari, A. Karaipekli, Preparation, thermal properties and thermal reliability of capric acid/expanded expanded perlite composite for thermal energy storage, Materials Chemistry and Physics 109 (2008) 459–464.
[13] "Perlite" Techninal Data Sheet/No. 2-4 1983. Perlite Institute USA. Available from: www.schundler.com/TD2-4.pdf (accessed 13.05.10).
[14] M. Pfundstein, R. Gellert, M.H. Spitzner, A. Rudolphi, Detail Practice: Insulating Materials: Principles, Materials and Applications, 2007, ISBN 978-3-7643-8654-2.
[15] "Evacuated Perlite" Perlite Institute USA. Available from: www.pdfport.com/view/535638-evacuated-perlite.html (accessed 24.05.10).
[16] S.D. Augustynowicz, J.E. Fesmire, J.P. Wikstrom, Cyrogenic insulation systems, in: 20th International Congress of Refrigeration, IIR/IIF, Sydney, 1999.
[17] J.P. Sass, J.E. Fesmire, Z.F. Nagy, S.J. Sojourner, D.L. Morris, S.D. Augustynowicz, Thermal performance comparison of glass microsphere and perlite insulation systems for liquid hydrogen storage tanks, in: American Institute of Physics Conference Proceedings, vol. 985, 2008, pp. 1375–1382.
[18] J. Fricke, H. Schwab, U. Heinemann, Vacuum insulation panel-exciting thermal properties and most challenging applications, International Journal of Thermophysics 27 (2006) 1123–1139.
[19] D. Zhang, S. Tian, D. Xiao, Experimental study on the phase change behavior of phase change material confined in pores, Solar Energy 81 (2007) 653–660.
[20] W.P. Bolen, Perlite – Mineral Year Book 2009. US Geological Survey. Available from: http://minerals.usgs.gov/minerals/pubs/commodity/perlite/index.html#pubs (accessed 26.07.12).
[21] Baltimore Innovations Ltd. Innovations House, Jackson's Business Park, Wessex Road, Bourne End, Buckinghamshire, SL8 5DT, UK, http://www.baltimoreinnovations.co.uk/
[22] Silvaperl – William Sinclair Horticulture Ltd. www.william-sinclair.co.uk
[23] H. Simmler, S. Brunner, U. Heinemann, H. Schwab, K. Kumaran, P. Mukhopadhyaya, et al. Vacuum Insulation Panels – Study on VIP-components and Panels for Useful life time Prediction in Building Applications (Subtask A). A Report for the IEA/ECBCS Annex 39 High Performance Thermal Insulation for Buildings and Building Systems 2005, Available

from: http://www.ecbcs.org/docs/Annex_39_Report_Subtask-A.pdf (accessed 26.04.10).
[24] J. Fricke, Materials research for the optimization of thermal insulations, High Temperatures-High Pressures 25 (1993) 379–390.
[25] R. Caps, J. Fricke, H. Reiss, Improving the extinction properties of an evacuated high-temperature powder insulation, High Temperatures-High Pressures 15 (1983) 225–232.
[26] M.F. Modest, Radiative Heat Transfer, 2nd ed., Academic Press, California, USA, 2003.
[27] G. Wei, Y. Liu, X. Zhang, X. Du, Thermal radiation in silica aerogel and its composite insulation materials, in: 9th International Mechanical Engineering Congress and Exposition IMECE, Denver, Colorado, USA, 2011.
[28] J. Feng, D. Chen, W. Ni, S. Yang, Z. Hu, Study of IR absorption properties of fumed silica-opacifier composites, Journal of Non-Crystalline Solids 356 (2009) 480–483.
[29] E. Hümmer, T.H. Rettelbach, X. Lu, J. Fricke, Opacified silica aerogel powder insulation, Thermochimica Acta 218 (1993) 269–276.
[30] J.S. Kwon, C.H. Jang, H. Jung, T.H. Song, Effective thermal conductivity of various filling materials for vacuum insulation panels, International Journal of Heat Mass Transfer 52 (2009) 5525–5532.
[31] R. Caps, U. Heinemann, M. Ehrmanntraut, J. Frick, Evacuated insulation panels filled with pyrogenic silica powders: properties and applications, High Temperatures-High Pressures 33 (2001) 151–156.

Applied Energy 88 (2011) 3592–3602

Contents lists available at ScienceDirect

Applied Energy

journal homepage: www.elsevier.com/locate/apenergy

Vacuum Insulation Panels (VIPs) for building construction industry – A review of the contemporary developments and future directions

M. Alam *, H. Singh, M.C. Limbachiya

Sustainable Technology Research Centre (STRC), Kingston University, Roehampton Vale, Friars Avenue, London SW15 3DW, UK

ARTICLE INFO

Article history:
Received 14 December 2010
Received in revised form 13 April 2011
Accepted 14 April 2011
Available online 6 May 2011

Keywords:
Vacuum Insulation Panel (VIP)
Thermal insulation
Thermal conductivity
Payback period
Thermal bridging effect
Useful life time

ABSTRACT

Demand for energy efficient buildings has increased drastically in recent years and this trend will continue in the future. Insulating building elements will play a key role in meeting this demand by reducing heat losses through the building fabric. Due to their higher thermal resistance, Vacuum Insulation Panels (VIPs) would be a more energy efficient alternative to conventional building insulation materials. Thus, efforts to develop VIPs with characteristics suitable for applications to new and existing buildings are underway. This paper provides a review of important contemporary developments towards producing VIPs using various materials such as glass fibre, foams, perlite and fibre/powder composites. The limitations of the materials currently used to fabricate VIPs have not been emphasised in detail in previous review papers published. Selection criteria, methods to measure important properties of VIPs and analytical and numerical models presented in the past have been detailed. Limitations of currently employed design tools along with potential future materials such as Nano/microcellular foams and SiO_x/SiN_x coatings for use in VIPs are also described.

Contents

* Corresponding author. Tel.: +44 208 4174873.
E-mail address: k0962421@kingston.ac.uk (M. Alam).

0306-2619/$ - see front matter © 2011 Elsevier Ltd. All rights reserved.
doi:10.1016/j.apenergy.2011.04.040

1. Introduction

In 2007, the UK government set a target to gradually improve the energy efficiency and carbon performance of buildings required via the Building Regulations 2006 Part L. The aim of this was to achieve a zero carbon emission level for new homes by 2016 [1]. This carbon reduction will initially be realised by a 25% improvement in the energy/carbon performance set in Building Regulations 2006 Part L achieving the Code for Sustainable Homes (CSH) level 3 by 2010; then secondly, in 2013, to a 44% improvement achieving the CSH level 4; and ultimately in 2016, to zero carbon emissions achieving the CSH level 6 [2]. Further, the UK government intends to set zero carbon targets for new nondomestic buildings by 2019 [3]. These standards are expected to assist the UK government significantly in reducing Carbon dioxide (CO_2) emissions from buildings and achieving the 2050 target to reach net carbon emissions at least 80% lower than the 1990 baseline as set in the Climate Change Act 2008 [4]. Buildings account for almost half of the UK's total carbon emissions [5] and are directly related to energy consumption. In the first quarter of 2010 domestic and services sectors were responsible for 50% of total UK energy consumption [6]. A major portion of supplied space heating energy is lost through poorly insulated building fabric. Heat losses can be reduced by lowering the heat transfer coefficient (*U*-value) of building fabric by applying insulation. It is evident from Fig. 1 that lowering the average *U*-value from the Building Regulation standard value (0.40 W m^{-2} K^{-1}) to that required by level 5 of the CSH standard will reduce the annual space heating demand and CO_2 emissions by 7.80 kW h m^{-2} a^{-1} and 1.56 kg CO_2 m^{-2} a^{-1} respectively. Average building *U*-value, energy savings and amount of CO_2 emission reduced were calculated using Eqs. (1) and (2) and fuel emission factor of 0.20 [7–9].

$$U = \{(U_1 \times A_1) + (U_2 \times A_2) + (U_3 \times A_3) + (U_3 \times A_3)\} / \{(A_1 + A_2 + A_3 + A_4)\} \quad (1)$$

$$\text{Energy saving per annum (kW h m}^{-2}) = (\text{HDD} \times \text{U} \times 24)/(1000 \times \eta) \quad (2)$$

where A is the insulated area (m^2); U is the average *U*-value (W m^{-2} K^{-1}); HDD is the heating degree day (°C day); η is the efficiency of heating system. Subscripts 1, 2, 3 and 4 denotes building elements wall, floor, roof and window respectively.

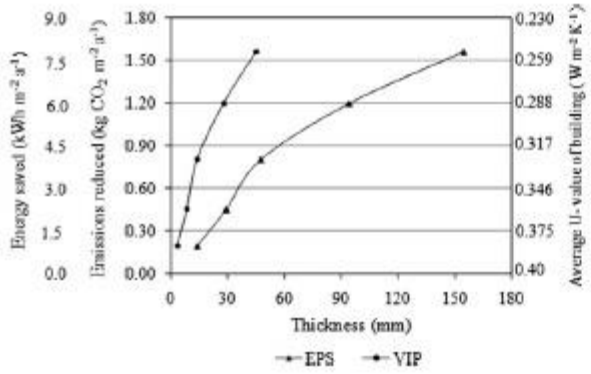

Fig. 1. Amount of heating energy saved and corresponding reduction in CO_2 emissions for varing thicknesses of EPS and VIP.

Conventional insulation materials such as expanded polystyrene (EPS) with a reported thermal conductivity (λ) of 0.035 W m^{-1} K^{-1} [10] requires a thickness of 4–5 times larger than Vacuum Insulation Panels (VIPs) (λ = 0.008 W m^{-1} K^{-1}) to lower the average *U*-value of building to that required by the CSH.

It is shown in Fig. 2 that conventional insulation materials such as rock wool and glass fibre require a large thickness to lower the *U*-value of a typical masonry cavity wall of a semi-detached UK dwelling (built between 1945 and 1964) from 0.53 W m^{-2} K^{-1} to 0.15 W m^{-2} K^{-1} as required by the PassivHaus standard [11]. This large thickness of insulation may not be feasible in existing and new buildings due to space and techno-economic constraints. VIPs with thermal resistance potentially 5–8 times higher than the

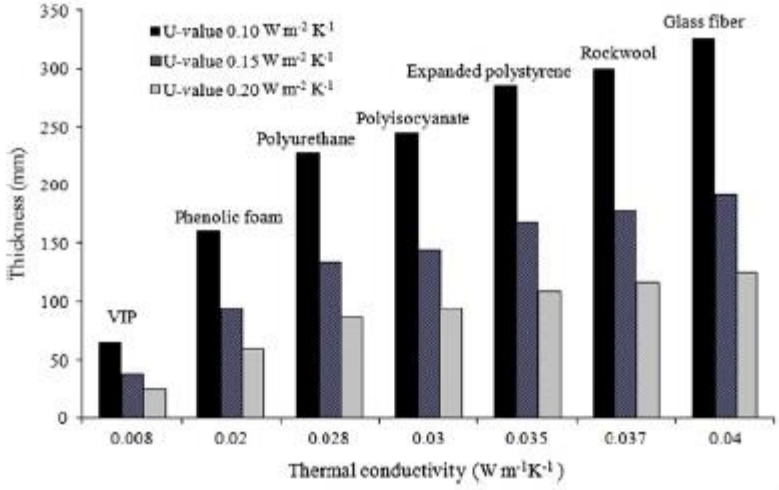

Fig. 2. Thicknesses of different insulation materials required to achieve different *U*-values (W m^{-2} K^{-1}) for a typical masonry cavity wall with a *U*-value 0.53 W m^{-2} K^{-1}.

conventional insulation [12] offer a solution to the problem. VIPs can be applied to buildings at various locations, for either external or internal surfaces, such as walls, roof, ground floor, window frames, and on hot water cylinders. However, the application of VIPs in buildings has two main barriers; high cost and uncertainty over useful life time. Recently, use of nanoinsulation materials and dynamic insulation materials were discussed by Jelle et al. [13]. However, these insulation materials are still at a conceptual stage and no real life or lab scale testing results have been reported yet.

2. Vacuum Insulation Panel (VIP) – Components and materials

A VIP can be described as an evacuated open porous material placed inside a multilayer envelope as shown in Fig. 3. The main components of a VIP are inner core, barrier envelope and getters and desiccants. The envelope could either consist of thick metal sheets or multilayer barrier of metalized polymeric layers to provide protection against environmental and handling stresses. A suitable getter or a desiccant is inserted inside the VIP core to adsorb gases and water vapours which might penetrate into a VIP through envelope barrier. In the case of conventional non-vacuum insulation materials convection in material pores causes the dominant heat transfer across such materials, whereas in VIP this mode of heat transfer is suppressed by creating a vacuum inside the core material. VIPs can either be classified as (i) sheet based VIPs and (ii) film based VIPs [14]. These are also called static VIPs because the vacuum can only be created at the time of manufacturing and cannot be created again over their useful life time. Sheet based VIPs use metal sheet envelope which exhibit better load bearing capacity and resistant to mechanical damages, but suffer from heavier weight and a greater thermal bridging effect [15,16]. On the other hand, thinner ($100–150 \times 10^{-6}$ m), and lighter multilayered metalized polymer film envelopes are easily punctured during handling.

2.1. VIP core

The core, fabricated from porous material of suitable pore size, is the inner part of a VIP as shown in Fig. 3. Its function is to maintain the vacuum below a minimum critical level and to physically support the VIP envelope. Gaseous heat transfer is suppressed within the core using small size porous materials such as open porous foams, powders and fibres.

2.1.1. Foams

Open cell foams such as polyurethane (PUR) and expanded polystyrene (EPS) with pore sizes in the range of $30–250 \times 10^{-6}$ m can be used as a core in VIPs. These foams have low thermal conductivity in evacuated conditions due to their low density ($60–100$ Kg m^{-3}) and small pore size of foam materials. However, a low gas pressure, $\leqslant 1 \times 10^{-4}$ bar, is required to achieve a reasonable thermal resistance in the case of foams, used as VIP core material. Kwon et al. [17] calculated the value for the total thermal conductivity of polyurethane foam of pore size 100 μm as 0.0078 W m^{-1} K^{-1} at 1×10^{-4} bar. However, such a low pressure is not feasible to maintain over the useful life time of the VIP, which is expected to be 100 years or longer for building applications. For foams with a density of 70 kg m^{-3} the radiative and solid conductivity at 300 K was reported as 0.0027 W m^{-1} K^{-1} and 0.003–0.007 W m^{-1} K^{-1} respectively [17], with a combined solid and radiative conductivity in the range of 0.0057–0.0097 W m^{-1} K^{-1}, a value higher than the normally accepted design thermal conductivity value for a VIP core of 0.004 W m^{-1} K^{-1}. Clearly it would be difficult to achieve this lower thermal conductivity value using foams in VIPs even with zero gaseous conductivity. Commercially available PUR foam (£6.03 m^{-2}) is capable of providing higher thermal resistance compared to other insulation materials such as glass fibre (£2.39 m^{-2}) and EPS (£2.39 m^{-2}) for the same insulation thickness [18]. However, PUR foam has higher fire toxicity due to the release of mainly carbon monoxide (CO), hydrogen cyanide (HCN) and other harmful emissions [19]. Thermal conductivity of foams can be reduced further by reducing the size of pores. Recently, rubber blended polypropylene and polyethylene nano/microcellular foam (average cell diameter ($0.5–2 \times 10^{-6}$ m) has been developed by CO_2 pressure quench method [20]. Nano/microcellular foams with improvised structural arrangement, though currently in the development phase, are potential candidates for VIP core materials in the medium term.

2.1.2. Powders

Currently fumed or pyrogenic silica, silica aerogels and expanded perlite individually or in a mixture form are employed in VIP cores. Fumed silica is commonly used due to its ability to yield a low thermal conductivity 0.003–0.006 W m^{-1} K^{-1} whilst requiring a pressure in the range of $20–100 \times 10^{-3}$ bar [21] owing to a favourable pore size of 300×10^{-9} m and a specific surface area in the range of $5–60 \times 10^{-2}$ m^2 Kg^{-1}. Its density is approximately 150–200 Kg m^{-3}. Fumed silica was first developed by Degussa AG (currently Evonik Industries) in Germany in 1942 [22]. Due to its

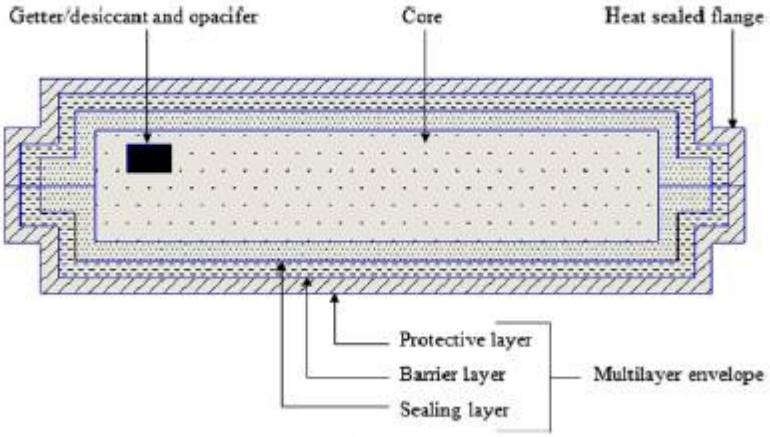

Fig. 3. Schematic of a VIP.

low density, high specific surface area and low thermal conductivity fumed silica is a suitable core material for VIPs to achieve the accepted core thermal conductivity design value of 0.004 $W m^{-1} K^{-1}$.

Silica aerogels, first developed by Kistler in 1931 using sodium silicate [23], are nanoporous materials with pore size of approximately 20 nm and a density in the range of 3–350 kg m^{-3}. In general, aerogels are made by two steps (i) wet gel formation by acidic condensation or sol–gel process (ii) drying of wet gel by using supercritical or ambient drying to produce silica aerogel [24]. A low density and a smaller pore size ($1–100 \times 10^{-9}$ m) render silica aerogel a thermal conductivity of (approximately 0.001–0.003 W $m^{-1} K^{-1}$ in evacuated and opacified conditions depending on temperature) and can even achieve a value of 0.004 W $m^{-1} K^{-1}$ at 50 mbar or less making it suitable for VIP applications [25]. Another advantage of Silica aerogel is that it is also considered as non reactive and nonflammable. However, due to its high cost it has not been widely used in VIPs for building applications.

Expanded perlite, was found to be less effective than silica aerogel and fumed silica requiring a low pressure below 0.1 mbar to achieve the desired design centre of panel thermal conductivity value [26]. Expanded perlite can be used in combination with fumed silica in different mass ratios and such a mixture can be optimised to achieve a low thermal conductivity at a comparatively high pressure for a specified useful life of the VIP. However, it is not expected to achieve typical design centre of panel value at reasonable pressure.

2.1.3. Glass fibre

Glass fibre can also be used as the core of a VIP for high temperature applications due to its low density and high thermal stability (>1000 °C). Kwon et al. [17] reported a radiative conductivity of 0.0007 W $m^{-1} K^{-1}$ and a solid conductivity of approximately 0.0021 W $m^{-1} K^{-1}$ for glass fibre (density of 250 kg m^{-3} and a fibre diameter of $0.5–0.7 \times 10^{-6}$ m) at 300 K. Collectively this results in a thermal conductivity of 0.0028 W $m^{-1} K^{-1}$ requiring a suppression of the gaseous conductivity within 0.0012 W $m^{-1} K^{-1}$ to achieve a VIP core thermal conductivity of 0.004 W $m^{-1} K^{-1}$. A pressure of approximately 0.01×10^{-3} bar was required to suppress the gaseous thermal conductivity to a negligible level [27]. Kwon et al. [17] also reported a theoretical total thermal conductivity value of 0.0036 W $m^{-1} K^{-1}$ for a glass fibre core at 0.1×10^{-3} bar. Araki et al. [28] investigated the performance of glass fibre based VIPs for insulating hot water cylinders. Glass fibre based VIPs are a good candidate for domestic ovens, furnaces, concentrated solar power plants and fuel cell power plants.

2.1.4. Fibre/powder composites

Mukhopadhyaya et al. [29] proposed the use of composites of glass and mineral oxide fibre with pumice and zeolite powder as VIP core material. Thermal conductivity of these materials was found to be comparable to precipitated silica and nanogels for a pressure range of $0.25–100 \times 10^{-3}$ bar. A lower embedded energy of such composites compared to that of silica based materials is expected to improve life cycle rating of VIP as they require. Low cost alternatives, such as, wood fibre composite with pumice powder [29], are also being considered, though their real time effectiveness in VIPs has not been reported yet.

2.2. VIP envelope

The envelope not only protects the VIP from air and water transmission but also provides mechanical strength to withstand atmospheric pressure and handling stresses during transportation and installation. Performance of the envelope depends upon its barrier properties and capability to resist thermal bridging across the edges. Envelope materials are expected to have a water vapour transmission rate (WVTR) of approximately 0.0001 g $m^{-2} d^{-1}$ and oxygen transmission rate (OTR) of 0.001 cm^3 m^{-2} d^{-1} to yield a useful life time of approximately 30–50 years for building applications [30]. However, the range of useful life time 30–50 years is wide and for building applications life time of 100 years needs to be considered and specified more precisely to build the confidence in manufacturers and users. A combination of polymers and thin metalized films or metal foils is currently employed to produce VIP envelope [30,31]. Generally, permeance of multilayer film envelope of a VIP depends on temperature, relative humidity and size of panel [32]. Barrier properties of envelope films can be improved by reducing the number and size of defects in the barrier layer [30]. A typical VIP envelope with three metalized films was reported to have a WVTR and an OTR of 0.003–0.005 g $m^{-2} d^{-1}$ and 0.001–0.002 cm^3 m^{-2} d^{-1} respectively at 23 °C and 50% RH [30]. For a two-layered metallised envelope panel estimated useful life time is 16–38 years depending upon panel size and climatic conditions [33]. Baetens et al. [34] calculated that aluminium foil can keep the thermal conductivity of core minimum as compared to multi-layered metalized films. Clearly, a significant improvement in barrier properties is needed to achieve a useful life time of 100 years or longer for a VIP for building applications. Higher barrier properties of aluminium foil envelope compared to a metalized polymeric envelope are evident. However, an aluminium foil envelope suffers from a higher thermal bridging effect. Linear thermal transmittance values of 0.01 W $m^{-1} K^{-1}$ for a metalized film envelope and 0.07 W $m^{-1} K^{-1}$ for an aluminium foil envelope were reported [35].

2.2.1. Structure of envelope

A typical VIP envelope consists of three material layers; (i) outer protective layer (ii) barrier layer (iii) inner sealing layer, each serving a distinct function. These layers are joined together as shown in Figs. 3 and 4 to form an envelope by using a suitable adhesive such as polyurethane. Kwon et al. [36] proposed a double envelope with an additional porous core material sandwiched between the inner envelope and outer envelope to reduce the gas permeation through the envelope as shown in Fig. 5. However, this may increase the thickness and cost of VIP and any increase in pressure in outer core will also contribute towards degradation of VIP performance.

2.2.2. Protective layer

It is the outer most layer of the envelope as shown in Fig. 3, which protects the VIP from environmental and handling stresses and also acts as a substrate for barrier layer. Currently, polyethylene terephthalate (PET) is used as protective layer due to its low cost and better barrier properties. Use of other materials for envelope is being investigated, for example Araki et al. [28] investigated Nylon 6 (Polyamide) as a protective layer in VIP envelope for high temperature application such as heat pumps and water storage tanks due to its high melting point (225 °C). A drawback of Nylon 6 is its high cost.

2.2.3. Barrier layer

The middle layer (Fig. 3) which acts as a barrier against air and water vapour transmission is known as the barrier layer. It is either an aluminium foil or metalized layers of polymers in which aluminium is attached to polymeric substrate. The number of barrier layers in a VIP envelope varies from one to three; though a three layer structure is widely used due to its better barrier properties against air and water vapour transmission. Currently polypropylene (PP) and polyethylene terephthalate (PET) are being used as substrates [37]. Araki et al. [28] investigated the use of metalized layer of ethylene vinyl alcohol copolymer (EVOH) and metallised layer of PET in VIP envelope and found that WVTR and OTR index for this type of envelope were high as compared to the envelope

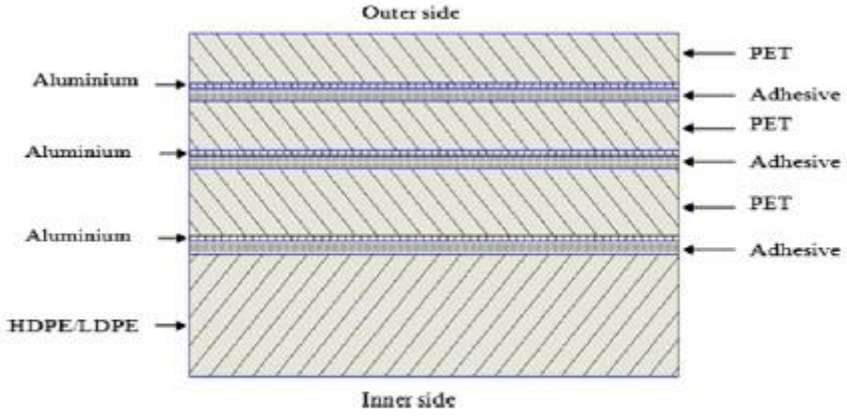

Fig. 4. A typical multilayer barrier envelope containing metalized barrier layers.

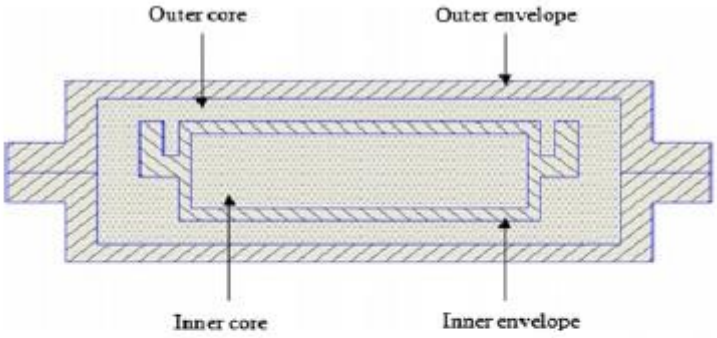

Fig. 5. Schematic of a double envelope VIP (redrawn from [36]).

with aluminium foil. Teniers [38] reported the better barrier properties of metalized layer of EVOH. However, due to the presence of high thermal conductivity metal in such barrier layers the thermal bridging effect on edges of VIP becomes dominant. Thermal bridging effect can be reduced by replacing the metalized barrier layer with silicon oxides (SiO_x) and silicon nitride (SiN_x) coatings. Barrier properties and mechanical properties of these materials are comparable to the metalized barrier layer [39–43]. Use of SiO_x and SiN_x coated PET in barrier layers for VIPs has not been reported to date. Nevertheless, these materials have great potential for VIP applications and required further investigation. Electrospun Methyltriethoxysilane (MTES) nanofiber fabric [44] is also a potential candidate for the barrier layer due to its high thermal stability and super hydrophobicity.

2.2.4. Sealing layer

The sealing layer is the inner most layer in a multilayered VIP envelope (Fig. 3). This layer seals the core material in the envelope. Imperfections in sealing seams generally contribute approximately 30% total gas permeation. Heat sealing is a commonly used process to join the laminates. In sealing process the film surfaces are heated between two hot bars under pressure. This creates a bond between two polymer layers due to diffusion. For achieving a better seal, the temperature and time allowed for sealing are very important factors. At a specific initiation temperature, the seal begins to form and its strength increases till a certain maximum value is achieved [45]. Conventionally Low Density Polyethylene (LDPE) and High Density Polyethylene (HDPE) have been used in VIPs as a sealing layer [37]. Malsene et al. [45] experimentally found no significant difference between the seal strength of these materials and concluded that a sealing layer material should be chosen on the basis of its air and water vapour permeability. Araki et al. [28] reported the use of other materials such as polybutylene (PBT) and high retort-cast polypropylene (HR-CPP) as sealing layers for high temperature applications.

2.3. Getters, desiccants and opacifiers

Getters and desiccants are placed inside the core to extend the useful life time of a VIP by continuously adsorbing water vapours (desiccants) and gases (getters) which may get into it over its useful life time through either permeation from the outside environment or via out gassing of core and envelope materials or both. In the case of silica core VIPs, core itself acts as a desiccant but for other core materials a small amount of silica gel desiccant is required. Araki et al. [28] used synthetic zeolites getters to adsorb gases for a glass fibre core. Opacifiers are used to reduce the radiative conductivity of the core material by making it opaque to infrared radiation. Silicon carbide (SiC) is the most commonly used opacifier in fumed silica core. Other opacifiers such as carbon black, titanium dioxide (TiO_2) and iron oxide (Fe_3O_4) are also being used.

2.4. Manufacturing of VIPs

Main steps involved in the manufacturing of a VIP are shown in Fig. 6. Heat sealing of the envelope could either be a three sided seal or a four-sided seal. Three sided seal has the advantage of reduced gas permeation through the seal flanges compared to four-sided seal [36].

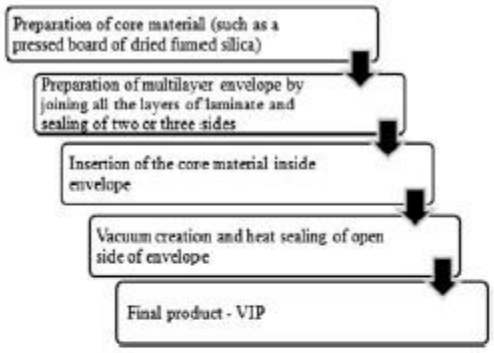

Fig. 6. Steps in manufacturing of VIP.

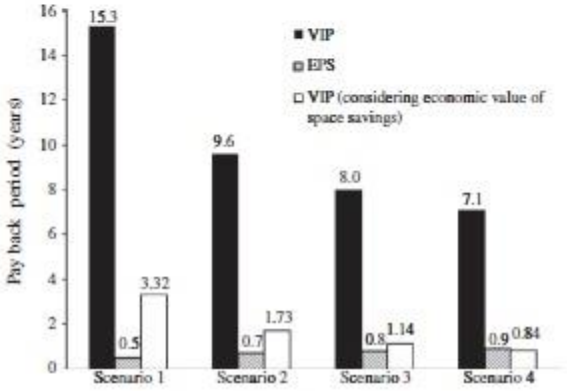

Fig. 7. Payback period of VIP and EPS in different scenarios of insulation (Table 1) for buildings.

Table 1
Insulation scenarios and main parameters used in payback period calculation.

		Parameters	Value
Scenario 1		Average building U-value	0.40 ($W m^{-2} K^{-1}$)
	(VIP)	Thickness	10 mm
		Cost	£70 m^{-2}
	(EPS)	Thickness	48.3 mm
		Cost	£2.40 m^{-2}
Scenario 2		Average building U-value	0.31 ($W m^{-2} K^{-1}$)
	(VIP)	Thickness	25 mm
		Cost	£80 m^{-2}
	(EPS)	Thickness	113 mm
		Cost	£6.19 m^{-2}
Scenario 3		Average building U-value	0.27 ($W m^{-2} K^{-1}$)
	(VIP)	Thickness	40 mm
		Cost	£80 m^{-2}
	(EPS)	Thickness	180 mm
		Cost	£8.38 m^{-2}
Scenario 4		Average U-value	0.24 ($W m^{-2} K^{-1}$)
	(VIP)	Thickness	60 mm
		Cost	£80 m^{-2}
	(EPS)	Thickness	256 mm
		Cost	£10.78 m^{-2}
Other parameters		Fuel	Natural gas
		Emission conversion factor	0.20
		HDD	1931 °C day
		C_f	£0.40 m^{-3}
		H_v	39.5×10^6 ($J m^{-3}$)
		η	0.9
		N	25
		i	10%

2.5. VIP economic analysis

Fig. 7 compares the payback period predicted for VIP and EPS when used as building insulation under different scenarios of interventions detailed in Table 1. For the purpose of calculations typical U-values for existing UK buildings; wall 0.51 $W m^{-2} K^{-1}$, roof 0.25 $W m^{-2} K^{-1}$, floor 0.18 $W m^{-2} K^{-1}$ and window 1.4 $W m^{-2} K^{-1}$ were assumed [46]. Payback period, an indication of the time required to recover the cost of insulation, is defined as the ratio of cost of insulation to the annual savings in heating cost as shown in Eq. (3). Annual heating cost (C_A) was calculated using the Eq. (4) [47]. Main parameters used in payback period calculation are detailed in Table 1.

$$PBP = C_{ins}/(C_{A,exis} - C_{A,imp}) \quad (3)$$

$$C_A = (86400 \times HDD \times C_f \times U \times PWF)/(H_v \times \eta) \quad (4)$$

$$PWF = N/(1 + i) \quad (5)$$

where PBP is the Payback period(year); C_{ins} is the cost of insulation (£); $C_{A,exis}$ is the annual heating cost with existing U-value (£ per annum); $C_{A,imp}$ is the annual heating cost with improved U-value (£ per annum); C_f is the cost of fuel (£ m^{-3}); H_v is the heating value of fuel ($J m^{-3}$); η is the efficiency of heating system; PWF is the present worth factor as shown in Eq. (5) if interest rate (i) is equal to inflation rate; N is the life time of insulation (years).

In scenario 1 VIP and EPS with a thickness of 10 mm and 48.3 mm respectively were considered for insulating the building, the average U-value was calculated as 0.40 $W m^{-2} K^{-1}$. In scenario 2 VIP and EPS with a thickness of 25 mm and 113 mm respectively were assumed, resulting in a average U-value of 0.31 $W m^{-2} K^{-1}$. Payback periods of VIP predicted for scenarios 1 and 2 are too long compared to those calculated for EPS. In scenario 3 a payback period of VIP and EPS insulation just sufficient to achieve a building average U-value of 0.27 $W m^{-2} K^{-1}$ were predicted. It was found that the payback period of VIP was 10 times longer than that for EPS. Scenario 4 compared the payback period of insulation required to achieve an average building U-value of 0.24 $W m^{-2} K^{-1}$. EPS had a payback period 8 years shorter than VIP although EPS required a prohibitively large thickness of 256 mm. Such a thick insulation layer cannot be employed to insulate the wall and floor area of most of the existing buildings. The main reason for the longer payback period of VIP insulation in all scenarios is its high initial cost, which must be reduced significantly if VIP is to provide a cost effective alternative to conventional insulation materials. In the case of existing commercial buildings, especially those which cannot be insulated on the outer surfaces such as listed buildings [48], VIP is an attractive alternative to conventional insulation materials as the facade of the building will not be modified as much. In Scenario 4, VIP was found to achieve a considerably shorter payback period when the economic value of the potential space savings due to thinner VIP was considered in all the scenarios, in scenario 4 it was even shorter than EPS. For calculating the economic value of space saved, an average rent of commercial buildings situated in London was assumed as £40 ft^{-2} [49].

3. Heat transfer phenomena in a VIP

With the VIP maintained at a pressure lower than a certain value, sufficient to suppress the convective heat transfer, the remaining modes of heat transfer include solid conduction, radiation and gaseous conduction. Total thermal conductivity of a VIP core can be expressed as [50]

$$\lambda_C = \lambda_S + \lambda_R + \lambda_G + \lambda_{cv} + \lambda_{coup} \quad (6)$$

where λ_S is the solid thermal conductivity ($W m^{-1} K^{-1}$); λ_R is the radiative thermal conductivity ($W m^{-1} K^{-1}$); λ_G is the gaseous ther-

mal conductivity (W m^{-1} K^{-1}); λ_{cv} is the gaseous convection within pores (W m^{-1} K^{-1}); λ_{coup} is the thermal conductivity due to the coupling effect (W m^{-1} K^{-1}).

The thermal conductivity λ_C of VIP core can be reduced by suppressing the thermal conductivity terms shown in the right hand side of Eq. (6) to minimum and is expected to be in the range of 0.004 W m^{-1} K^{-1} [31,50]. In Eq. (6) λ_{coup} represents coupling effect which becomes evident at higher pressures for powders and fibre materials due to interaction between them in the VIP core.

3.1. Solid conduction

Solid conduction occurs through the skeleton of core material, whereby the heat is transferred through the physical contact of the constituent particles of the core material. Its magnitude depends upon material structure, density and external pressure on the core. The following correlation was proposed for the variation of solid conductivity with density of the core material [50].

$$\lambda_S = \rho^{\alpha} \tag{7}$$

where ρ is the density (kg m^{-3}) and the index α has a value of unity for foams and ranges over 1.5–2 for nanomaterials. It is clear from Eq. (7) that the materials with a low density will yield a smaller solid conductivity.

3.2. Radiation

Radiative heat transfer in the form of electromagnetic waves requires no medium and is a significant mode of transferring heat in vacuum conditions. It can be calculated by using Eq. (8) [50].

$$\lambda_R = (16n^2\sigma T_r^3)/(3E(T_r)) \tag{8}$$

where n is the mean index of refraction; σ is the Stefan–Boltzmann constant (5.67×10^{-8} W m^{-2} K^{-4}); T_r is the average temperature within the insulation material (K); E is the extinction coefficient of the insulating material (m^{-1}).

Radiative heat transfer can be reduced by adding opacifier to the core material. Caps and Fricke [19] reported that at room temperature thermal conductivity of pure silica is higher by 0.002–0.003 W m^{-1} K^{-1} than that of silicon carbide opacified precipitated silica.

3.3. Gaseous thermal conduction

Heat transfer occurs through convection and conduction processes in gases. Its intensity depends on the ratio of mean free path of gas molecules and the pore size of the material i.e., Knudsen Number. Kaganer [51] proposed the following correlation Eq. (9) to estimate the gas conductivity, λ_G, as a function of Knudsen Number.

$$\lambda_G = \lambda_0/(1 + 2\beta Kn) \tag{9}$$

where λ_0 is the thermal conductivity of air at atmospheric pressure (W m^{-1} K^{-1}); ß is the coefficient which depends on accommodation coefficient and the adiabatic coefficient of the gas; Kn is the Knudsen Number which is equal to the ratio of molecular mean free path length (l) to the pore size diameter (Φ) as shown in Eq. (10)

$$Kn = l/\Phi = (k_B T)/(\sqrt{2}\phi d^2 p\Phi) \tag{10}$$

where k_B is the Boltzmann's constant (1.38×10^{-23} J K^{-1}); T is the thermodynamic temperature (K); d is the diameter of gas molecule (m); p is the gas pressure (Pa).

Kwon et al. [17] employed the following correlation, Eq. (11), to estimate the gaseous thermal conductivity of air at 25 °C using $\beta = 0.0016/P$.

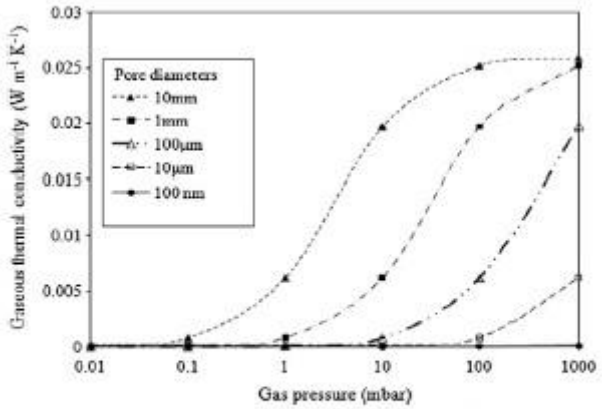

Fig. 8. Dependence of gaseous thermal conductivity on pore diameter as a function of gas pressure.

$$\lambda_G = \lambda_0/((1 + (0.0032/P\Phi)) \tag{11}$$

where P is the pressure (Pa); Φ is the pore width of the porous insulation material (m).

By using Eq. (11) the calculated values of gaseous thermal conductivity of air for different pore sizes are shown as a function of pressure in Fig. 8. It can be seen that materials with pore size in the nanometeric range have negligible gaseous thermal conductivity even at atmospheric pressure. It is clear from Fig. 8 that with increasing pore size comparatively lower pressure is required to suppress gaseous thermal conductivity.

4. Measurement of basic properties of VIPs

Gas pressure rise inside a VIP core is an important criterion to predict its service life. Pressure increase can be due to addition of gases from one or more of these sources (i) residual gases present inside VIP after manufacturing (ii) out gassing of materials present in envelope and core (iii) permeation through barrier envelope and seal flange [36,52]. Pressure measurement in a VIP is a challenging process as the core is sealed inside an outer envelope. Table 2 details different techniques employed to measure pressure inside a VIP, water vapour transmission and thermal conductivity.

5. Ageing of VIP

5.1. Useful life time prediction of VIP

Useful life time of a VIP is the time period in which total VIP thermal conductivity (i.e., centre of panel thermal conductivity) exceeds a certain limiting value [59,60]. The variation in gas and water vapour pressure inside the core material determines the change in thermal conductivity of the VIP core. This rate of change of thermal conductivity is employed to predict the useful life time of a VIP [30]. The moisture transmission through a VIP core can be attributed to the Knudsen diffusion and surface diffusion [61]. Knudsen diffusion is molecule-wall collision due to the larger mean free path of the molecules as compared to the pore size and surface diffusion is the movement of molecules along the pore wall [62].

Simmler and Brunner [35] predicted the useful life time for a VIP with silica core and metalized envelope for constant environmental conditions using Eq. (12) and suggested the preliminary thermal design values of change in core thermal conductivity for useful life time of 25 years for silica VIP 0.006 W m^{-1} K^{-1} for alu-

Table 2
Measurement of basic properties of VIP.

Property	Method	Principle	Advantages	Disadvantages
Pressure	Spin rotor gauge [53]	Suspension of steel ball in magnetic field spinning at specific speed in a stainless steel tube attached to the VIP	Accurate and fast	Risk of leakage on attaching the tube, dependent on gas type, not feasible for large number of VIPs
	Foil lift off [35,53]	Pressure equilibrium between inside and outside the panel	Fast and no special preparation of panel required	Not feasible for large number of VIPs, limited pressure measurement range
	Radio frequency identification technique (RFID) [53,54]	Identification of radio waves emitted by RFID tag placed in VIP	Fast, post installation measurement suitable for large number of VIPs	Not suitable for thick aluminium foil envelope
	Thermal measurement [53,54]	Thermal conductivity of thin fibre sensor fleece and relation of pressure increase		Slow and requires Helium gas for fast measurement, multiple tests for accuracy
WVTR	Gravimetric method [55]	Difference in weight due to water vapour permeation	Less expensive	Slow, Less accurate, not suitable for high barrier materials
	Electrolytic detection sensor method [30]	Gas flowing underneath the sample foil carries moisture and leads to electrolysis		
	Infrared detection sensor method	Relative humidity measurement using infra red sensor		
Thermal conductivity	Guarded hot box [56,57]	Heat transfer between hot and cold chambers at steady conditions across the test sample is measured	Slow, expensive, requires auxiliary guard section and edge insulation	
	Heat flow meter [57,58]	Heat flux is measured between hot and cold plates across the test sample	Fast, inexpensive	Requires frequent calibration

minium foil and 0.008 W m^{-1} K^{-1} for metalized polymeric envelope due to air and water infiltration for at least 20 mm thick and 250 mm wide panel.

$$\frac{\partial \lambda_c}{\partial t} = \frac{\partial \lambda_c}{\partial P}\frac{\partial P}{\partial t}(T,\varphi) + \frac{\partial \lambda_c}{\partial u}\frac{\partial u}{\partial t}(T,\varphi) \tag{12}$$

where λ_c is the core thermal conductivity (W m^{-1} K^{-1}); u is the moisture content (% mass); T is the temperature (K); φ is the relative humidity (%).

Schwab et al. [33] presented a correlation (13) for predicting thermal conductivity as a function of time for a fumed silica kernel VIP. In correlation (13) initial thermal conductivity was limited to only solid and radiative conductivity and thermal conductivity due to increase in gas pressure and water content over time was added to calculate the time dependent thermal conductivity, $\lambda(t)$

$$\lambda(t) = \lambda_{evac} + \frac{\lambda_{free\ gas}}{1 + (p_{1/2,gas}/p_{gas(t)})} + bX_w(t) \tag{13}$$

where λ_{evac} is the thermal conductivity (in evacuated conditions) (W m^{-1} K^{-1}); $\lambda_{free\ gas}$ is the thermal conductivity of the free and still gas (W m^{-1} K^{-1}); $p_{1/2,gas}$ is the pressure at which the gaseous thermal conductivity equals one half of $\lambda_{free\ gas}$ (Pa); p_{gas} is the gas pressure (Pa); b is the sorption isotherm constant; X_w is the water content (% mass).

At 10 °C thermal conductivity increased by 0.0005 W m^{-1} K^{-1} per mass% of adsorbed water and a 30 mbar increase in gas pressure led to a rise of 0.001 W m^{-1} K^{-1} in thermal conductivity [30]. Tenpierik et al. [59,63] based on the Eq. (12) proposed an analytical model equation for estimating changes in thermal conductivity over time and useful life time for a VIP with silica core and aluminium foil envelope. This Eq. (14) includes the rate of change of thermal conductivity due to gas and water vapours as separate terms.

$$\Delta\lambda_c(t) \approx \frac{\partial \lambda_c}{\partial p_g} p_{ge}\left(1 - e^{\frac{t-t_{get}}{t_g}}\right) + \frac{\partial \lambda_c}{\partial p_{wv}} p_{wve}\left(1 - e^{\frac{t-t_{des}}{t_w}}\right) + \frac{\partial \lambda_c}{\partial u} \times \frac{du}{d\varphi}\left(1 - e^{\frac{t-t_{des}}{t_w}}\right) \tag{14}$$

where p_g is the pore gas pressure (Pa); p_{ge} is the atmospheric gas pressure (Pa); p_{wve} is the partial water vapour pressure outside the VIP (Pa); t is the time (s); t_{get} is the time shift due to a getter (s); t_{des} is the time shift due to a desiccant (s); t_g is the time constant for gas pressure increase (s); t_w is the time constant for water content increase (s); φ is the relative humidity of the air outside the VIP (%).

For compressed fumed silica a simplified model, (15), was used to approximate rapid estimation of useful life time by assuming nil extension of VIP life using getter and desiccant [59,63].

$$Tsl \approx a e^{b(\lambda_w - \lambda_0 - \lambda_w)} \cdot d_p \cdot \left(\frac{l_p}{s_p}\right) c \cdot \frac{T_0}{T} e^{E_a/R\left(\frac{1}{T} - \frac{1}{T_0}\right)} \tag{15}$$

where a (s m$^{-(1+c)}$), b (m K W^{-1}) and c are regression parameter; E_a is the activation energy for permeation through the barrier envelope (J mol^{-1}); R is the universal gas constant (J mol^{-1} K^{-1}); l_p is the perimeter length of VIP (m); s_p is the surface area of VIP (m^2); λ_w is the thermal conductivity of liquid water and water vapour at equilibrium (W m^{-1} K^{-1}); λ_0 is the thermal conductivity of air at atmospheric pressure (W m^{-1} K^{-1}).

This approximating model is limited to VIP thickness in the range of 0.01–0.05 m, temperature in the range of 268–318 K, perimeter length to surface area ratio in the range of 2–12 m^{-1} and a constant relative humidity of 50%. However, for building applications constantly changing environmental conditions require a model that is able to predict VIP useful life time under real life transient conditions. Recently, Beck et al. [61] proposed a dynamic simulation model for a silica VIP core under dynamic hygrothermal conditions and was able to simultaneously calculate the moisture transmission and temperature profile of the VIP core. Wegger et al. [64] performed accelerated ageing testing of VIPs to evaluate the effect of various factors such as temperature, moisture and pressure on thermal performance. The results of the ageing tests showed acceptable agreement with that of the accompanying theoretical analysis. A parametric regime for accelerated ageing tests of VIPs in laboratories was also proposed.

5.2. Thermal bridging effect

It is customary to express the performance of VIPs in terms of either the centre of panel or effective thermal conductivity with later incorporating the effect of thermal bridges around the edges.

These thermal bridges appear at three levels for VIP application; (i) VIP level (ii) building components level (iii) facade level [65]. Thermal bridges or linear thermal transmittance at VIP level occurs at edges due to the difference in thermal conductivity of evacuated core and surrounding envelope materials. The linear thermal transmittance depends upon the panel thickness, length of perimeter and surface area. Effective thermal conductivity of a VIP can be calculated by adding linear thermal transmittance to centre of panel thermal conductivity as described in Eq. (16) [30,66].

$$\lambda_{eff} = \lambda_{cop} + \Psi_{VIP\ edge} \cdot d_p \cdot l_p / S_p \quad (16)$$

where λ_{cop} is the centre of panel thermal conductivity (W m^{-1} K^{-1}); $\Psi_{VIP\ edge}$ the is linear thermal transmittance (W m^{-1} K^{-1}); λ_{eff} is the effective thermal conductivity (W m^{-1} K^{-1}); d_p is the thickness of VIP (m).

Wakili et al. [66] employed a two-dimensional numerical simulation tool TRISCO to predict the effective thermal conductivity and reported measurements using a guarded hot box. Values of linear thermal transmittance calculated by Wakili et al. [66] for a square-shaped VIP of size 1 m^2 are shown in Fig. 9. It can be seen that linear thermal transmittance values are higher for a VIP with an aluminium foil (8 μm) envelope as compared to the aluminium coated polymeric foil envelopes. Linear thermal transmittance values for a VIP, 10–40 mm thick, lie in the range of 0.008–0.010 W m^{-1} K^{-1} for envelopes consisting of three 12 μm metalized PET layers, while for a 6 μm aluminium foil it varied between 0.022 and 0.040 W m^{-1} K^{-1} [67]. Simmler and Brunner [35] calculated the safe design values for linear thermal transmittance to be 0.007 W m^{-1} K^{-1} and 0.01 W m^{-1} K^{-1} respectively for an aluminium foil and a metallised envelope. Clearly an aluminium foil envelope is not suitable for use in VIP envelope.

Thorsell and Kallebrink [68] proposed the serpentine edge design to minimise the linear thermal transmittance at VIP edges. For the stainless steel envelope with 17 serpentines of 20 mm depth the linear thermal transmittance was reported as 0.0096 W m^{-1} K^{-1} compared to 0.028 W m^{-1} K^{-1} for a straight steel edge. These values were calculated by using simulation tool Femlab. However, these linear thermal transmittance values were still larger as compared to the values obtained by the Wakili et al. [66] for the metallised and aluminium foil envelopes. Schwab et al. [69] reported similar results and recommended that a minimum panel size of 1 m^2 for aluminium foil VIP.

Tenpierik et al. [63,70] and Tenpierik and Cauberg [71] assuming steady state boundary conditions, no lateral heat transfer between adjacent VIPs and zero thermal conductivity of core presented an analytical model to calculate thermal bridges due to VIP envelope. The results of model for nonzero core thermal conductivity were validated against the predictions obtained from a commercially available software, TRISCO. Linear thermal transmittance was found to be a complex function of laminate thickness, laminate thermal conductivity, panel thickness and core thermal conductivity. The difference in results of the model and that obtained by TRISCO simulations was much larger for metalized VIP panel with core thermal conductivity 0.002 W m^{-1} K^{-1} and a panel thickness of 20 mm. The results of linear thermal transmittance obtained by simulations for 0.004 W m^{-1} K^{-1} core thermal conductivity with aluminium foil, stainless steel foil and metalized film envelope are shown in Fig. 10. It is evident from Fig. 10 that metalized film results into a smaller thermal bridge effect than in the case of aluminium foil and stainless steel envelope. Linear thermal transmittance due to metalized films, though smaller than aluminium foil and stainless steel, still has a value in the range of 0.001–0.004 W m^{-1} K^{-1} depending upon the thickness of panel and core thermal conductivity. Results of both model and simulations show that materials with higher thermal conductivity in the VIP envelope generated larger thermal bridging effect. Clearly, it is imperative to use low thermal conductivity materials in the VIP envelope to reduce the thermal bridging effect. Thin films of SiO_x and SiN_x coated on a polymer substrate can be used to reduce this thermal bridging effect, which is expected to enhance the thermal performance of VIPs.

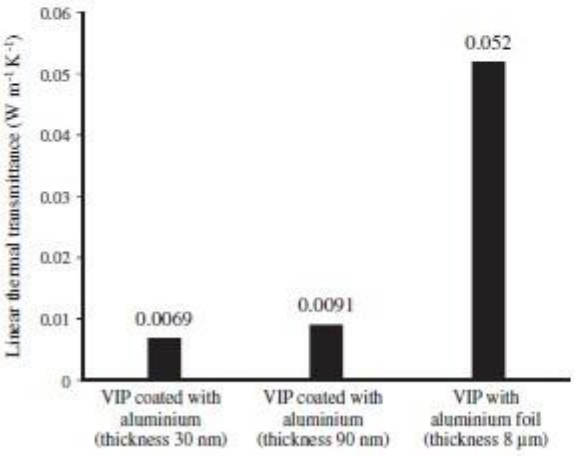

Fig. 9. Linear thermal transmittance for different envelope configurations (adapted from [66]).

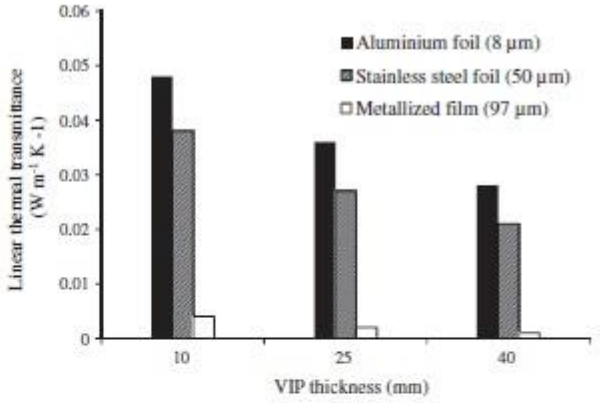

Fig. 10. Comparison of linear thermal transmittance of different envelope materials with specified thicknesses (adapted from [70]).

VIPs often consist of two protecting facings on both sides of the panels linked with a spacer. Schwab et al. [69] estimated the linear thermal transmittance values of expanded polystyrene covered VIPs with aluminium foil and aluminium coated envelopes and found that the presence of expanded polystyrene facing reduced the thermal bridging losses. Nussbaumer et al. [72] also observed the reduced thermal bridging effect when expanded polystyrene was used as a facing in building components. Tenpierik et al. [73] and Quenard and Sallee [65] calculated thermal bridging effect of facing and spacers and found that aluminium and stainless steel facing caused larger values of linear thermal transmittance as compared to polyester facing. Same trend was observed for spacers made up of aluminium as compared to thermoplastic spacer. EPS strips along the perimeter of an encapsulated VIP were reported to cause an additional thermal bridging effect depending upon their thicknesses [74]. To reduce this thermal bridging effect, designers should either completely remove EPS strip or minimise the thickness of perimeter insulator or use a better insulator for perimeter.

6. Conclusions and future directions

VIP is a high performance thermal insulation, with a large potential to reduce the CO_2 foot prints of buildings (1.56 kg CO_2 $m^{-2}a^{-1}$) and in conforming to stringent energy standards whilst using minimal existing space. The adoption of VIPs is presently constrained by their limitations namely, susceptibility to damage during installation and development, uncertain useful life time, thermal bridging and high cost. Presently, research is limited to only a few materials which are being used in core and envelope of VIPs and test results available to date are limited to a narrow range of climatic conditions. Thus, new materials, concepts and computer models experimentally validated under realistic climatic conditions are required. The aim of such activities should be to enhance the properties of VIP and reduce their cost making them more attractive to manufacturers, consumers and the construction industry.

VIP envelope consisting of PET multiple sheets coated with SiO_x and/or SiN_x have a good potential to replace the conventional aluminium and metalized PET films. Silicon coatings are expected to improve the thermal and barrier performance of the VIP envelope. Research needs to be focussed on developing a barrier material which will achieve an OTR of $<10^{-3}$ cm^3 m^{-2} d^{-1} at 23 °C, 50% RH, and a WVTR of $<10^{-4}$ g m^{-2} d^{-1} at 32 °C, 90% RH which is expected to yield a useful life time of 50 years or more for VIPs. These coatings are also expected to reduce the thermal bridging effect and improve thermal resistance. A comprehensive computer model able to resolve the coupled complex heat and mass (gas and water vapour) exchange phenomena that occur in a VIP system would be a useful tool for researchers to predict VIP performance parameters, thermal conductivity, WVTR and OTR, over a prolonged duration subject to realistic ambient conditions of temperature and humidity. Such a model would assist in identifying the optimum configurations of VIP envelope specifying the type and thicknesses of coatings required for varying thickness of the substrate.

One criticism that the fumed silica core material faces is its high market prices (leading to a higher VIP cost). There is a definite scope of cost reduction for VIP core materials by preparing fumed silica–perlite composite, though this might result into some thermal resistance being sacrificed. Optimal proportions for these two materials in the core yielding the lowest possible thermal conductivity need to be ascertained. Open-celled polystyrene modified by employing a suitable filler material is also being seen as a potential core material due to low out gassing properties. The challenge here is to optimise the type, amount and distribution of filler material in the composite to achieve and maintain a suitable vacuum level inside the core to result in design thermal conductivity values with intended useful life of 100 years or more.

There is a need of identifying newer adhesive materials, which have a low thermal conductivity and are chemically and physically stable under vacuum conditions and least outgas. Among various components in the surrounding air, water vapour has the highest transmission rate and it permeates about 30,000 times faster than oxygen and nitrogen and is therefore one of the major contributor to increasing pressure along with oxygen and nitrogen. It is felt that a new class of super hydrophobic sealants and sealing processes is required to overcome the problem of permeation of water vapours through the seal areas.

Finally, it is utmost important to employ the knowledge generated in the laboratories to manufacture example VIPs with experimentally validated test results under realistic climatic conditions to earn the confidence of the builders, architects and building managers and owners.

References

[1] Department for Communities and Local Government. Building a Greener Future:policy statement. <http://www.communities.Gov.uk/documents/planningandbuilding/pdf/building-greener.pdf>; 2007 [accessed 01.07.10].

[2] Department for Communities and Local Government. The Code for Sustainable Homes setting the standard in sustainability for new homes. <http://www.communities.gov.uk/documents/planningandbuilding/pdf/codesustainhomesstandard.pdf>; 2008 [accessed 01.07.10].

[3] Department for Communities and Local Government. Zero carbon for new nondomestic buildings consultation policy options. <http://www.Communities.gov.uk/documents/planningandbuilding/pdf/13991110.pdf>; 2009 [accessed 17.04.10].

[4] Climate Change Act 2008, Crown copyright. <http://www.opsi.gov.uk/acts/acts2008/pdf/ukpga20080027_en.pdf>; 2008 [accessed 19.06.10].

[5] Department of Trade and Industry. Meeting the energy challenge a white paper on energy. <http://www.berr.gov.uk/files/file39387.pdf>; 2007 [accessed 12.05.10].

[6] Department of Energy and Climate Change. Energy trends; June 2010.

[7] The Building Regulations 2000, Conservation of fuel and power L1A, Crown Copy Rights.

[8] Çomaklı K, Yüksel B. Optimum insulation thickness of external walls for energy saving. Appl Therm Eng 2003;23:473–9.

[9] Pout C. Revised emission factors for national calculation methodologies, Technical papers supporting SAP 2009, BRE 2009. <http://www.bre.co.uk/filelibrary/SAP/2009/STP09CO201_Revised_emission_factors.pdf>; [accessed 18.09.10].

[10] Charted Institute of Building Engineers (CIBSE). Environmental design, CIBSE guide A; 2006.

[11] BRE-PassivHaus Primer. <http://www.passivhaus.org.uk/filelibrary/BRE-PassivHaus-Primer.pdf>; [accessed 20.04.10].

[12] Brunner S, Simmler H. In situ performance assessment of vacuum insulation panels in a flat roof construction. Vacuum 2008;82:700–7.

[13] Jelle BP, Gustavsen A, Baetens R. The Path to the high performance thermal building insulation materials and solutions of tomorrow. J Build Phys 2010;34:99–123.

[14] Tenpierik M, Cauberg H. Vacuum insulation panel: friend or foe? In: Proceeding of 23rd conference on passive and low energy architecture, Geneva, Switzerland; 2006.

[15] Willems WM, Schild K. The next generation of insulating materials: vacuum insulation. In: Proceedings of the 7th symposium of building physics in the Nordic countries, Reyjhavik, Iceland; 2005.

[16] Willems WM, Schild K, Hellinger G. Numerical investigation on thermal bridge effects in vacuum insulating elements. In: Zimmermann M, editor. Proceedings of the 7th international vacuum insulation symposium, Duebendorf, Switzerland; 2005. p. 145–52.

[17] Kwon JS, Jang CH, Jung H, Song TH. Effective thermal conductivity of various filling materials for vacuum insulation panels. Int J Heat Mass Trans 2009;52:5525–32.

[18] Al Homoud MS. Performance characteristics and practical applications of common building thermal insulation material. Build Environ 2005;40:353–66.

[19] Hull TR, Stec AA. Assessment of the fire toxicity of building insulation materials. Energy Build 2011;43:498–506.

[20] Nemoto T, Takagi J, Ohshima M. Control of bubble size and location in nano-/microcellular poly(propylene)/rubber blend foams. Macromol Mater Eng 2008;293:574–80.

[21] Wang X, Walliman N, Ogden R, Kendrick C. VIP and their applications in buildings: a review. Constr Mater 2007;160:145–53.

[22] Evonik Industries. Basic properties and characteristics of Aerosil® products. Technical bulletin Fine Particles, Number 11.

[23] Kistler SS, Caldwell AG. Thermal conductivity of silica aerogel. Ind Eng Chem 1934;26:658–62.

[24] Potter FJ. Nanogel™, Production, properties, applications. In: Zimmermann M, Bertschinger H, editors. In: Proceedings of the international conference and workshop on high performance thermal insulation, Duebendorf, Switzerland; 2001. p. 33–6.

[25] Baetens R, Jelle BP, Gustavsen A. Aerogels for building applications: a state-of-the-art review. Energy Build 2011;43:761–9.

[26] Caps R, Fricke J. Thermal conductivity of opacified powder filler materials for vacuum insulations. Int J Thermophys 2000;21:445–52.

[27] Swimm K, Reichenauer G, Vidi S, Ebert HP. Gas pressure dependence of the heat transport in porous solids with pores smaller than 10 μm. Int J Thermophys 2009;30:1329–42.

[28] Araki K, Kamoto D, Matsuoka S. Optimization about multilayer laminated film and getter device materials of vacuum insulation panel for using at high temperature. J Mater Process Technol 2009;209:271–82.

[29] Mukhopadhyaya P, Kumaran K, Normadin N and Reen DV. Fibre–powder composite as core material for vacuum insulation panel. In: 9th international vacuum insulation symposium, London, UK; 2009.

[30] Simmler H, Brunner S, Heinemann U, Schwab H, Kumaran K, Mukhopadhyaya P, et al. Vacuum insulation panels – study on VIP-components and Panels for Useful life time Prediction in Building Applications (Subtask A). A Report for the IEA/ECBCS Annex 39 High Performance Thermal Insulation for Buildings and Building Systems 2005. <http://www.ecbcs.org/docs/Annex_39_Report_Subtask-A.pdf>; [accessed 26.04.10].

[31] Fricke J, Schwab H, Heinemann U. Vacuum insulation panel-exciting thermal properties and most challenging applications. Int J Thermophys 2006;27:1123–39.
[32] Schwab H, Heinemann U, Beck A, Ebert HP, Fricke J. Permeation of different gases through foils used as envelopes for vacuum insulation panels. J Therm Envelope Build Sci 2005;28:293–317.
[33] Schwab H, Heinemann U, Beck A, Ebert HP, Fricke J. Prediction of useful life time for vacuum insulation panels with fumed silica kernel and foil cover. J Build Phys 2005;28:357–74.
[34] Baetens R, Jelle BP, Thue JV, Tenpierik MJ, Grynning S, Uvslokk S, et al. Vacuum insulation panels for building applications: a review and beyond. Energy Build 2010;42:147–72.
[35] Simmler H, Brunner S. Vacuum insulation panels for building application: basic properties, aging mechanisms and service life. Energy Build 2005;37:1122–31.
[36] Kwon JS, Jang CH, Jung H, Song TH. Vacuum maintenance in vacuum insulation panels exemplified with a staggered beam VIP. Energy Build 2010;42:590–7.
[37] Brunner S, Gasser P, Simmler H, Wakili KG. Investigation of multilayered aluminium-coated polymer laminates by focused ion beam (FIB) etching. Surf Coatings Technol 2006;200:5908–14.
[38] Teniers C. How laminates with EVALTM EVOH film improve the performance of VIPs. In: 9th international vacuum insulation symposium, London, UK; 2009.
[39] Lange J, Wyser Y. Recent innovations in barrier technologies for plastic packaging – a review. Pack Technol Sci 2003;16:149–58.
[40] Amrerg-Schwab S, Hoffmann M, Badera H, Gessler M. Inorganic-organic polymers with barrier properties for water vapour, oxygen and flavours. J Sol–Gel Sci Technol 1998;13:141–6.
[41] Howells DG, Henry BM, Laterrier Y, Manson JAE, Madocks J, Assender HE. Mechanical properties of SiO_x gas barrier coatings on polyester films. Surf Coating Technol 2008;202:3529–37.
[42] Wolf R, Wandel K, Boeffel C. Moisture barrier films deposited on PET by ICPECVD of SiN. Plasma Process Polym 2007;4:S185–9.
[43] Yun-Jin S, Ya-Bo F, Qiang C, Chun-Mei Z, Li-Jun S, Yue-Fei Z. Silicon dioxide coating deposited by PDPs on PET films and influence on oxygen transmission rate. Chin Phys Lett 2008;25:1753–6.
[44] Lim HS, Baek JH, Park K, Shin HS, Kim J, Cho JH. Multifunctional hybrid fabrics with thermally stable super hydrophobicity. Adv Mater 2010;22:2138–41.
[45] Malsen JV, Tenpierik MJ, Looman RHJ, Cauberg JJM. Heat seal strength of barrier film used in vacuum insulation panels at room temperature and at −130 °C. J Plastic Film Sheet 2008;24:35–52.
[46] Technology Assessment for Radically Improving the Built Asset (TARBASE). Carbon Vision grant GR/S94285/01-TARBASE, <http://www.sbe.hw.ac.uk/hostedsites/tarbase/>; 2008 [accessed 10.01.11].
[47] Altan Dombayci Ö, Gölcü M, Pancar Y. Optimization of insulation thickness for external walls using different energy-sources. Appl Energy 2006;83:921–8.
[48] Jenkins DP, Singh H, Eames PC. Interventions for large-scale carbon emission reductions in future UK offices. Energy Build 2009;41:1374–80.
[49] http://www.findalondonoffice.co.uk/toolbox/rental-guide/ [accessed 29.01.11].
[50] Fricke J. Materials research for the optimization of thermal insulations. High Temp–High Press 1993;25:379–90.
[51] Kaganer MG. Thermal insulation in cryogenic engineering, translated by A. Moscona, Israel programme for scientific translation Ltd.; 1969.
[52] Porta PD. Gas problem and gettering in sealed-off vacuum devices. Vacuum 1996;47:771–6.
[53] Caps R, Beyrichen H, Kraus D, Weismann S. Quality control of vacuum insulation panels: methods of measuring gas pressure. Vacuum 2008;82:691–9.
[54] Caps R, Beyrichen H. Monitoring gas pressure in vacuum insulation panels. In: Zimmermann M, editor. Proceedings of the 7th international vacuum insulation symposium. Switzerland: Duebendorf; 2005. p. 57–66.
[55] British Standards Institution. BS EN 12086:1997. Thermal insulating products for building applications-Determination of water vapour transmission properties, BSI London; 1999.
[56] British Standards Institution. BS EN 12667:2001. Thermal performance of building materials and products – determination of thermal resistance by means of guarded hotplate and heat flow meter methods – products of high and medium thermal resistance, London BSI; 2001.
[57] Grynning S, Jelle BP, Uvslokk S, Gustavsen A, Baetens R, Caps R, et al. Hot box investigations and theoretical assessments of miscellaneous vacuum insulation panel configurations in building envelopes. J Build Phys 2011. doi:10.1177/1744259110382229.
[58] Frawley E, Kennedy DM. Thermal testing of building insulation materials. Eng J 2007;61:552–8.
[59] Tenpierik M, van Der Spoel W, Cauberg H. Simplified analytical model for useful life time prediction of a vacuum insulation panel. In: Proceedings of 8th international vacuum insulation symposium, Würzburg, Germany; 2007.
[60] ASTM C 1484. Standard specification for vacuum insulation panels. West Conshohocken, US: American Society for Testing and Materials International; 2001.
[61] Beck A, Binder M, Frank O. Dynamic simulation of VIP moisture and heat transport. In: Proceedings of 9th international vacuum insulation symposium, London, UK; 2009.
[62] Krishna R, Wesselingh JA. The Maxwell–Stefan approach to mass transfer. Chem Eng Sci 1997;52:861–911.
[63] Tenpierik MJ. Vacuum insulation panels applied in building constructions (VIP ABC). Ph.D. Thesis, Delft University of Technology (Delft, The Netherlands); 2009.
[64] Wegger E, Jelle BP, Sveipe A, Graynnig S, Gustavsen A, Baetens R, et al. Aging effects on thermal properties and service life of vacuum insulation panels. J Build Phys 2011. doi:10.1177/1744259111398635.
[65] Quenard D and Sallee H. From VIP's to building facades: three levels of thermal bridges. In: Zimmermann M, editor. Proceedings of the 7th international vacuum insulation symposium, Duebendorf, Switzerland; 2005. p. 113–20.
[66] Wakili KG, Bundi R, Binder B. Effective thermal conductivity of vacuum insulation panels. Build Res Inform 2004;32:293–9.
[67] Binz A, Moosmann A, Steinke G, Schonhardt U, Fregnan F, Simmler H, et al. Vacuum insulation in the building sector. Systems and applications (Subtask B). Final Report for the IEA/ECBCS Annex 39 HiPTI-project High performance thermal insulation for buildings and building systems 2005. <http://www.ecbcs.org/docs/Annex_39_Report_Subtask-B.pdf>; [accessed 20.04.10].
[68] Thorsell T, Kallebrink I. Edge loss minimization in vacuum insulation panels. In: Proceedings of 7th symposium on building physics in the Nordic countries, Reykjavik, Iceland; 2005.
[69] Schwab H, Stark C, Wachtel J, Ebert HP, Fricke J. Thermal bridges in vacuum-insulated building facades. J Therm Envelope Build Sci 2005;28:345–55.
[70] Tenpierik M, van Der Spoel W, Cauberg H. Analytical model for predicting thermal bridge effects due to vacuum insulation panel barrier envelope. Bauphysik 2008;30:38–45.
[71] Tenpierik M, Cauberg H. Analytical models for calculating thermal bridge effects caused by thin high barrier envelopes around vacuum insulation panels. J Build Phys 2007;30:185–215.
[72] Nussbaumer T, Wakili KG, Tanner Ch. Experimental and numerical investigation of the thermal performance of a protected vacuum-insulation system applied to a concrete wall. Appl Energy 2006;83:841–55.
[73] Tenpierik M, van Der Spoel W, Cauberg H. An Analytical model for calculating thermal bridge effects in high performance building enclosure. J Build Phys 2008;31:361–87.
[74] Tenpierik MJ, Cauberg JJM. Encapsulated vacuum insulation panel: theoretical thermal optimization. Build Res Inform 2010;38:660–9.